



UNIVERSIDADE FEDERAL DE SANTA CATARINA
CENTRO TECNOLÓGICO
PROGRAMA DE PÓS-GRADUAÇÃO EM ENGENHARIA DE ALIMENTOS

Édipo da Silva Almeida

**Technologies applied to the recovery of bioactive compounds from
food fluids and their performance in the biosynthesis of nanometals:**

*a case study with *Morinda citrifolia**

Florianópolis, SC

April 2022

Édipo da Silva Almeida

**Technologies applied to the recovery of bioactive compounds from
food fluids and their performance in the biosynthesis of nanometals:**

a case study with *Morinda citrifolia*

Doctoral thesis submitted to the Graduate Program
in Food Engineering at the Federal University of
Santa Catarina to obtain the title of Doctor in Food
Engineering.

Advisor: Prof. Débora de Oliveira, Dr.

Co-advisor: Prof. Dachamir Hotza, Dr.

Florianópolis, SC

April 2022

Ficha de identificação da obra elaborada pelo autor,
através do Programa de Geração Automática da Biblioteca Universitária da UFSC.

Almeida, Édipo da Silva

Technologies applied to the recovery of bioactive compounds from food fluids and their performance in the biosynthesis of nanometals : a case study with Morinda citrifolia / Édipo da Silva Almeida ; orientadora, Débora de Oliveira, coorientador, Dachamir Hotza, 2022.

167 p.

Tese (doutorado) - Universidade Federal de Santa Catarina, Centro Tecnológico, Programa de Pós-Graduação em Engenharia de Alimentos, Florianópolis, 2022.

Inclui referências.

1. Engenharia de Alimentos. 2. Morinda citrifolia. 3. Compostos bioativos. 4. Crioconcentração. 5. Nanopartículas de prata. I. Oliveira, Débora de . II. Hotza, Dachamir. III. Universidade Federal de Santa Catarina. Programa de Pós-Graduação em Engenharia de Alimentos. IV. Título.

Édipo da Silva Almeida

Technologies applied to the recovery of bioactive compounds from food fluids and their performance in the biosynthesis of nanometals:

a case study with *Morinda citrifolia*

The present study at the doctoral level was evaluated and approved by an examining board composed of the following members:

Prof. Acácio Zielinski, Dr.

Universidade Federal de Santa Catarina (UFSC)

Prof. Lizandro Manzato, Dr.

Instituto Federal de Educação, Ciência e Tecnologia do Amazonas (IFAM)

Universidade Federal do Amazonas (UFAM)

Prof. Lorenzo Pastrana, Dr.

International Iberian Nanotechnology Laboratory (INL)

Universidade de Vigo (UVigo)

We certify that this is the original and final version of the final work that was considered suitable for obtaining the title of Doctor in Food Engineering.

Prof. Sandra Regina Salvador Ferreira, Dr.
Coordinator of the Postgraduate Program in
Food Engineering (PPGEAL/UFSC)

Prof. Débora de Oliveira, Dr.
Advisor (PPGEAL/UFSC)

Florianópolis, SC

April 2022

*“Deixe tudo acontecer a você, beleza e terror.
Apenas continue.
Nenhum sentimento é final.”*

Rainer Maria Rilke (1875-1926)

Dedico esse trabalho aos meus pais, Dona Maria
Betânia e meu velho Sr. Ruy José.

Nossa! Como vocês *“aperream”* o meu juízo durante meu colegial.
De tanto insistirem em dizer que *“...você tem que ir embora daqui. Pombal não tem nada pra você!”* Resultado: *“peguei o beco”* de casa aos 17 anos pra fazer faculdade de engenharia e vejam onde vim parar! Já se vão 12 anos e o irônico é que hoje vocês me querem por perto.

Valeu a pena ir tão longe? Confesso que até aqui ainda não arquitetei uma resposta categórica, mas quando certo dia, perante olhares circunspectos dos meus pais pude ouvir destes um: *“...a gente tá contigo!”* Senti que esse era o combustível que precisava pra seguir e concluir essa empreitada maluca.

Obrigado por confiarem nesse filho desajuizado, compassivo e perseverante.
Amo vocês!

AGRADECIMENTOS

A tal felicidade parece mesmo estar por trás de tudo que fazemos ou pensamos, não é mesmo?! Basta ir vasculhando as razões para as nossas decisões. Meio à moda de criança chata e perguntona. Estudar no domingo, pra quê? Ir bem na prova? Passar de ano? Faculdade? Diploma? Estágio? Emprego? Salário? Viajar? Casar? Ter filhos? Uma casa em Balneário Camboriú? Ah, vai! Um apê nas montanhas geladas de Aspen? Vixe! Pegamos um caminho meio pobre de espírito quando pensamos demais sobre o futuro. E olha que, enquanto criança eu só queria ser goleiro do Flamengo e da Seleção...

Essas e muitas outras dúvidas me vem à tona quando encontro pessoas que acham estranho eu dizer que a fé comporta muitas dúvidas. Sempre coloco o nome de Deus perante tantas incertezas. Diante de minhas limitações, não me abstenho dos temas polêmicos de Deus: Por quê ele se esconde? O que ele reserva pra mim? Pra quê essa implicância meio “Parkinson” de escrever certo por linhas tortas? É imerso nesse oceano de incertezas que cheguei a uma conclusão. Ao comprometer-me sinceramente a tais dúvidas que descobri que não possuo fé suficiente para não crer Nele, embora minha natureza às vezes me guie por um caminho oposto. Meio contraproducente, não?! Graças a Deus, pude receber esse privilégio do livre arbítrio de questionar, de tentar achar uma lógica sobre seus planos. E é nesse misterioso mar de dúvidas que alguma lógica pode ser encontrada. Provavelmente morrerei afogado em virtude das câimbras de tanto nadar e não achar p... nenhuma. Mas eu só cheguei até aqui graças a Ele. Ele é a lógica pela qual perduro, e é a Ele que primeiramente agradeço.

Deus! Olha só... antes de baixar meu olhar, agora apontado para o céu e migrá-lo para seus demais servos humanos aqui na Terra para continuar os agradecimentos, permita-me indagar: se você realmente é amor, perdoe esse servo atrevido que vos escreve (sorriso envergonhado), ele te ama profundamente.

Aos meus pais pela incansável paciência ante esse filho que teima em não seguir a cartilha da conduta pela qual, por eles fui educado.

- Dona Betânia, meu velho pai, Sr. Ruy José, obrigado por terem até aqui, me permitido ser só aquilo que consigo ser nesse momento. Obrigado por me acolherem do jeito que eu sou. Obrigado por amarem a minha realidade, e não minha expectativa. Obrigado pelo amor traduzido, mesmo à distância, em olhares mansos, afáveis e carinhosos. Amo vocês por me olharem devagar, num mundo onde tanta gente nos olham depressa demais.

- Amo vocês!

- Seu filho tá virando doutor!

Aos amigos, que fiz, às parcerias que firmei. A esse amor de amizade, que contempla tão poucos, mais que é abarrotado de estima e afeto. Foram vocês que me aceitaram expressar esse sentimento, da maneira menos natural, orgânica e instintiva. Não cabe a mim verbalizar nomes, pois se algum dia vocês lerem esse texto, saberão que sempre amei vocês.

Aos meus orientadores da pós-graduação, Professora Débora de Oliveira, com seu “*jeitão bizarro, porém fabulosa*”, e ao Professor Dachamir Hotza, das quais os elogios não cabem nessa página, afinal é mais prudente adotar o “*menos é mais*” nesse momento. Direta e indiretamente, foi devido a paciência e confiança de vocês que estou conseguindo mais essa conquista. Professores, muito obrigado!

Aos laboratórios que me permitiram executar esse trabalho, em especial, o Laboratório de Transferência de Massa (LABMASSA/EQA/UFSC) e o Laboratório de Separação por Membranas (LABSEM/EQA/UFSC).

A UFSC e em especial, o Departamento de Engenharia Química e de Alimentos, graduação e pós-graduação. Vocês não imaginam o tamanho da minha gratidão.

Embarcar na Engenharia de Alimentos virou minha vida de ponta-cabeça! Me reinventei! MUITÍSSIMO obrigado!

À cidade de Florianópolis que me proporcionou um misto de tantas alegrias e tristezas, que passei a amá-la e considerá-la minha nova casa longe da minha cultura e raízes. Guardarei com carinho, cada esquina, cada casa e cada aventura que vivi nesta cidade.

A todos os demais amigos, parceiros e colegas que de alguma maneira contribuíram nesta minha conquista; do meu orientador ao porteiro do laboratório, meus sinceros agradecimentos de coração.

A todos vocês, muito obrigado!

RESUMO

A *Morinda citrifolia*, também conhecida como “noni”, fornece frutos que são matéria-prima no preparo de alimentos e bebidas. No entanto, o processamento do fruto resulta na geração de grande quantidade de resíduos, dos quais as folhas representam ampla maioria. Levando-se em consideração que as folhas de noni são comprovadamente detentoras de alta quantidade de compostos bioativos com alto teor nutricional e propriedades fitoterápicas comprovadas, este estudo propõe a aplicação da concentração por congelamento em bloco multiestágio realizada pelo método de degelo passivo, conhecido como crioconcentração. Objetivando promover uma maior rapidez e eficiência no processo de retenção dos componentes bioativos presentes nas folhas de *Morinda citrifolia*, dois métodos de crioconcentração foram estudados: o degelo gravitacional e o método assistido por micro-ondas. A execução de ambos os processos de crioconcentração resultou em extratos concentrados que posteriormente foram utilizados como meio de reação para síntese de nanopartículas de prata. O efeito das etapas de crioconcentração sobre as características físicas e químicas das frações concentradas resultou em maior teor de fenólicos e sólidos totais, com alta eficiência na retenção de fenólicos comparado a suas respectivas porções iniciais. A aplicação dos extratos concentrados na biossíntese de nanopartículas de prata resultou em um material polidisperso, estável, com propriedades ainda mais destacadas quando comparadas com a biossíntese via uso dos extratos não concentrados. Pôde-se concluir que a utilização de ambos os sistemas de crioconcentração permitiu a obtenção de frações concentradas com promissor valor biológico e nutricional; indicando que a técnica também pode contribuir como referência no uso de uma tecnologia sustentável na geração de nanometais com propriedades aprimoradas.

Palavras-chave: *Morinda citrifolia*. Compostos bioativos. Crioconcentração. Biossíntese de nanometais. Nanopartículas de prata.

ABSTRACT

Morinda citrifolia, also known as “noni”, provides fruits that are raw materials in the preparation of food and beverages. However, the processing of the fruit results in the generation of a large amount of waste, of which the leaves represent the vast majority. Taking into account that noni leaves are proven to contain a high amount of bioactive compounds with high nutritional content and proven phytotherapeutic properties, this study proposes the application of concentration by freezing in a multistage block performed by the passive thaw method, known as cryoconcentration. Aiming to promote greater speed and efficiency in the retention process of the bioactive components present in the leaves of *Morinda citrifolia*, two cryoconcentration methods were studied: the gravitational thaw and the microwave-assisted method. The execution of both cryoconcentration processes resulted in extract concentrates that were later used as a reaction medium for the synthesis of silver nanoparticles. The effect of the cryoconcentration steps on the physical and chemical characteristics of the concentrated fractions resulted in greater phenolic content and total solids, with higher efficiency in phenolic retention than their respective initial portions. The application of concentrated extracts in the biosynthesis of silver nanoparticles resulted in a polydisperse, stable material with even better properties when compared to biosynthesis via the use of non-concentrated extracts. We conclude that the use of both cryoconcentration systems allowed obtaining concentrated fractions with promising biological and nutritional value; indicating that the technique can also contribute as a reference to the use of sustainable technology in the generation of nanometals with improved properties.

Keywords: *Morinda citrifolia*. Bioactive compounds. Cryoconcentration. Biosynthesis of nanometals. Silver nanoparticles.

RESUMO EXPANDIDO

INTRODUÇÃO Atualmente, entende-se que a preferência do consumidor por alimentos é influenciada principalmente pelas informações nutricionais. Frutas e vegetais fornecem não apenas nutrientes essenciais à vida, mas também outros componentes biologicamente ativos para a promoção da saúde e prevenção de doenças. Uma estratégia inovadora envolvendo a possibilidade de aquisição de componentes bioativos, baseia-se no uso de todas as partes das plantas. Este estudo propõe uma alternativa de utilização de uma tecnologia limpa e de baixo custo para promover tal possibilidade, focando apenas em alimentos líquidos. Assim, a concentração de alimentos líquidos é considerada atualmente uma inovação na indústria de alimentos. O objetivo dessa técnica basicamente é remover a água e aumentar o teor de sólidos dos alimentos, prolongando a vida de prateleira e consequentemente promovendo estabilidade microbiana. Por outro lado, a nanotecnologia, um novo campo emergente e fascinante da ciência, permite pesquisas avançadas em muitas áreas, uma delas está centrada na busca por novas rotas de biossíntese nanometais com propriedades funcionais. As novas e sustentáveis metodologias sobre a ditada “nanotecnologia verde” foram recentemente desenvolvidas para a síntese de nanopartículas, das quais os estudos estão voltados na utilização de extratos vegetais como meio para produção de nanopartículas. Valendo-se do fato já exposto de que a biossíntese de nanometais por intermédio do uso de plantas envolve a participação direta de componentes fitoquímicos no mecanismo de bioprodução, e que a concentração de bioativos de líquido alimentares, sobretudo de origem vegetal, abrange o aumento do conteúdo de componentes bioquímicos desses alimentos. Temos em posse a possibilidade de obtenção de uma nova ferramenta dinâmica e inovadora que promova a compilação da técnica de concentração de ativos de líquidos alimentares de origem vegetal, e uso desses ativos na biossíntese de nanometais com propriedades funcionais.

OBJETIVOS O objetivo geral desta tese visou avaliar as técnicas de crioconcentração em blocos gravitacional (CCG) e crioconcentração assistida por micro-ondas (CCM) na separação e acúmulo de compostos bioativos do extrato aquoso de folhas de *Morinda citrifolia* e o uso das frações concentradas como meio de reação para biorredução posterior síntese de nanopartículas de prata (AgNPs), a fim de se

verificar se de fato, seria possível obter nanopartículas com propriedades físico-químicas aprimoradas, tais como menor tamanho e estabilidade em meio coloidal, baseado na hipótese de que o uso de extratos com maior deposição de bioativos via crioconcentração, permitiria a formação de AgNPs melhoradas.

METODOLOGIA O processamento das folhas de *M. citrifolia* incluiu uma etapa de branqueamento, secagem e trituração para posterior preparo do extrato por meio da infusão em água do material triturado em um sistema fechado com agitação contínua e temperatura controlada de 40 °C composto por 40 g de folhas suspensas em 1 L (4% (p / v)) de água ultrapura por 20 min. Após a extração, a solução foi submetida a filtração a vácuo com papel de filtro qualitativo para remoção dos sólidos em suspensão. A primeira parte da metodologia desta tese centrou-se no processo de crioconcentração, na qual foi executado por meio de dois métodos de degelo passivo em blocos ou etapas, onde os métodos foram designados como crioconcentração gravitacional (CCG) e crioconcentração assistida por micro-ondas (CCM). Entretanto, na CCM o descongelamento passivo ocorreu com o auxílio da técnica assistida por micro-ondas para promover uma maior velocidade e eficiência no processo de concentração dos componentes bioativos presentes nas folhas de *M. citrifolia*. As frações crioconcentradas em ambos os métodos prescritos foram então caracterizadas quanto ao teor de sólidos e fenólicos totais, viscosidade, identificação de grupamentos orgânicos funcionais por espectroscopia FTIR, por HPLC para a identificação e quantificação de compostos fenólicos, e a atividade biológica foi descrita por meio da determinação da atividade antioxidante e testes *in vitro* de biodisponibilidade gastrointestinal. A segunda parte da metodologia desta tese está centrada na utilização e comparação da amostra *in natura*, e dos extratos concentrados por CCG e CCM, na biossíntese de nanopartículas de prata. A biossíntese seguiu-se por meio da inserção do precursor metálico AgNO₃ no meio reacional contendo os extratos crioconcentrados por CCG e CCM, bem como também no extrato *in natura*. As AgNPs produzidas via uso dos extratos obtidos por CCG e CCM foram caracterizadas via determinação de tamanho de partícula, potencial zeta (ZP), espectroscopia UV-Vis, FTIR e por Absorção atômica com chama, EDS e ensaios de microscopia eletrônica. Por fim, o comportamento das AgNPs perante o tamanho de partícula e estabilidade via ZP foi mensurado a partir da variação dos parâmetros de biossíntese.

RESULTADOS OBTIDOS

Ambos os métodos CCG e CCM foram altamente efetivos na recuperação de sólidos e consequentemente de fenólicos totais, das quais foi possível obter extratos até 6 vezes mais concentrados quando comparados com o extrato *in natura*, culminando com uma eficiência do processo superior a 80% em ambos os métodos de crioconcentração executados. O comportamento da viscosidade das amostras foi significativo conforme as etapas de CCG e CCM progrediam, na qual o aumento da viscosidade foi um reflexo direto da maior deposição de sólidos no meio mais concentrado. Os ensaios em HPLC revelou a detecção de 10 diferentes tipos de compostos fenólicos nos extratos crioconcentrados, com um aumento superior a 12 e 7 vezes maior de fenólicos para as técnicas de CCG e CCM respectivamente. O composto catequina foi o fenólico identificado em maior quantidade nos extratos concentrados tanto por CCG, quanto por CCM. As etapas de ambos os métodos de crioconcentração tiveram efeito significativo no aumento da atividade antioxidante para os extratos mais concentrados bem como na manutenção da quantidade de sólidos totais após biodigestão *in vitro*. O uso dos extratos concentrados por CCG e CCM também proporcionaram um efeito relevante na biossíntese das AgNPs quando comparadas ao uso do extrato *in natura*. As AgNPs quando biossintetizadas utilizando os extratos crioconcentrados apresentaram menor tamanho médio de partícula bem como valores de ZP que refletiram em nanopartículas estáveis em meio coloidal. Os valores de pH entre 5 e 6 no decurso da biossíntese sugerem a ação efetiva de ácidos orgânicos no processo de biorredução do precursor metálico bem como no processo de estabilização das AgNPs. Os melhores valores de ZP foram obtidas em faixa de pH alcalina, sugerindo melhor dispersividade das nanopartículas, corroborado posteriormente via ensaios de microscopia eletrônica. A interferência da variação de diversos parâmetros de biossíntese no tamanho e estabilidade das AgNPs também foi estudada. Notou-se que tanto o aumento do precursor metálico quanto o volume do crioconcentrado causaram melhores resultados de estabilidade medida por ZP em função do pH. Notou-se que as melhores condições para menores valores de ZP, consequentemente melhor estabilidade, ocorreram em pH na faixa neutra. e alcalino. No entanto, maiores volumes de extrato concentrado não causaram redução no tamanho das AgNPs, sugerindo uma grande quantidade de substrato vegetal com pouco sal redutor metálico disponível. Notou-se também que a temperatura mais adequada para biossíntese de AgNPs permaneceu abaixo de 30°C, uma vez que o aumento da temperatura causou um aumento abrupto no tamanho das partículas, bem como maior instabilidade refletida em

valores de ZP próximos a 0 mV. Também foi possível verificar o comportamento das NPs frente ao tempo de armazenamento das AgNPs, a partir do qual foi possível obter partículas de nanop prata estáveis, com tamanho médio abaixo de 100 nm em até 30 dias. No geral, ambos os métodos de crioconcentração ofereceram um substrato valioso na promoção da biossíntese de AgNPs. Ambos os extratos concentrados foram altamente eficazes em termos de menor tamanho e estabilidade das AgNPs quando comparados à biossíntese envolvendo o extrato *in natura*. O fato de a biossíntese envolvendo o uso do extrato do CCG ter apresentado melhor desempenho do que o extrato do CCG, deve-se à deposição de compostos bioativos presentes no extrato após o CCG.

CONSIDERAÇÕES FINAIS

Levando em consideração que as folhas de *M. citrifolia* são comprovadamente detentoras de alta quantidade de compostos bioativos com propriedades fitoterápicas, o presente estudo comprovou que a aplicação de uma tecnologia não térmica, conhecida como crioconcentração, para a separação e concentração de compostos bioativos de *Morinda citrifolia* não somente foi altamente benéfica, como também abriu precedentes para exploração do produto obtido no amplo campo da nanobiotecnologia, tornando inédita a utilização da técnica na referida matéria-prima vegetal. Os resultados apresentados também sugerem que o presente estudo pode contribuir como referência na utilização de uma tecnologia barata e sustentável no reaproveitamento e tratamento de resíduos da indústria alimentícia, na geração de um produto promissor de alto valor biológico, visando potencializar a aquisição de bioativos, como compostos fenólicos; com ampla funcionalidade, bem como propriedades nutricionais e fitoterápicas aprimoradas.

PALAVRAS-CHAVE

Morinda citrifolia; Crioconcentração; Compostos Bioativos; Nanotecnologia; Nanopartículas de prata; Caracterização físico-química.

LIST OF FIGURES

Figure 1 - Basic schematic diagram of a freezing concentration industrial module.....	39
Figure 2 - Basic schematic illustration of the block cryoconcentration process.	41
Figure 3 - Schematic outline of some one-step systems of the cryoconcentration process. a) Microwave-assisted; b) Centrifugal freeze/Vacuum-assisted concentration and c) Progressive freeze concentration system. Illustrations a), b) and c) were adapted from Aider & Ounis (2012), Muñoz et al. (2019) and Orellana-Palma et al. (2017) respectively.....	43
Figure 4 - <i>Morinda citrifolia</i> leaves crushed before preparation of the extract.	51
Figure 5 - Illustrative representation of the gravitational cryoconcentration method....	53
Figure 6 - Illustrative representation of the CCM process.	54
Figure 7 - Schematic sketch of the experimental apparatus of the general flowchart for both methods of cryoconcentration.....	54
Figure 8 - TSC present in the concentrated and ice fractions for both methods of cryoconcentration used: a) CCG and b) CCM.....	62
Figure 9 - Behavior of the C_f for the TSC in the concentrated fractions in all concentration stages for both methods of cryoconcentration used.....	65
Figure 10 - Total phenolics content present in the concentrated and ice fractions for both methods of cryoconcentration used: a) CCG and b) CCM.....	67
Figure 11 - Efficiency in the accumulation of TPC in both methods of cryoconcentration used.....	69
Figure 12 - Behavior of the concentration factor for the TPC for both methods of cryoconcentration used.....	69
Figure 13 - Visual comparison and summary of the properties of TSC, TPC, concentration factor and percentage efficiency of the phenolic retention process between the extracts <i>in natura</i> and after the last stage of cryoconcentration for both the CCG and CCM methods employed.....	73
Figure 14 - FTIR spectroscopy for the concentrated fractions of both cryoconcentration methods used: a) gravitational and b) microwave-assisted.	75

Figure 15 - Apparent viscosity versus shear rate for each stage of both cryoconcentration methods used in the aqueous extract of <i>M. citrifolia</i> leaves: a) CCG and b) CCM.	79
Figure 16 - Chromatogram containing the identification of the main phenolic species present in the sample <i>in natura</i> and in the cryoconcentrated samples of the aqueous extracts of the leaves of <i>M. citrifolia</i> by CCG method. The wavelengths, the retention time and the identification of each compound are detailed in Table 10.	83
Figure 17 - Chromatogram containing the identification of the main phenolic species present in the sample <i>in natura</i> and in the cryoconcentrated samples of the aqueous extracts of the leaves of <i>M. citrifolia</i> by CCM method. The wavelengths, the retention time and the identification of each compound are detailed in Table 11.	85
Figure 18 - Antioxidant activity via the ORAC method verified in the concentrated extracts of leaves of <i>M. citrifolia</i> in each stage for both cryoconcentration methods used.	89
Figure 19 - Behavior of TPC in the <i>in vitro</i> simulation of gastrointestinal digestion for extracts of leaves of <i>M. citrifolia</i> cryoconcentrated in both studied methods. Note that the cryoconcentrated fractions (samples) evaluated were those corresponding to the last executed cryoconcentration stage (CC4). The analysis was performed comparing the concentrated samples with the fresh samples for each portion (region) of the simulated digestion.	91
Figure 20 - Behavior of antioxidant activity via ABTS method in the <i>in vitro</i> simulation of gastrointestinal digestion for extracts of leaves of <i>M. citrifolia</i> cryoconcentrated in both studied methods. Note that the cryoconcentrated fractions (samples) evaluated were those corresponding to the last executed cryoconcentration stage (CC4). The analysis was performed comparing the concentrated samples with the fresh samples for each portion (region) of the simulated digestion.	94
Figure 21 - Size comparisons where objects range in size from 1 meter to 1 picometer.	103
Figure 22 - Main methods of nanoparticles synthesis via biological and physicochemical approaches.	106
Figure 23 - Bottom-up mechanisms of nanoparticle synthesis (M^+ - Metal ion).	107

Figure 24 - Schematic representation of mechanism of synthesis of AgNPs.....	108
Figure 25 - Summary of process variables in the AgNPs Biosynthesis methodology from <i>M.citrifolia</i> extracts concentrated by the CCG and CCM method (CC4-CCG and CC4-CCM).	115
Figure 26 - AgNPs produced from extracts <i>in natura</i> and from concentrated extracts (CC4-CCG and CC4-CCM) of <i>M. citrifolia</i> leaves following Assays Protocol 1.	119
Figure 27 - UV-Vis spectra for the AgNPs produced from the <i>in natura</i> extract of <i>M. citrifolia</i> leaves. The change in color from brownish to almost black after 48h of biosynthesis is indicative of the effectiveness of the bioreduction from Ag ⁺ to Ag ⁰ ..	121
Figure 28 - UV-Vis spectra for the AgNPs produced from the CC4 extract via CCG method of <i>M. citrifolia</i> leaves. The change in color from brownish to almost black after 48h of biosynthesis is indicative of the effectiveness of the bioreduction from Ag ⁺ to Ag ⁰	122
Figure 29 - UV-Vis spectra for the AgNPs produced from the CC4 extract via CCM method of <i>M. citrifolia</i> leaves. The change in color from brownish to almost black after 48h of biosynthesis is indicative of the effectiveness of the bioreduction from Ag ⁺ to Ag ⁰	123
Figure 30 - Variation of zeta potential as a function of pH of AgNPs produced according to Assays Protocol 1 (<i>in natura</i> extracts and CCG and CCM method).....	125
Figure 31 - DLS assays for particle size detection from the cumulative and percentage distribution of AgNPs produced from the <i>M. citrifolia</i> leaves extract <i>in natura</i> and via extracts cryoconcentrated by the CCG and CCM methods.....	126
Figure 32 - Effect of AgNO ₃ concentration, on maximum absorbance wavelength (a) and b)) and ZP as a function of pH (c) and d)) on AgNPs.	127
Figure 33 - Percentage and cumulative distribution assays of AgNPs produced from extracts obtained by CCG and CCM with variation in the concentration of the metallic precursor.....	130
Figure 34 - Effect of volume of the cryoconcentrated extract, on maximum absorbance wavelength (a) and b)) and ZP as a function of pH (c) and d)) on AgNPs.	131

Figure 35 - Percentage and cumulative distribution assays of AgNPs produced from extracts obtained by CCG and CCM with variation in the volume of the cryoconcentrated.....	134
Figure 36 - Effect of treatment temperature variation, on maximum absorbance wavelength (a) and b)) and ZP as a function of pH (c) and d)) on AgNPs.....	135
Figure 37 - Percentage and cumulative distribution assays of AgNPs produced from extracts obtained by CCG and CCM with variation in the treatment temperature.....	137
Figure 38 - Effect of storage time variation of AgNPs, on maximum absorbance wavelength (a) and b)) and ZP as a function of pH (c) and d)) on AgNPs.....	138
Figure 39 - Percentage and cumulative distribution assays of AgNPs produced from extracts obtained by CCG and CCM with variation in the storage time of AgNPs.	141
Figure 40 - Comparison between the FTIR spectra of cryoconcentrated samples and AgNPs produced by the same sample: CC-CCG (a) and CC4-CCM (b).	144
Figure 41 - SEM-EDS micrograph of AgNPs related to the <i>in natura</i> extract of <i>M. citrifolia</i> leaves.	147
Figure 42 - SEM-EDS micrograph of AgNPs related to CC4-CCG extract from <i>M. citrifolia</i> leaves.	148
Figure 43 - SEM-EDS micrograph of AgNPs related to CC4-CCM extract from <i>M. citrifolia</i> leaves	149
Figure 44 - TEM micrographs of AgNPs biosynthesized using the <i>in natura</i> extract and the extracts concentrated by CCG and CCM from the leaves of <i>M. citrifolia</i>	150

LIST OF TABLES

Table 1 - Summary of the main bioactive compounds present in <i>M. citrifolia</i> leaves...	34
Table 2 - Summary of the application of different techniques of cryoconcentration in food liquids.....	44
Table 3 - TSC for the cryoconcentrated and ice fractions of the aqueous extract of <i>M. citrifolia</i> leaves in CCG and CCM used methods.	63
Table 4 - Concentration factor (C_f) for the total solids content for the cryoconcentrated and ice fractions of the aqueous extract of <i>M. citrifolia</i> leaves in both cryoconcentration methods used.	65
Table 5 - Total phenolics content for the cryoconcentrated and ice fractions of the aqueous extract of <i>M. citrifolia</i> leaves in both cryoconcentration methods used.....	68
Table 6 - FTIR spectra and their respective functional groups found in the samples of the aqueous extract of cryoconcentrated <i>M. citrifolia</i> leaves by the CCG method.	76
Table 7 - FTIR spectra and their respective functional groups found in the samples of the aqueous extract of cryoconcentrated <i>M. citrifolia</i> leaves by the microwave-assisted method.....	77
Table 8 - Rheological parameters obtained by adjusting the data to the Power Law model and adjusting data to the Newton model, for the aqueous extract of cryoconcentrated <i>M. citrifolia</i> leaves by the CCG method.....	80
Table 9 - Rheological parameters obtained by adjusting the data to the Power Law model and adjusting data to the Newton model, for the aqueous extract of cryoconcentrated <i>M. citrifolia</i> leaves by the CCM method.	81
Table 10 - Major phenolic compounds identified via HPLC-DAD-MS assays for <i>in natura</i> and cryoconcentrated samples by CCG method.....	84
Table 11 - Major phenolic compounds identified via HPLC-DAD-MS assays for <i>in natura</i> and cryoconcentrated samples by CCM method.	86
Table 12 - Summary of the results of the analysis of antioxidant activity via ABTS and DPPH methods for the cryoconcentrated and ice fractions in both cryoconcentration methods for the aqueous extract of <i>M. citrifolia</i> leaves.	88

Table 13 - Behavior of TPC and antioxidant activity via ABTS method during <i>in vitro</i> simulation of gastrointestinal digestion for CC4 samples extracts of leaves of <i>M. citrifolia</i> cryoconcentrated in both studied methods.....	92
Table 14 - Summary of some studies involving the biosynthesis of nanometals by <i>M. citrifolia</i>	109
Table 15 - Summary of process variables in the AgNPs Biosynthesis methodology from <i>M.citrifolia</i> extracts concentrated by the CCG and CCM method (CC4-CCG and CC4-CCM).....	114
Table 16 Average particle size, zeta potential and initial pH values for AgNPs for samples developed in Assays Protocol 1.....	125
Table 17 - Influence of metallic precursor concentration on size, zeta potential and UV-Vis spectrum of AgNPs produced by cryoconcentrated <i>M. citrifolia</i> extracts.....	128
Table 18 - Influence of volume of cryoconcentrated on size, zeta potential and UV-Vis spectrum of AgNPs produced by cryoconcentrated <i>M. citrifolia</i> extracts.	132
Table 19 - Influence of treatment temperature on size, zeta potential and UV-Vis spectrum of AgNPs produced by cryoconcentrated <i>M. citrifolia</i> extracts.	136
Table 20 - Influence of storage time on size, zeta potential and UV-Vis spectrum of AgNPs produced by cryoconcentrated <i>M. citrifolia</i> extracts.	139
Table 21 - Concentration of AgNPs determined by FAAS, produced through the use of cryoconcentrated extracts of <i>Morinda citrifolia</i> via CCG, CCM method and by extract <i>in natura</i>	145

LIST OF ABBREVIATIONS AND SYMBOLS

ABTS	2,2'-azino-bis (3-ethylbenzothiazoline-6-sulfonic acid)
AgNPs	Silver nanoparticles
CCG	Cryoconcentration, via gravitational method
CCM	Cryoconcentration via microwave-assisted method
CCn	Samples corresponding to the fractions concentrated in steps (n) 1, 2, 3, and 4 of the cryoconcentration process
C_f	Concentration factor
DLS	Dynamic Light Scattering
DPPH	2,2-Diphenyl-1-picrylhydrazyl
EDS	Energy-Dispersive x-ray Spectroscopy
FAAS	Flame Atomic Absorption Spectrometry
FC	Freezing Concentration
FTIR	Fourier-Transform Infrared Spectroscopy
Gn	Samples corresponding to the residual ice fractions referring to steps (n) 1, 2, 3, and 4 of the cryoconcentration process;
K	Consistency index
n	Rheological behavior index
ORAC	Oxygen Radical Absorbance Capacity
PFC	Progressive Freezing Concentration
SEM	Scanning Electron Microscopy
TEM	Transmission Electron Microscopy
TPC	Total Phenolics Content
TSC	Total Solids Content
ZP	Zeta Potential
η	Efficiency of the cryoconcentration process
μ	Absolute or dynamic viscosity

γ Shear rate

τ Shear stress

SUMMARY

PART I	27
1. INTRODUCTION.....	29
2. AIMS	31
2.1. General aim	31
2.2. Specific aims	31
3. LITERATURE REVIEW	32
3.1. What is noni?.....	32
3.2. Biochemical composition of <i>M. citrifolia</i>	33
3.3. Concentration of food liquids.....	38
3.4. Concentration of food liquids by cryoconcentration	40
3.5. State of the art considerations	50
4. MATERIALS AND METHODS.....	51
4.1. Raw material.....	51
4.2. Preparation of the extract	52
4.3. Cryoconcentration assays.....	52
4.3.1. Gravitational block cryoconcentration (CCG).....	52
4.3.2. Microwave-assisted cryoconcentration (CCM).....	53
4.4. Analysis of the physical-chemical properties of the concentrates.....	55
4.4.1. Quantification of total phenolic content (TPC)	55
4.4.2. Total solids content (TSC).....	55
4.4.3. FTIR spectroscopy assays	55
4.4.4. Rheological behavior of cryoconcentrated samples.....	56
4.4.5. Identification of phenolic compounds by HPLC	56
4.5. Evaluation of process parameters of cryoconcentration	57

4.6.	Biological properties of concentrates	58
4.6.1.	Antioxidant activity via ABTS method.....	58
4.6.2.	Antioxidant activity via DPPH method.....	58
4.6.3.	Antioxidant activity via ORAC method.....	59
4.6.4.	Simulation of in vitro gastrointestinal digestion of concentrates.....	59
4.7.	Statistical analysis.....	60
5.	RESULTS AND DISCUSSION	61
5.1.	Total solids content.....	61
5.2.	Total phenolics content	67
5.3.	FTIR Spectroscopy	74
5.4.	Rheological analysis of cryoconcentrate extracts.....	78
5.5.	HPLC-DAD-MS assays	81
5.6.	Biological activity of cryoconcentrate extracts	87
5.6.1.	Antioxidant activity via ABTS, DPPH and ORAC methods	87
5.6.2.	<i>In vitro</i> assays of simulation of gastrointestinal digestion	90
6.	CONCLUSIONS OF PART I.....	95
	PART II.....	97
1.	INTRODUCTION.....	99
2.	AIMS	102
2.1.	General aim	102
2.2.	Specific aims	102
3.	LITERATURE REVIEW	103
3.1.	Nanotechnology inspired by living organisms	103
3.2.	Nanotechnology and the principle of sustainable and green chemistry.....	104
3.2.1.	Biosynthesis of nanometals by plants	106
3.2.2.	Biosynthesis of nanometals by <i>Morinda citrifolia</i>	109

3.3. State of the art considerations	111
4. MATERIALS AND METHODS	112
4.1. Plant extract used in biosynthesis	112
4.2. Methodology for biosynthesis of AgNPs.....	112
4.3. Characterization of the silver nanoparticles	116
4.3.1. Dynamic light scattering	116
4.3.2. Zeta potential	116
4.3.3. UV-visible	116
4.3.4. Fourier transform infrared	117
4.3.5. Flame atomic absorption	117
4.3.6. Electron microscopy and energy-dispersive X-Ray.....	118
5. RESULTS AND DISCUSSION	119
5.1. Biosynthesis analysis	119
5.1.1. Standard conditions: Assays protocol 1	119
5.1.2. Influence of biosynthesis conditions on the size and stability of AgNPs	
127	
5.1.3. Considerations about the size and stability of AgNPs	142
5.2. Structure analysis of AgNPs.....	143
5.3. Microstructure analysis of AgNPs.....	146
6. CONCLUSIONS OF PART II.....	151
FINAL CONCLUSION	153
REFERENCES.....	155

PART I

Technologies for the concentration of bioactive components from aqueous extract of *M. citrifolia* (noni) leaves


Conceptual diagram of Part I

Why?

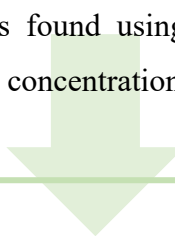
- It is known that large amounts of food are wasted every year as a result of processing. It is also known that a substantial part of the waste from the agri-food industries comes from the production of fruits and vegetables. Consequently, a strategy to reduce huge volumes of food waste involves using all parts of plants for human consumption.
- *Morinda citrifolia* is the scientific name of the vegetable, which is widely known by the commercial name of "Noni". One of the striking features of this plant is that noni leaves are also characterized by a large number of bioactive components with phytotherapeutics properties.
- In fact, due to the complexity of biochemical components present in the extract of noni leaves, cryoconcentration appears as a technology able to promote the removal of water and the increase of solids content, thus extending the shelf life of related food products.
- The study of the biochemical properties of the different structures that make up *Morinda citrifolia* is not widespread in Brazil. In addition, the processing of the Noni fruit results in a large generation of residues from which the leaves make up a large part. Such residues can be considered an excellent source for processes aimed at the concentration of biochemically active compounds.

What has already been done?


- Several studies have already been carried out involving the concentration of bioactive compounds from different plant sources. The method of cryoconcentration




applied to the separation of bioactive components from plant extracts is widely exposed in the literature. Some studies may be highlighted, such as those carried out by Adorno et al. (2017), Wu et al. (2017), and Orellana-Palma et al. (2017). All of the aforementioned authors reported promising results. However, after a search in several databases, no work was found using both membrane nanofiltration and cryoconcentration aiming at the concentration of phenolic compounds in *Morinda citrifolia* leaves.



Study hypotheses:

- Will the cryoconcentration method be efficient in the recovery of bioactive compounds from *M. citrifolia* leaves?
 - Will bioactive compounds maintain or increase their activity after the application of both concentration techniques?
 - How will the concentration affect the bioavailability of these compounds?
 - Will the product's antioxidant biological activity be maintained after concentration?
- 

Experimental methods:

- Physical-chemical characterization of the different fractions of the concentrates of the cryoconcentration techniques used.
 - Determination of the antioxidant activity of different fractions of cryoconcentrate.
 - Evaluation of the bioavailability of concentrated bioactive compounds using cryoconcentration.
- 

Responses

- Quantification of antioxidant activity and content of total phenolic compounds, as well as phenolic compounds in the fractions obtained by cryoconcentration.
- Determination of the bioavailability of concentrated phenolic compounds after the simulated digestion process.
- Evaluation of the viscosity parameters of the different fractions of the samples of the extract of leaves of cryoconcentrated *Morinda citrifolia*.

1. INTRODUCTION

According to the Food and Agriculture Organization of the United Nations (FAO), about 1.3 billion tons of food are likely to be wasted every year, where around 15% of the waste from the agri-food industries comes from the production and processing of fruit and vegetables (FAO, 2011). How to combine an emerging and sustainable technology that promotes the reduction of the waste previously mentioned? One strategy to reduce such alarming amounts of food waste involves the use of all parts of plants for human consumption. In this study, we will limit ourselves to proposing an alternative of using low-cost and clean technology to solve this problem, only focusing on food liquids.

Morinda citrifolia is the scientific name of the vegetable widely known by the commercial name of "noni". The processing of the noni fruit results in a remarkable generation of residues from which the leaves make up a large part (NELSON; ELEVITCH, 2006). Besides the use in tea preparation, noni leaves are also characterized by bioactive components with phytotherapeutic properties. It is proven that the solution elaborated with the leaf extract of noni presents a phytotherapeutic effect against various diseases such as cancer and obesity disorders, besides presenting antibacterial properties and antioxidant activity (ALMEIDA; DE OLIVEIRA; HOTZA, 2019). In fact, due to the complexity of biochemical components present in noni tea, technologies that promote the increase of solids content are valid for the aqueous leaf extract of noni (WU et al., 2017). Also, the production of aqueous extracts from industrial waste has been the subject of several studies, since these can be excellent sources of bioactive compounds (PRUDÊNCIO et al., 2012).

The concentration of liquid foods had led to innovation in the food industry (ORELLANA-PALMA et al., 2018), considering that the removal of water will increase the solids content of food, prolonging shelf-life and consequently promoting microbial stability. Seeking to reuse the nutritional value of the structural components of vegetables, which are generally rejected, the goal of this part of the study was to evaluate the potential of the gravitational and microwave-assisted cryoconcentration technique on the behavior of the physical, chemical, and biological properties of bioactive compounds present in extracts of *Morinda citrifolia* leaves (noni), quantitatively checking the presence and content of phenolics and solids total, viscosity, antioxidant activity and gastrointestinal bioavailability *in vitro*.

This method presents the advantage of being a one-step procedure, characterized by simple construction and operation of the equipment, where all liquid food is frozen, then thawed and the concentrated fraction is separated from the ice fraction by the gravitational method. The use of microwaves will have an auxiliary role, acting as an external force to promote a solid/liquid separation more quickly and efficiently (AIDER; DE HALLEUX; MELNIKOVA, 2009; ORELLANA-PALMA et al., 2017a). Besides, considering that *M. citrifolia* leaves have large amounts of bioactive compounds with phytotherapeutic properties, this work presents to the best of our knowledge the first application of cryoconcentration for the separation and accumulation of bioactive substances of this plant species. It is expected that the results of this study provide useful information on the application of cryoconcentration in the development of the nutritional and phytotherapeutic properties of *M. citrifolia* leaves.

This thesis will use methods that include clean, low-cost, and high-yield technologies, integrating the use of residues from the food industry with high biological value. The originality of this study is related to the comparison of two processes aimed at the concentration of bioactive components of a liquid leaf extract with a large accumulation of phytochemical species. According to the literature, there are no reports of the use of previously mentioned processes for this product.

2. AIMS

2.1. General aim

The general objective of this part of the study is to evaluate two processes of cryoconcentration for promoting the concentration of bioactive compounds present in the aqueous extract of noni leaves (*Morinda citrifolia*), as well as characterizing the process and the final fractions obtained.

2.2. Specific aims

The respective specific aims are:

- Analyze the concentration process of bioactive compounds of noni leaves by cryoconcentration.
- Evaluate the physical-chemical characteristics of the concentrated fractions obtained.
- Evaluate the *in vitro* bioavailability and antioxidant properties of the concentrated extract.

3. LITERATURE REVIEW ¹

3.1. What is noni?

Morinda citrifolia is the scientific name of the vegetable, which is widely known by the trade name “noni”. It is a perennial, fruitful plant, with an average size ranging from 10 to 20 meters in height and is originally from Southeast Asia (NELSON, 2001; SANG et al., 2001a). Noni plants belong to the family *Rubiaceae* (family of coffee) and the subfamily *Rubioideae* (LACHENMEIER et al., 2006), and are characterized by having large lanceolated leaves, their stem is straight and their fruits are oval and fleshy with a rigid and rough skin, measuring about 3 to 10 cm long and 3 to 6 cm wide (LIN et al., 2014; MOTSHAKERI; GHAZALI, 2015).

Noni fruits have a shade varying between green, yellow and white depending on their stage of ripeness, and can contain up to 260 seeds. The fruit is also known to have a very unpleasant sour odor when it is already in an advanced stage of ripeness (NELSON, 2005; LIN et al., 2014). Its popular name varies according to the place of cultivation, with names such as “Indian mulberry” or “nuna” in India (CHAN-BLANCO et al., 2006), “mengkudu” in Malaysia (CARRILLO-LÓPEZ; YAHIA, 2011) or “fruit of cheese” in Australia (ROSS, 2001). Its most popular name, noni, was introduced by Polynesian immigrants when they arrived in the territory where the island of Hawaii is today approximately 2000 years ago (WANG et al., 2002).

Different parts of the plant such as the root, stem, fruits, and leaves are traditionally used by various East Asian cultures for the treatment of numerous diseases such as arthritis, headaches, burns, and even disorders related to tuberculosis, diabetes, and hypertension (DIXON; MCMILLEN; ETKIN, 1999; CHAN-BLANCO et al., 2006; ALI; KENGANORA; MANJULA, 2016). As reported by Solomon (1999), scientific evidence on the therapeutic properties of Noni juice was quite limited. Currently, Dussosoy et al. (2014), found that Noni juice has antioxidant and anti-inflammatory properties, as well as Motshakeri & Ghazali (2015) stated that Noni juice is an important protagonist in the thriving market for functional drinks.

According to Deng; West and Jensen (2010), it is known that the commercialization of Noni components as herbal food and dietary supplement made it possible to increase

¹ Partially published in *Comprehensive Reviews in Food Science and Food Safety*, as “Properties and Applications of *Morinda citrifolia* (Noni): A Review”, <https://doi.org/10.1111/1541-4337>

its availability worldwide. Its use has brought benefits to more people, paving the way for countless products from Noni as well as the development and investigation of new research in several technological domains of medicine, pharmacy, food industry, biotechnology, and even in the scope of materials science, whatever considering the studies developed by Suman et al. (2014) and Sundrarajan et al. (2017) in the elaboration of metallic nanostructures from extracts of *Morinda citrifolia*.

3.2. Biochemical composition of *M. citrifolia*

Chemical and nutritional analyses found that *Morinda citrifolia* has a high nutritional value (SHALAN; MUSTAPHA; MOHAMED, 2017a). There are almost 200 phytochemical compounds with bioactive properties that have already been identified and isolated from different parts of the plant (INADA et al., 2017). It is important to note that the biochemical composition of these compounds differs completely not only depending on the structure of the plant, but also in relation to the place of origin and the harvest period (CHAN-BLANCO et al., 2006; DENG; WEST; JENSEN, 2010; ASSANGA et al., 2013).

Regarding the leaves of *M. citrifolia*, it is important to mention that the vast majority of bioactive compounds present in different regions of *Morinda citrifolia* have confirmed biological activity. In fact, as noni leaves will be our raw material for use in this study, Table 1 summarizes a list of the many biochemical components detected in noni leaves together with their respective identified biological properties.

Table 1 - Summary of the main bioactive compounds present in *M. citrifolia* leaves.

Biochemical classification	Bioactive compound	Amount	Biological activity	Reference
Aminoacids	Alanine	6% (w/w)	--	(DITTMAR, 1993; ELKINS, 1998)
	Arginine	7% (w/w)	--	(DITTMAR, 1993; ELKINS, 1998)
	Aspartic acid	10% (w/w)	--	(DITTMAR, 1993; ELKINS, 1998)
	Cysteine	1% (w/w)	--	(DITTMAR, 1993; ELKINS, 1998)
	Glutamic acid	1% (w/w)	--	(DITTMAR, 1993; ELKINS, 1998)
	Glycine	6% (w/w)	--	(DITTMAR, 1993; ELKINS, 1998; SINGH; SINGH, 2013)
	Histidine	3% (w/w)	--	(DITTMAR, 1993; ELKINS, 1998)
	Isoleucine	16 (w/w)	--	(DITTMAR, 1993; ELKINS, 1998)
	Lysine	16% (w/w)	--	(DITTMAR, 1993; ELKINS, 1998; SINGH; SINGH, 2013)
	Methionine	3% (w/w)	--	(DITTMAR, 1993; ELKINS, 1998; SINGH; SINGH, 2013)
	Phenylalanine	5% (w/w)	--	(DITTMAR, 1993; ELKINS, 1998; SINGH; SINGH, 2013)
Proline	5% (w/w)	--	(DITTMAR, 1993; ELKINS, 1998)	

-- Data not informed by the author.

Table 1 - Summary of the main bioactive compounds present in *M. citrifolia* leaves. (continued)

Biochemical classification	Bioactive compound	Amount	Biological activity	Reference
Amino acids	Serine	5% (w/w)	--	(DITTMAR, 1993; ELKINS, 1998)
	Tryptophan	1-3% (w/w)	--	(DITTMAR, 1993; ELKINS, 1998)
	Treonine	5% (w/w)	--	(DITTMAR, 1993; ELKINS, 1998)
	Tyrosine	2% (w/w)	--	(DITTMAR, 1993; ELKINS, 1998; SINGH; SINGH, 2013)
	Valine	8% (w/w)	--	(DITTMAR, 1993; ELKINS, 1998)
Anthraquinones	Damnacanthal	--	Antitumor and anticancer	(THANI et al., 2010)
Carotenoids	β -carotene	12.4 mg/100g	Cytotoxic, antioxidant and antiviral	(AALBERSBERG et al., 1993)
Coumarins	Scopoletin	--	Anticancer	(THANI et al., 2010)
Flavonoids	Rutin	7.93 mg/g		(DENG; WEST; JENSEN, 2008)
	Quercetin-3-O- β -D- glucopyranoside	--	Anti-inflammatory, antioxidant, anticancer	(SANG et al., 2001a)

-- Data not informed by the author.

Table 1 - Summary of the main bioactive compounds present in *M. citrifolia* leaves. (continued)

Biochemical classification	Bioactive compound	Amount	Biological activity	Reference
Flavonoids	Quercetin-3- <i>O</i> - α -L-rhamnopyranosyl-(1 \rightarrow 6)- β -D-glucopyranoside	--	Anti-inflammatory, antioxidant, anticancer	(SANG et al., 2001a)
	Quercetin-3- <i>O</i> - β -D-glucopyranosyl-(1 \rightarrow 2)-[α -L-rhamnopyranosyl-(1 \rightarrow 6)]- β -D-galacopyranoside	--	Anti-inflammatory, antioxidant, anticancer, antihistaminic	(SANG et al., 2001a)
Iridoids	Asperulosidic acid	--	Immunostimulant, hypotensive	(SANG et al., 2001a)
	Asperuloside	--	Anti-obesity	(DENG; WEST; JENSEN, 2008)
	Citrifolinoside A	--	Hypoglycemic	(SANG et al., 2001a)
Minerals	Calcium	5.462 mg/g	--	(PETER; PETER, 2018)

-- Data not informed by the author.

Table 1 - Summary of the main bioactive compounds present in *M. citrifolia* leaves. (continued)

Biochemical classification	Bioactive compound	Amount (mg/g)	Biological activity	Reference
Minerals	Cooper	0.00233	--	(PETER; PETER, 2018)
	Iron	0.00447	--	(PETER; PETER, 2018)
	Magnesium	0.57	--	(PETER; PETER, 2018)
	Potassium	1.219	--	(PETER; PETER, 2018)
Nucleoside	Cytidine	--	--	(SANG et al., 2002)
Saccharide	β -D-glucopyranose-penta-acetate	--	--	(SU et al., 2005)

3.3. Concentration of food liquids

The demand for new tools in the food industry that promotes the elevation and maintenance of the organoleptic characteristics of food is increasing, mainly due to the growing demand for differentiated products by consumers (SAFIEI et al., 2017). In order to meet this demand for new products, concentration techniques are gaining acceptance among the food processing industries. Concentration processes also contribute to reducing transportation, handling, and storage costs, since these costs are mainly linked to the product's mass (MUÑOZ et al., 2019).

Taking into account that food liquids such as fruit juices, milk, whey (*lactoserum*), tea or coffee extracts, are complex aqueous solutions in which water makes up the majority. It is known that water constitutes up to 95% of the composition of these foods (AIDER; DE HALLEUX; AKBACHE, 2007). In order to reduce storage costs, preserving the best quality of these food solutions, the idea of concentrating these solutions to reduce water activity and, thus, prevent microbial growth was validated in industrial processing (VAN BEEK; BUDDE; VAN ESCH, 2018).

Thus, there are the processes of concentration of food solutions, which basically is the process of removing a certain part of the water content of these solutions. Regardless of recent advances in separation science and process automation, liquid food concentration methods require careful selection and a thorough understanding of the biochemical transformations involved. An incorrect selection of the process conditions can cause harmful effects on the sensory and nutritional profile of the final product and/or impose high production costs. A wide range of fruit juice concentration methods, mainly based on thermal evaporation, lyophilization, membrane filtration/distillation, direct/reverse osmosis, or clathrate hydrate drying, have been developed and are frequently practiced (ADNAN; MUSHTAQ; ISLAM, 2018). In summary, the concentration of these food liquids can be carried out by three main methods: evaporation, reverse osmosis, and cryoconcentration (freeze concentration) (AIDER; DE HALLEUX; AKBACHE, 2007).

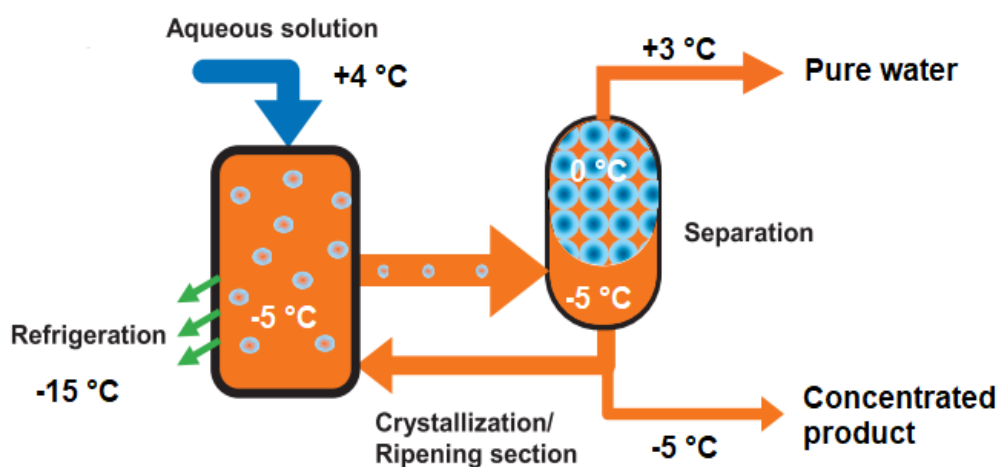
The evaporation concentration technique is considered one of the best consolidated processes in the acquisition of concentrated fractions of food liquids in the industry. However, considered a conventional method, the disadvantages of using this type of treatment to obtain a concentrate are summarized mainly in changes in the physical and

chemical properties of the product (such as soluble solids, pH, and color). In addition, high-temperature processes produce an important degradation of bioactive components, such as minerals, antioxidants, and vitamins (LEWICKI, 2006; AIDER; DE HALLEUX; AKBACHE, 2007; ORELLANA-PALMA et al., 2018).

Reverse osmosis as a technique for concentrating food liquids is based mainly on the selectivity of membranes (DOVA; PETROTOS; LAZARIDES, 2007). The effectiveness of this operation is dependent on the pressure applied compared to the osmotic pressure. It also depends on the intrinsic properties of the reverse osmosis membranes used (CONIDI; DRIOLI; CASSANO, 2018).

However, the limitations regarding the use of membranes are focused on the fouling phenomenon. This phenomenon is responsible for decreasing the efficiency of the separation process and requires periodic stops for cleaning the membrane. An alternative to removing water from a food solution is to freeze the water in ice crystals, with subsequent removal of water in the form of ice crystals. The positive aspects of the freezing concentration are the low temperature and absence of thermal stress, a closed system with no vapor space that prevents loss of volatile components, and absence of microbial activity that allows weeks of continuous operation without intermediate cleaning (VAN BEEK; BUDDE; VAN ESCH, 2018). Industrially, this principle is illustrated in Figure 1.

Figure 1 - Basic schematic diagram of a freezing concentration industrial module.



Adapted from Van Beek; Budde and Van Esch (2018).

3.4. Concentration of food liquids by cryoconcentration

Cryoconcentration is a technology widely used in the food industry to concentrate various liquid foods and to recover biological compounds sensitive to heat such as proteins, polyphenols, water-soluble vitamins, and aromatics. The cryoconcentration technology is very suitable in the food industry due to its ability to retain the nutritional quality and volatile aromatic compounds in the product. This feature is attributed to the low operating temperatures that are suitable to prevent the degradation of sensitive liquid food components (AIDER; DE HALLEUX, 2009).

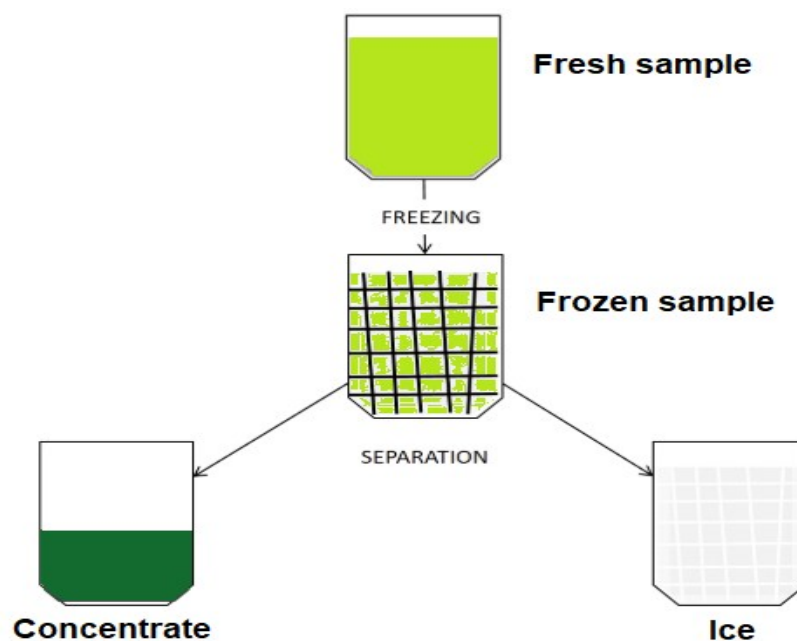
Theoretically, cryoconcentration should be more effective than evaporation for given water removal (latent melting heat: 0.33 kJ/g of water; latent evaporating heat: 2.26 kJ/g of water). However, investment in conventional freezing concentrators is more expensive when compared to the purchase of evaporators. The high operating costs are mainly due to the loss of juice that accompanies the formation of ice crystals and the difficulty of removing the ice crystals without losing the food solids. Furthermore, the degree of concentration achieved is less than by evaporation. Therefore, the priority of freezing concentration over evaporation is explained by the quality of the concentrated products: the freezing concentration is known to be the best among the concentration methods, giving greater retention in flavors and thermally fragile compounds (AIDER; DE HALLEUX, 2008; PETZOLD et al., 2015; ORELLANA-PALMA; GONZÁLEZ; PETZOLD, 2019).

Although the industrial process of cryoconcentration appears to be complex due to the need for a structural framework. Other methods that prioritize equipment minimization and ease of operation have gained ground. Some techniques such as suspension crystallization and eutectic cryoconcentration are described in the literature (AIDER; DE HALLEUX, 2009). However, it is aware that the industrial future of cryoconcentration has been linked to developments in the configuration of one-step systems (block freeze concentration or progressive freeze concentration) than conventional freeze concentration systems (suspension crystallization), due to the separation step is simpler (PETZOLD et al., 2016).

An advantage of these one-step systems is their simplicity in terms of construction and operation of the equipment. In block cryoconcentration, for example, all liquid food

is frozen (ice block), then thawed and the concentrated fraction is separated from the ice fraction by the gravitational method. The process consists of three steps that are freezing, thawing, and separation. Under these conditions, control of the thawing process is critical to achieving efficiency of close to 90% (ORELLANA-PALMA et al., 2017a). However, to increase the efficiency of the cryoconcentration process in blocks, assisted techniques or the so-called external forces, such as ultrasound, centrifugation, microwave or vacuum can be coupled to the process (AIDER; DE HALLEUX; MELNIKOVA, 2008; PETZOLD; AGUILERA, 2013; ORELLANA-PALMA et al., 2017b, 2017a). A basic schematic illustration of the block cryoconcentration process is shown in Figure 2.

Figure 2 - Basic schematic illustration of the block cryoconcentration process.



From the author.

The progressive freezing concentration (PFC) is based on a similar concept, because a large mass of ice is formed and grown on the cooling surface, so that separation from the other solution is relatively easy (DEMIRBAS et al., 2018). The main difference between the PFC process and other freezing concentration systems is related to the growth of ice crystals. The PFC system produces ice crystals layer by layer on a cooled surface to form a single, substantial block of crystal. As there is only one block of ice

crystal, the separation between the ice crystal and the concentrated solution occurs quickly, resulting in a low operating cost. In a vertical PFC system, for example, the solution is poured into a stirred cylindrical tank equipped with a cooling jacket. The ice layer grows on the cooling wall and mechanical agitation can be used to reduce the solute's occlusion in the ice (PETZOLD; AGUILERA, 2013; MUÑOZ et al., 2019)

Assisted techniques that promote improvement in processing efficiency in one-stage cryoconcentration configurations are important to achieve commercial viability. The alternatives of assisted techniques applied to block freeze concentration are external forces such as centrifugation or vacuum. The centrifugation technique was proposed by Bonilla-Zavaleta; Vernon-Carter and Beristain (2006), to promote the cryoconcentration of pineapple juice. Luo; Chen and Han (2010) managed to obtain high-purity ice crystals during the cryoconcentration of brackish water. Petzold & Aguilera (2013) recovered high values of solute, reaching approximately 0.73 kg of sucrose obtained by 1 kg of sucrose in a block cryoconcentration process by centrifugation. More recently, Orellana-Palma; González, and Petzold (2019) proposed this same cryoconcentration technique in obtaining orange juice concentrate.

The vacuum cryoconcentration process (suction by a pump) was proposed by Petzold et al. (2016) in obtaining concentrated fractions of wine. Petzold; Niranjani; Aguilera (2013) applying a vacuum (80 kPa) promoted an improvement in atmospheric conditions in the process of cryoconcentration of sucrose solutions. Moreno et al. (2013) found that vacuum separation treatments (27 kPa) were the ones that obtained the highest concentration factor, due to the positive effect of the pressure difference on the movement of the concentrated liquid fraction during the cryoconcentration process of coffee blocks. Figure 3 presents a schematic outline of some one-step systems of the cryoconcentration process.

As already well demonstrated, the cryoconcentration process using the configuration of a one-step system is widespread, encompassing different types of food products. In order to present a small outline of this variety of applications, Table 2 summarizes some studies addressing different cryoconcentration techniques in obtaining different food concentrates.

Figure 3 - Schematic outline of some one-step systems of the cryoconcentration process. a) Microwave-assisted; b) Centrifugal freeze/Vacuum-assisted concentration and c) Progressive freeze concentration system. Illustrations a), b) and c) were adapted from Aider & Ounis (2012), Muñoz et al. (2019) and Orellana-Palma et al. (2017) respectively.

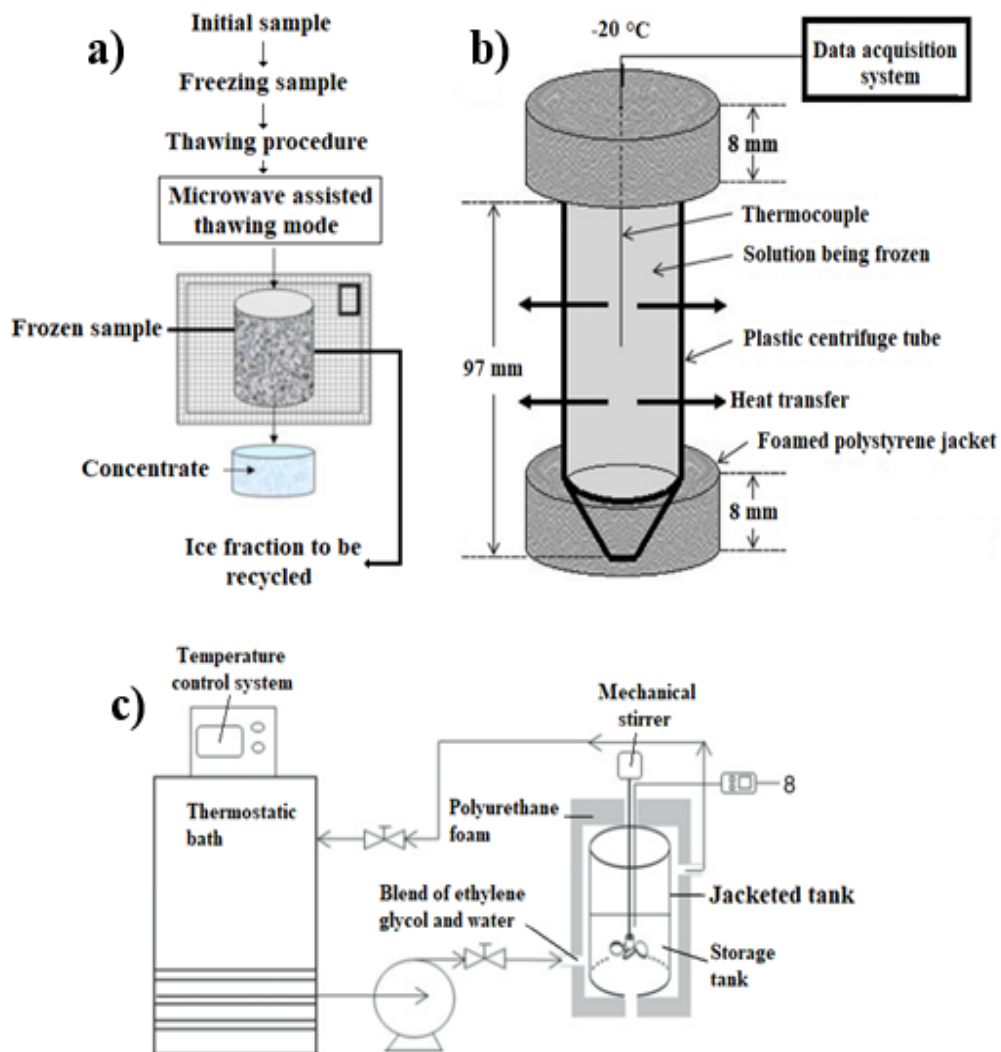


Table 2 - Summary of the application of different techniques of cryoconcentration in food liquids.

Cryoconcentration method	Food solution used	Characterization of the concentrate	Result obtained	Reference
Gravitational block cryoconcentration	Banana juice	Total polyphenolics content; Reducing sugars; Minerals composition and Volatile compounds composition	The concentrations of polyphenols and minerals were threefold more than the banana juice without concentrate.	(ESCALANTE-MINAKATA et al., 2013)
	Red cabbage (<i>Brassica oleracea</i> var. capitata, f, rubra)	Total anthocyanin content; Total polyphenol content; Antioxidant activity and Electrochemistry analysis	Cryoconcentration increased anthocyanin activity and total phenol content approximately 10 times compared with common extraction techniques.	(DEMIRBAS et al., 2018)
	Skim Milk Whey	Total Dry Matter; Lactose Content; Characterization and Total Proteins	Results showed that the fat matter is an important factor for protein and lactose distribution between the concentrated and the ice fractions.	(AIDER; DE HALLEUX; MELNIKOVA, 2009)
	Whey	Total dry matter content; Total proteins and Lactose content	It was possible to concentrate the whey up to 35% of dry matter after four levels. Total proteins were concentrated up to 20% of the total dry matter.	(AIDER; DE HALLEUX; AKBACHE, 2007)

Table 2 - Summary of the application of different techniques of cryoconcentration in food liquids. (continued)

Cryoconcentration method	Food solution used	Characterization of the concentrate	Result obtained	Reference
Gravitational block cryoconcentration	Strawberry juice	Total solids content; Colour intensity; Phenolic compounds; HPLC-DAD analyses of anthocyanins and Antioxidant activity	An increase in the values of phenolic content was observed in the concentrate fraction for all the freeze concentration stages	(ADORNO et al., 2017)
	Skim milk	Total dry matter; Concentration factor and process efficiency; Total proteins and Ash and mineral fraction analysis	Process efficiency to cryoconcentrated skim milk in up to $43.72 \pm 0.69\%$ (w/w) total dry matter after four cryoconcentration cycles. The total protein fraction was concentrated up to $22.49 \pm 0.31\%$ (w/w).	(AIDER; OUNIS, 2012)
Gravitational and microwave-assisted	Milk whey	Total dry matter; Total proteins and Lactose content	Microwave-assisted thawing mode was an efficient procedure and was faster than gravitational mode. Whey concentrates with $37.72 \pm 0.69\%$ of total dry matter was obtained. Proteins were concentrated up to $6.49 \pm 0.31\%$ (w/v).	(AIDER; DE HALLEUX; MELNIKOVA, 2008)

Table 2 - Summary of the application of different techniques of cryoconcentration in food liquids. (continued)

Cryoconcentration method	Food solution used	Characterization of the concentrate	Result obtained	Reference
Gravitational and microwave-assisted	Fresh maple sap	Degree Brix measurement; Process efficiency; Electrical conductivity and Light transmittance analysis	High concentration levels were achieved at four cryoconcentration stages.	(AIDER; DE HALLEUX, 2008)
	Blueberry and pineapple juices	Percentage of concentrate; Efficiency of concentration and Recovered solute	Performed well after the third cycle, reaching an increase of approximately 2.5 times the initial concentrations of solids.	(PETZOLD et al., 2015)
Falling-film freeze concentration	Feijoa (<i>Acca sellowiana b.</i>) pulp powder	Product yield; Water activity; Hygroscopicity; Color and Solubility	Freeze concentration was an effective technology to make the spray drying process of feijoa pulp feasible, avoiding adherence of the product on the dryer walls, increasing the fruit content in the final product, and reducing the maltodextrin content.	(HENAO-ARDILA; QUINTANILLA-CARVAJAL; MORENO, 2019)
	Coffee extract	Quantification of bioactive compounds; Antioxidant activity and Total phenolic compounds	The process effectively removes water from the aqueous coffee extract. Specifically, this technique increased the solids content of coffee 2.1 times in 2 process steps.	(CORREA; RUIZ; MORENO, 2018)

Table 2 - Summary of the application of different techniques of cryoconcentration in food liquids. (continued)

Cryoconcentration method	Food solution used	Characterization of the concentrate	Result obtained	Reference
Centrifugation-assisted block freeze concentration	Blueberry juice	Concentration of solids; Color; Total polyphenol content and Flavonoid and non-flavonoid content by HPLC;	Centrifugal cryoconcentration of blueberry juice was effective in obtaining a cryoconcentrate with high retention of polyphenol monomers, as well as notable values in terms of solutes, color and process parameters.	(ORELLANA-PALMA et al., 2017a)
	Aqueous solutions of sucrose	Percentage of concentrate; Efficiency of concentration and Recovered solute	High values of solute had recovered, reaching approximately 0.73 kg of sucrose obtained per 1 kg of initial sucrose at 1600 RCF of centrifugation speed, independent of initial concentration of sucrose and freezing procedure.	(PETZOLD; AGUILERA, 2013)
	Orange juice	Efficiency of concentration; Solid concentration and Percentage of concentrate	The solutes in the concentrated samples increased progressively six times after three cycles compared to the initial concentration of solids.	(ORELLANA-PALMA; GONZÁLEZ; PETZOLD, 2019)

Table 2 - Summary of the application of different techniques of cryoconcentration in food liquids. (continued)

Cryoconcentration method	Food solution used	Characterization of the concentrate	Result obtained	Reference
Centrifugation-assisted block freeze concentration	Apple juice	Total phenolic content; Total flavonoid content; Individual phenolic compounds; Antioxidant activity and Color	The levels of phenolics increased significantly with each freeze concentration cycle that was performed.	(ZIELINSKI et al., 2019)
	Grape juice	Total Phenolic Content and Effective Partition Constant	The results suggest that PFC may contribute a great potential in concentrating grape juice, therefore could contribute to the economy of the juice industry.	(SAFIEI et al., 2017)
Progressive freeze concentration	Skim milk	Solids concentration; Concentrated yield and Average ice growth rate	The progressive freeze concentration technique showed promise as an alternative for the dairy industry since it makes the development of new dairy products possible.	(MUÑOZ et al., 2019)
Vacuum-assisted block freeze concentration	Wine	Total polyphenol content; Color; Percentage of concentrate and Solute yield	By applying vacuum (40 kPa), the solids content in the concentrated fraction increased significantly compared to the initial value (8°Brix).	(PETZOLD et al., 2016)

Table 2 - Summary of the application of different techniques of cryoconcentration in food liquids. (continued)

Cryoconcentration method	Food solution used	Characterization of the concentrate	Result obtained	Reference
Vacuum-assisted block freeze concentration	Blueberry juice	Concentration of solids; Color; Total polyphenol content; Percentage of concentrate and Efficiency	Results showed a significant solute increase in the concentrated fraction in all treatments.	(ORELLANA-PALMA et al., 2017b)
	Orange juice	Percentage of concentrate; Efficiency of concentration; Color and Ascorbic acid content	The block freeze concentration assisted by vacuum allows producing an orange juice concentrate with excellent physicochemical properties.	(ORELLANA-PALMA et al., 2018)

3.5. State of the art considerations

The use of technologies aimed at the purpose of retaining and concentrating biochemically active components in food liquids is widespread in the literature and in the food processing industry. However, it is noteworthy that there is a trend towards the execution and elaboration of methods that allow lower energy consumption and waste production. Thus, one-step techniques linked to the cryoconcentration process provide less expensive tests and easy operation.

As already described, *M. citrifolia* leaves are the result of discarding fruit processing, this part of study seeks to support the insertion of two different techniques of cryoconcentration aimed at the process of retention and concentration of bioactive components of *M. citrifolia* leaves and to characterize the product obtained.

4. MATERIALS AND METHODS

4.1. Raw material

The main raw material was obtained from different *Morinda citrifolia* trees, kindly provided by farmers in the city of Pombal, state of Paraíba, Brazil. The leaves of the species mentioned were pruned randomly belonging to the same crop lot, thus aiming at standardizing the composition of the material. The species was identified at the collection site by the producers and later confirmed by a botanist. *Morinda citrifolia* is an authenticated plant as per the International Plant Names Index (IPNI Life Sciences Identifier (LSID)).²

After collecting the material, the leaves were washed running and immersed in a solution with chlorinated water (200 ppm) for 15 min and rinsed with running water. The end of the treatment of the raw material occurred with the process of bleaching the sheets, as described by Xavier, Machado, & Costa (2014), followed by drying the material at 45 °C for a period not exceeding 24 hours. Finally, the noni sheets were then ground in a Wiley mill (Tecnal, TE-605/1), packed in polyethylene bags, and stored at -24 °C until extract preparation. The crushed leaves are shown in Figure 4.

Figure 4 - *Morinda citrifolia* leaves crushed before preparation of the extract.



From the author.

² <http://www.theplantlist.org/tpl1.1/record/kew-129789>

4.2. Preparation of the extract

The preparation of *M. citrifolia* leaf extract followed the methodology proposed by Shalan, Mustapha, & Mohamed (2017), with few modifications. Briefly, the tests were conducted in a closed system with continuous agitation and a controlled temperature of 40 °C, where 40 g of leaves were suspended (4% w/v) in 1 L of ultrapure water for 20 min. After extraction, the solution was subjected to vacuum filtration with a qualitative filter paper to remove suspended solids. After filtration, the material was cooled (~4 °C) for 30 min, with the subsequent start of the cryoconcentration process.

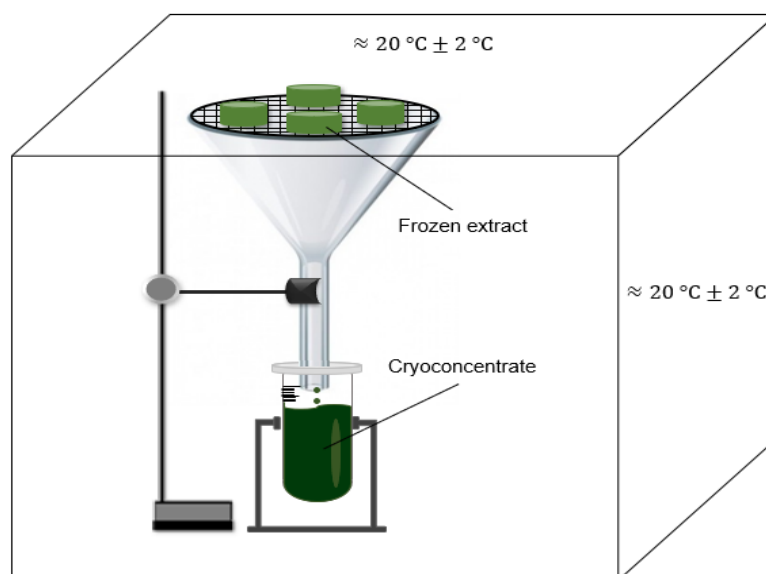
4.3. Cryoconcentration assays

4.3.1. Gravitational block cryoconcentration (CCG)

The process of cryoconcentration of the leaves of *Morinda citrifolia* followed the protocol described by Adorno et al. (2017) and Aider & Ounis (2012) with minor modifications. An initial feed volume of 2000 mL of the aqueous extract of the leaves of *M. citrifolia* was divided into containers with 200 mL each.

The samples were frozen by chilled air until the temperature was reduced to -20 ± 2 °C. After freezing the extract in small blocks, the defrosting mode was used to separate the entire frozen block into two phases: the concentrated fraction and the fraction of residual ice. Cryoconcentration was performed by passive thawing (gravitational method of thawing) of the frozen extract blocks during which the initial solution containing the frozen extract of *M. citrifolia* leaves was left at 20 ± 2 °C. The thawing for the formation of the concentrated samples was divided into four steps or cycles. In each cycle, 50% of the frozen volume was thawed. The volume thawed during the first cryopreservation cycle was again frozen and used as feed solution for the second cryopreservation cycle. This procedure was repeated in the third and fourth cryoconcentration cycles, resulting in four volumes of concentrates: CC1 to CC4 and four volumes of residual ice. At each cryoconcentration cycle, 50 mL of the concentrated sample was collected and frozen again at -24 °C for further analyses. In this study, the Gravitational block cryoconcentration method will be designated by the abbreviation CCG. A general outline for the gravitational cryoconcentration is illustrated in Figure 5.

Figure 5 - Illustrative representation of the gravitational cryoconcentration method.



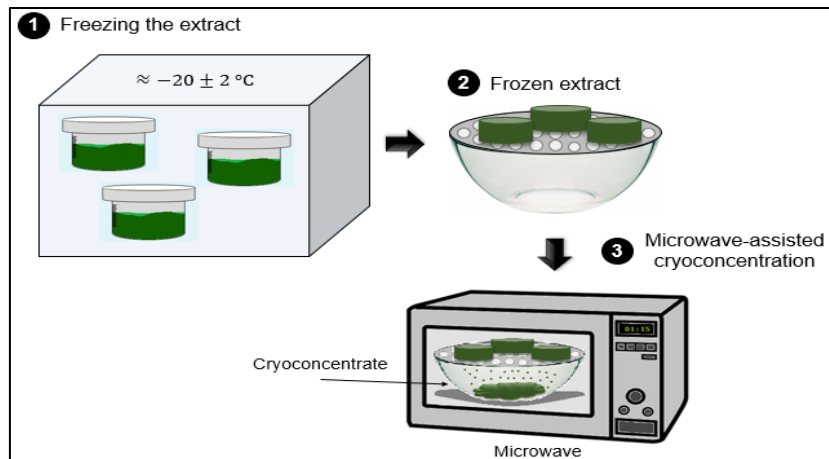
From the author.

4.3.2. Microwave-assisted cryoconcentration (CCM)

The microwave-assisted cryoconcentration (CCM) method is very similar to the CCG method. The CCM assays were based on studies developed by Adorno et al. (2017); Aider & Ounis (2012) with few modifications. As in the CCG method, the same initial volume of 2000 mL of the aqueous extract of the leaves of *M. citrifolia* was divided into containers containing 200 mL of extract volume in each. In this method, the passive thawing followed with the aid of the microwave-assisted technique to promote a greater speed and efficiency in the process of concentration of the bioactive components present in the noni leaves. In the microwave-assisted defrosting of portions of the frozen extract, the frozen initial solution was kept under controlled temperature of $20 \pm 2\text{ }^{\circ}\text{C}$. The melting for the formation of the concentrated samples was divided into four steps or cycles; in each cycle, 50% of the volume of the frozen samples was thawed. The volume thawed during the first cryopreservation cycle was again frozen and used as feed solution for the second cycle. This procedure was repeated in the third and fourth cycles, resulting in four cryoconcentrated volumes: CC1, CC2, CC3 and CC4; and four volumes of residual ice. A general outline for the microwave-assisted cryoconcentration is illustrated in Figure 6, which presents a schematic sketch of the experimental apparatus of the general flowchart for both methods of freezing and

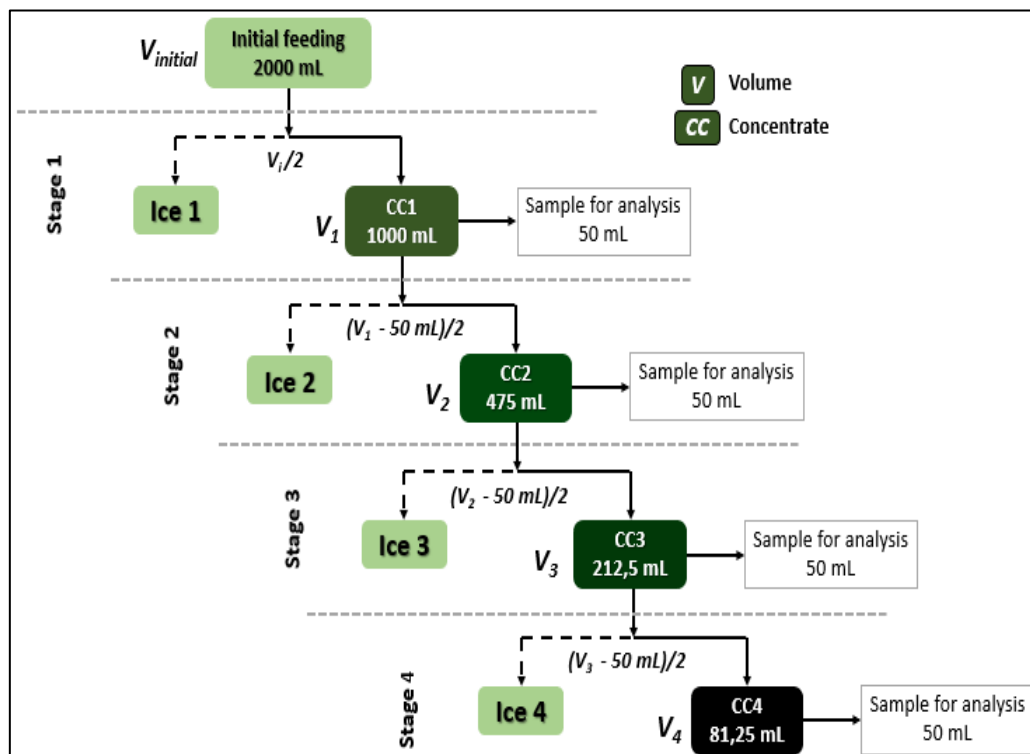
separating the fractions in stages (blocks) for both methods of cryoconcentration (CCG and CC method).

Figure 6 - Illustrative representation of the CCM process.



From the author.

Figure 7 - Schematic sketch of the experimental apparatus of the general flowchart for both methods of cryoconcentration.



From the author.

4.4. Analysis of the physical-chemical properties of the concentrates

4.4.1. Quantification of total phenolic content (TPC)

The determination of the content of total phenolic compounds present in the cryoconcentrated fractions and the fractions of ice for each stage of the cryoconcentration process was carried out following the methodology presented by Singleton; Rossi (1965), described by Martin-Diana et al. (2017), via colorimetric scanning of Folin-Ciocalteu. The method consists of the reaction of 100 μL of the sample, 7 mL of ultrapure water, 0.5 mL of Folin-Ciocalteu, and 1.5 mL of 20% (w/v) sodium carbonate solution. The mixture was kept in the dark at room temperature (24 °C) for 120 min. The absorbance was determined with wavelength adjustment at 765 nm in a spectrophotometer (UV-Vis mini-1240 Tokyo, Japan) using ultrapure water as white. The same procedure was used to construct the analytical curve, elaborated from solutions of gallic acid in the range of 200-800 $\text{mg}\cdot\text{mL}^{-1}$ and the results expressed as milligram equivalent to gallic acid per milliliters of extract ($\text{mgGAE}\cdot\text{mL}^{-1}$).

4.4.2. Total solids content (TSC)

All samples concerning the cryoconcentrated fractions and the ice fractions of the extract of leaves of *M. citrifolia* were analyzed for the TSC. The method is described by AOAC (2010), and is determined by the mass loss measure after drying the samples at 105 °C for 24 h and expressed as dry matter/total mass content ($\text{g}\cdot 100\text{ g}^{-1}$).

4.4.3. FTIR spectroscopy assays

FTIR measurements were performed (Shimadzu, IR Prestige-21, 8400S) in the diffuse reflectance mode, operating at a resolution of 4 cm^{-1} with a scanning range of 400-4000 cm^{-1} in potassium bromide (KBr). Samples for the cryoconcentrated and ice fractions for each step of the process were centrifuged at ~ 10.000 rpm for 12 min. The supernatant was discarded, and the pellet was again dispersed in ultrapure water to remove any non-absorbed biological molecules, then the sample was oven-dried and then subjected to FTIR analysis.

The proposed FTIR spectroscopy in this study is based on the possible identification of functional groups and binders present in the cryoconcentrated samples of the leaves

of *M. citrifolia*. These results would show evidence of the presence of the bioactive components characteristic of *Morinda citrifolia* leaves.

4.4.4. Rheological behavior of cryoconcentrated samples

The rheological measurements of the cryoconcentration steps of the initial and concentrated volume samples of the *M. citrifolia* leaves extract were conducted on a Thermo Haake DC 10 rotational viscometer (model VT 550, Thermo Haake, Karlsruhe, Germany) with concentric cylinders (NV ST 807-0713 CE and NV 807-0702). Data were collected through Pro Rheowin® software (version 2.93). The rheological analyses were obtained with a variation of the deformation rate of 200 to 1800 s⁻¹ (ascending curve) and 1800 to 200 s⁻¹ (descending curve), with a time of 3 min duration for each curve. The measurements were made at 25 ± 0.1 °C by circulating the water in a temperature-controlled thermostatic bath and coupled to the equipment (Phoenix P1, Thermo Haake, Karlsruhe, Germany). The analyses were performed in duplicate, and in each measurement a new sample was used. The rheological behavior was described by Newton's model, Equation (1), and power law, Equation (2), as follows:

$$\tau = \mu\gamma \quad (1)$$

$$\tau = K\gamma^n \quad (2)$$

where τ is the shear stress (N.m² or Pa); μ the absolute or dynamic viscosity (Pa.s) and γ the shear rate (s⁻¹); K the consistency index (Pa.sⁿ); and n the behavior index (dimensionless). The tests of the rheological behavior of the cryoconcentrated samples were carried out at the Ceramic & Composite Materials Laboratory (CERMAT/UFSC).

4.4.5. Identification of phenolic compounds by HPLC

The detection analyses of the major phenolic compounds present on *Morinda citrifolia* leaves extracts concentrated by NF and cryoconcentrated extracts by CCG and CCM methods were performed using high-performance liquid chromatography (HPLC-

DAD-MS) (Shimadzu, Kyoto, Japan). The HPLC-DAD-MS assay followed the methodology described by Pilatti-Riccio et al. (2019). The equipment consisted of a binary pump, an automatic injector, and a diode array detector with a coupled mass spectrometer containing an electrospray ionization source and a quadrupole analyzer (LCMS-2020, Shimadzu, Kyoto, Japan).

The identification of the phenolic compounds was carried out by comparing the retention times and absorption spectra of the peaks of the *Morinda citrifolia* leaves cryoconcentrated extracts samples with those of standard compounds. Quantitative analysis was performed through standard calibration curves using the diode array detector (SPD-20A/20AV, Shimadzu, Kyoto, Japan) adjusted in the wavelengths for the compounds: gallic acid; vanillic acid; catechin; epicatechin; caffeic acid; p-coumaric acid; quercetin; ferulic acid; trans-resveratrol and myricetin. The method was validated for the parameters of the linear band (analytical curve of 7 points, in random triplicates), limits of quantification and detection (with 3 and 6 times the height of the signal noise, respectively), and precision in three levels (limit of intermediate point, quantification, and maximum point of the analytical curve), with n=3 for each level. Analysis of variance (ANOVA) was used to validate the data presented by the analytical curve models.

4.5. Evaluation of process parameters of cryoconcentration

The concentration factor for each concentrated fraction and ice at different stages of cryoconcentration was calculated according to Aider et al. (2008). The concentration factor (C_f) was calculated as a function of the increase of the total solids content in each step of the process (TS_i) in relation to the total solids content in the initial extract (TS_0). The concentration factor is calculated by the Equation (3):

$$C_f = \frac{TS_i}{TS_0} \quad (3)$$

where TS_i is the total solids content for each cryoconcentration stage ($i = 1, 2, 3$ and 4^{th} stage) (mg.L^{-1}); and TS_0 is the total solids content in the initial extract (mg.L^{-1}).

The efficiency of the cryoconcentration process was defined as increasing the content of the phenolic compounds for each step of the process relative to the residual phenolic content present in each fraction of ice for each stage of the process. Theoretically, the lower the content of phenolic compounds present in each fraction of ice, the higher the concentration of the concentrated solution in its respective cryopreservation step. The efficiency of the process η (%) was calculated by the Equation (4):

$$\eta(\%) = \frac{P_i - P_f}{P_i} \cdot 100 \quad (4)$$

where P_i is the amount of total phenolic compounds (mgGAE.mL⁻¹) present in the cryoconcentration solutions for each stage of the process; and P_f is the content of phenolic compounds (mgGAE.mL⁻¹) present in the corresponding fraction of ice.

4.6. Biological properties of concentrates

4.6.1. Antioxidant activity via ABTS method

The ABTS free radical scavenger activity was determined according to the ABTS^{•+} (2,2'-azino-bis (3-ethylbenzothiazoline-6-sulfonic acid) method described by Martin-Diana et al. (2017). In summary, absorbances were measured 6 min after addition of the sample and the spectrophotometer reading (UV-Vis mini-1240 spectrometer Tokyo, Japan) was performed at the wavelength of 30 μ L of the diluted sample, each sample was reacted as 3 mL of ABTS radical solution. The same assay was used to construct the analytical curve, using solutions of gallic acid solutions in the range of 200-800 mg mL⁻¹. The results were expressed in milligrams equivalent to gallic acid by milliliter of extract (mgGAE ml⁻¹). All readings were performed in duplicate.

4.6.2. Antioxidant activity via DPPH method

Also known as 2,2-Diphenyl-1-picrylhydrazyl, the method of evaluating the antioxidant potential via DPPH assay was first established by Brand-Williams;

Cuvelier, and Berset (1995) and performed as described by Martin-Diana et al. (2017) and Adorno et al. (2017) with few modifications.

The method consists of reacting 100 μL of each sample with 3.9 mL of DPPH (2,2-Diphenyl-1-picrylhydrazyl) methanolic solution (60 μM). After 30 min of reaction, absorbances were measured at a 515 nm wavelength spectrophotometer (UV-Vis mini-1240 spectrometer Tokyo, Japan) using methanol as white. The same procedure was used to construct the analytical curve, using solutions of gallic acid solutions in the range 200-800 mg mL^{-1} , and the results were expressed in milligrams equivalent to gallic acid per milliliter of extract (mgGAE mL mL^{-1}). All readings were performed in duplicate.

4.6.3. Antioxidant activity via ORAC method

Also known as Oxygen Radical Absorbance Capacity, the ORAC method performed in this study is based on the exposition by Mazzucotelli et al. (2018) with few modifications.

A reaction mixture was prepared by mixing 25 μL of the sample under analysis with 150 μL of 10 nM fluorescein. The reaction was initiated by the addition of 25 μL of the APPH radical; [2,2'-azobis (2-amidinopropane) dihydrochloride of the AAPH radical, 240 mM]. Phosphate buffer (75 mM, pH 7,0) was used as a solvent in each solution for each sample. The fluorescence reduction was measured every 90 s for 30 min with an excitation wavelength of 485 nm, and a wavelength of 520 nm in a microplate reader (FLUOstar Omega). Phosphate buffer (75 mM, pH 7,0) was used as a blank, and dilutions retained with Trolox were used as standard (6,25-200 mM). The results were calculated from the standard Trolox curve and are expressed as mg TE/100 g FW.

4.6.4. Simulation *in vitro* of gastrointestinal digestion of concentrates

The gastrointestinal digestion simulation assays were performed following the methodology developed by Laurent; Besançon and Caporiccio (2007) and Yuan et al. (2019) with some modifications. The test simulates the conditions of digestion of the cryoconcentrates and nanofiltration products in the mouth, stomach, duodenum, and ileum in sequence. Samples for the last stage of cryoconcentration and ice were

prepared in test tubes; peristaltic movements and temperature (37 ± 1 °C) were simulated in a thermostated bath.

For the mouth, the pH was adjusted to 6.9 by adding a solution of sodium bicarbonate (1 mol.L^{-1}) and saliva solution (100 U/mL in 1 mmol.L^{-1} solution of calcium chloride) which was added to volume of $24 \mu\text{L.min}^{-1}$ for 2 min, with constant stirring at 200 rpm.

In the stomach stage, the pH was adjusted to 2.0 via the addition of hydrochloric acid (1 mol.L^{-1}), followed by the gradual addition of $50 \mu\text{L}$ of pepsin solution (25 mg.mL^{-1} in 0.1 mol.L^{-1} solution of hydrochloric acid), the solution was kept under constant stirring at 130 rpm for 90 min.

During digestion simulation in the duodenum, the pH was adjusted to 5.0 via the addition of sodium bicarbonate (1 mol L^{-1}), simultaneously a solution of pancreatin and bile salts of bovine (2 g.L^{-1} of pancreatin and 12 g.L^{-1} of bovine bile salts in $0,1 \text{ mol.L}^{-1}$ solution of sodium bicarbonate) was added. The solution was kept under constant stirring at 45 rpm for 20 min.

Finally, for the digestion step in the ileum, the pH was raised to 6.5 via the addition of sodium bicarbonate (1 mol L^{-1}) and kept under constant stirring at 45 rpm for 90 min. After the experimental procedure, all samples were stored at -24 °C for further analysis.

4.7. Statistical analysis

All data were presented as mean \pm standard deviation (SD). The differences between means were compared by *Tukey's* least significant difference test (LSD), with a significance level of 5%. The Pearson correlation analysis (*r*) was applied to verify the strength of the correlation between the responses evaluated at $p < 0.05$. All analyses were performed using Software Statistica® v. 9.0 (TIBCO Software Inc., Palo Alto, CA, USA).

5. RESULTS AND DISCUSSION³

5.1. Total solids content

Figure 8 shows the content (mg.L^{-1}) of total dry matter in the cryoconcentrate extracts of *M. citrifolia* leaves in both cryoconcentration methods performed in this study. Note that these results include each step of the process, both for the concentrated samples (CC1 to CC4) and the ice fractions formed (G1 to G4). Statistical analysis of the data showed that the cryoconcentration stage had a significant effect on the evolution of total dry matter ($p < 0.05$). In both cryoconcentration methods, there is a significant increase in TSC, where the statistical analysis for the data of the concentrated fractions (CC1 to CC4) revealed a significant difference for each value corresponding to the cryoconcentration step ($p < 0.05$). The analytical data of the TSC together with the statistical analysis of the data can be seen in Table 3.

For the CCG method, the concentrated fractions for the four stages of the process showed TSC values ranging from 16.82 mg.L^{-1} in the first stage to 76.97 mg.L^{-1} in the last stage of the process. Such results confirm the technique of accumulating solids via freezing and gravitational thawing as satisfactory. Such TSC value at the end of the fourth stage was higher than those presented in the studies carried out by Aider & Ounis (2012) and Orellana-Palma et al. (2017a), who applied the cryoconcentration process to retain solids in samples of skim milk and blueberry juice, respectively.

As for the CCM method, the significant increase in TSC at each stage of the process makes the method, just as it was for the gravitational technique, satisfactory, but the accumulation of solids at the end of the last stage for the microwave-assisted method was lower than that presented by the gravitational method. The increase in TSC ranged from 15.40 mg.L^{-1} to 35.29 mg.L^{-1} for samples CC1 and CC4, respectively. The value presented by CC4 in the CCM method represented a reduction of approximately 45.85% in relation to the TSC value presented in the gravitational method, which made this method of cryoconcentration more effective in retaining solids from the extract of *M. citrifolia* leaves in this study.

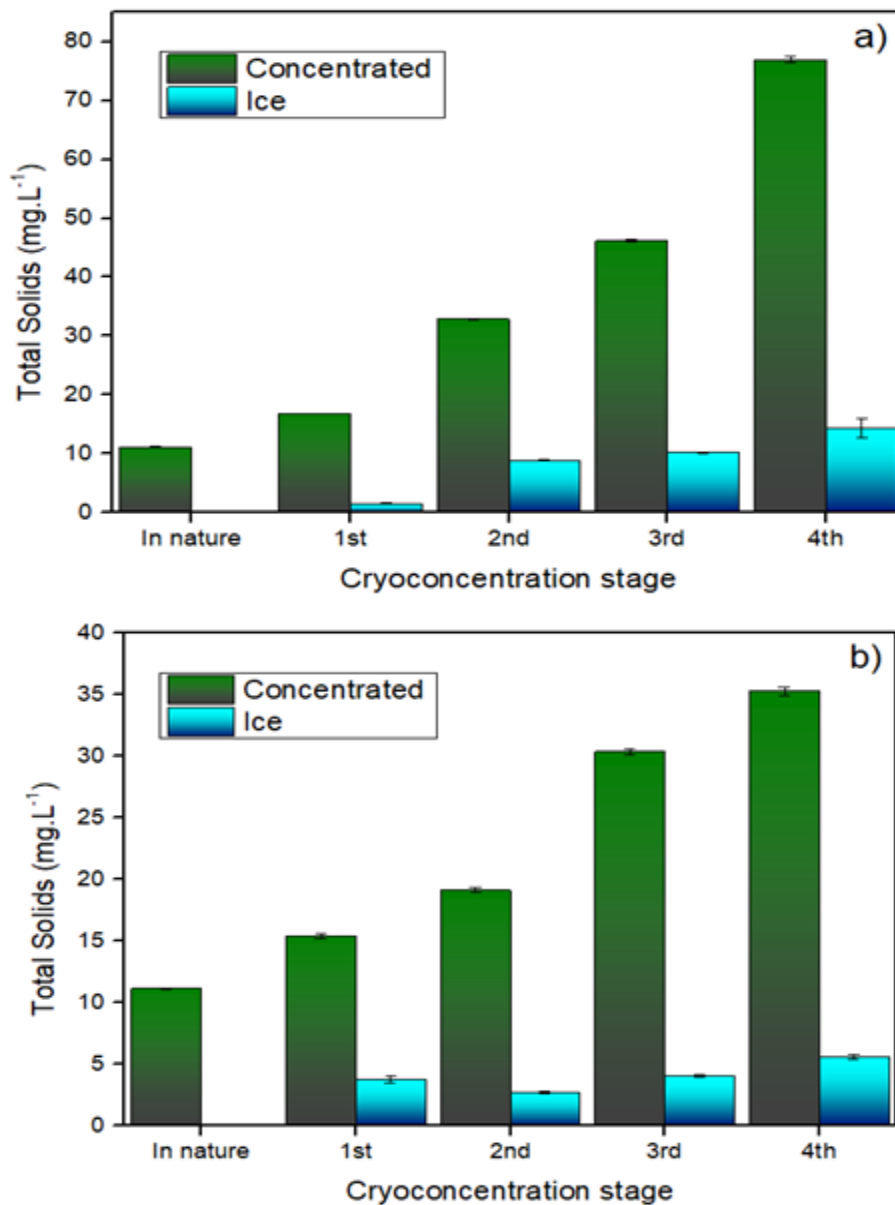
³ The results of Part II of this Thesis were submitted for publication as:

Physicochemical and phytotherapeutic properties of *Morinda citrifolia* (noni) leaf extracts submitted to a cryoconcentration process: A study on a promising functional food. Journal of Food Science. ID: JFDS-2022-0186. Submitted on: 31 Jan. 2022

Effect of the multi-stage block freeze concentration process on the physicochemical and biological properties of noni tea (*Morinda citrifolia*): a case study in Brazil to obtain a promising functional food. Journal of Food Measurement and Characterization. ID: SEIN-D-22-00481. Submitted on: 10 Feb. 2022

Although the TSC value presented by CC4 in the CCM method was lower than in the gravitational method; this same value proved to be practically identical when compared to the similar study prepared by Aider; De Halleux and Melnikova (2008), in the cryoconcentration of milk whey via the microwave-assisted method.

Figure 8 - TSC present in the concentrated and ice fractions for both methods of cryoconcentration used: a) CCG and b) CCM.



An important data to be considered during the cryoconcentration process refers to the TSC present in the residual ice. For the CCG method, the TSC present in G1 was quite low when compared to the fresh sample. However, in the second, third, and fourth

stages of the process, the TSC values increased significantly, varying between 8.86; 10.18, and 14.31 mg.L⁻¹ for samples G2, G3, and G4, respectively, in addition, such values for G2, G3, and G4 in the gravitational method did not show a statistically significant difference, being equivalent to the TSC of the *in natura* sample ($p < 0.05$). Although the TSC values present in the ice residues showed an increase corresponding to each stage of the gravitational process, such values are quite reduced when compared to the concentrated samples (CC1 to CC4), except for G4 ($p < 0.05$).

The behavior of the TSC present in the ice samples resulting from the microwave-assisted cryoconcentration process was similar to that presented by the gravitational method, where the TSC was much lower when compared to the concentrated fractions (Figure 8). It is noted that the representative TSC values for samples G1, G2, and G3 remained statistically similar, with a small increase in TSC in G4 ($p < 0,05$), a result that was already expected due to the accumulation of solids present in CC4 for this method of cryoconcentration. The TSC present in the ice residue for microwave-assisted cryoconcentration ranged from 3.78 to 5.59 mg.L⁻¹ between G1 and G4, respectively.

Table 3 - TSC for the cryoconcentrated and ice fractions of the aqueous extract of *M. citrifolia* leaves in CCG and CCM used methods.

Sample/ Cryoconcentration method	Total solids content (mg.L ⁻¹)	
	Gravitational	Microwave-assisted
<i>In natura</i>	11.12 ^{ab} ± 0.04	11.12 ^d ± 0.04
CC1	16.82 ^b ± 0.05	15.40 ^e ± 0.20
G1	1.49 ^c ± 0.09	3.78 ^{ab} ± 0.31
CC2	32.83 ^d ± 0.16	19.12 ^f ± 0.20
G2	8.86 ^a ± 0.13	2.70 ^a ± 0.09
CC3	46.18 ^e ± 0.20	30.37 ^g ± 0.23
G3	10.18 ^a ± 0.10	4.02 ^b ± 0.10
CC4	76.97 ^f ± 0.46	35.29 ^h ± 0.32
G4	14.31 ^{ab} ± 1.57	5.59 ^c ± 0.19

Note: Data are expressed as mean ± SD (n = 4). Values followed by the same letter do not differ (ANOVA, followed by Tukey's test; $p < 0.05$). Different symbols indicate significant differences ($P < 0.05$) for each stage of cryoconcentration analyzed in each method separately.

According to Orellana-Palma et al. (2018), the increase in the dry matter content in the ice can be explained due to the high content of solids retained in the ice fractions with the advance of the process steps. The same behavior was reported by Aider; De

Halleux and Melnikova (2008) in the milk whey concentration, Benedetti et al. (2015) for whey tofu concentration, and Orellana-Palma; González and Petzold (2019) on the concentration of orange juice.

Although satisfactory for both cryoconcentration processes, TSC results, mainly related to residual ice, need further analysis. Based on the high concentration of occluded solutes in the ice fraction in G3 and G4 (10.18 and 14.31 mg.L⁻¹, respectively) for the gravitational method, such results indicate the need to recirculate these fractions of ice. Statistically, there are no significant differences in the TSC referring to CC1 and the sample *in natura* ($p < 0.05$) (Table 3). This suggestion is also reported in the study by Orellana-Palma; González and Petzold (2019); in this case, centrifugal cryoconcentration of orange juice, the fractions of ice referring to the last stages of the process had a high content of residual solids.

As expected, extract *in natura* from the leaves of *M. citrifolia* has a low concentration of solute when compared to the concentrated fractions (CC1 to CC4). That is, the results obtained with the different methods of cryoconcentration showed that, as the cycles progressed, the trapped solutes were higher than the initial concentration.

Figure 9 illustrates the behavior of the TSC concentration factor for samples of *M. citrifolia* leaf extracts concentrated in both cryoconcentration methods. As previously described, C_f is calculated as a function of the increase of the total solids content in each step of the process, that is, it indicates how many times the sample was concentrated compared to the sample *in natura*. The analytical values for the C_f are shown in Table 4.

Considering the CCG method, the statistical analysis of the data obtained showed that the cryoconcentration steps had a significant effect on the TSC concentration factor, as expected ($p < 0.05$). It is noted that for this method, the CC4 sample obtained a TSC content almost 7 times greater when compared to the sample *in natura*. This result indicated that the recovery of the total dry matter was very high. Considering the CCM method, the TSC referring to CC4 was concentrated at 3.18 times when compared to the sample *in natura* (Table 4).

In fact, the parameter corresponding to the TSC C_f , is nothing more than a reflection of the behavior obtained for the retention of solids obtained during the stages of the cryoconcentration process. This aspect corroborates with what was exposed by Aider

and Ounis (2012), i.e. regardless of the type of defrosting method used, the total dry matter content increased with the increase of cryoconcentration cycles.

Figure 9 - Behavior of the C_f for the TSC in the concentrated fractions in all concentration stages for both methods of cryoconcentration used.

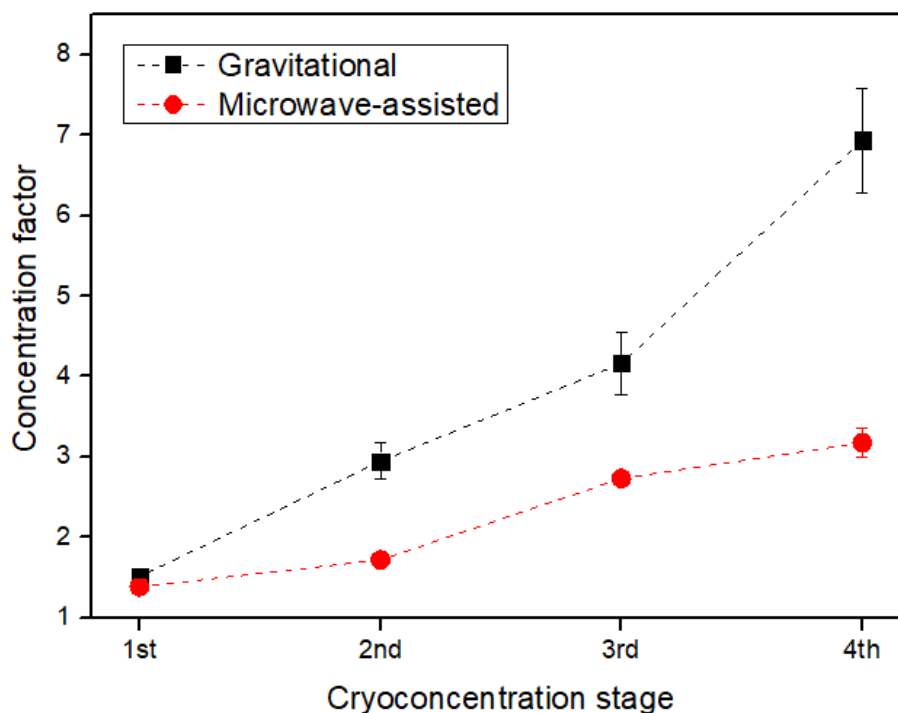


Table 4 - Concentration factor (C_f) for the total solids content for the cryoconcentrated and ice fractions of the aqueous extract of *M. citrifolia* leaves in both cryoconcentration methods used.

Cryoconcentration method/ Thawing stage	Gravitational	Microwave-assisted
	Concentration factor	Concentration factor
1st	1.51 ^a ± 0.01	1.39 ^a ± 0.04
2nd	2.95 ^{ab} ± 0.23	1.72 ^a ± 0.02
3rd	4.16 ^b ± 0.39	2.73 ^b ± 0.02
4th	6.94 ^c ± 0.65	3.18 ^c ± 0.18

Note: Data are expressed as mean ± SD (n = 3). Values followed by the same letter do not differ (ANOVA, followed by Tukey's test; $p < 0.05$). Different symbols indicate significant differences ($p < 0.05$) for each stage of cryoconcentration analyzed in each method separately.

Under the experimental conditions used in the present study, the CCG method had a significant effect on the total dry matter evolution. According to Aider and Halleux

(2008), this effect occurs because the amount of free water in the solution decreases when passing from one stage to another. In fact, when analyzing the values referring to the C_f for the gravitational method (Table 4), it is noticed that the TSC increases significantly in the third and fourth stages of the process. Considering that part of water, called the free water, can easily freeze, the remaining bound water is organized very differently from the free water. Therefore, it is expected that the amount of this water (non-bound) will increase, thus increasing the total dry matter content in the samples and, consequently, increasing with the cryoconcentration steps (PRAWITWONG; TAKIGAMI; PHILLIPS, 2007). Thus, an increase in the total dry matter from the first stage of cryoconcentration to the second is much smaller than that recorded in the last two stages of the process (Table 4). In addition, the solute concentration behavior attributed to both cryoconcentration methods can also be related to the phenomenon of elution, where the movement of solutes occurs during the formation of ice crystals, and due to this phenomenon, the solutes were expelled and accumulated in the liquid fraction. Similar results are presented by Petzold and Aguilera (2013) and Moreno et al. (2013) during the cryoconcentration of the sucrose solution and coffee extract, respectively.

The microwave-assisted cryoconcentration of the aqueous extract of leaves of *M. citrifolia* was an effective method and allowed to obtain samples with larger C_f at the end of the process than the samples *in natura* thus obtained by the CCG method. Although the C_f results obtained by the CCM method were inferior to the CCG method, the microwave defrosting technique was faster and the time required to reach the separation procedure was sufficient to keep the ice crystals relatively pure in the solid state. According to Aider; De Halleux and Melnikova (2008) and Aider & De Halleux (2008) the effectiveness of the retention of solids via CCM method occurs due to the low dielectric constant of the ice, compared to that of pure water or aqueous solution present in the extracts of the leaf of *M. citrifolia*. According to the authors, the dielectric of pure water is approximately 78.13. It is well known that microwaves in the range of 300 MHz up to 300 GHz can effectively heat solid and liquid foods. However, some particularities regarding the use of the microwave in the defrosting process should be discussed.

Unlike laser lights, whose photon energy is several eV, the microwave photon energy is as small as 10 and 5 eV, and its period is orders of magnitude greater than the

electronic processes that occur in molecules. However, microwaves can control the heating of solids and liquids with high energy efficiency. It has been shown that water in the liquid phase is heated by microwaves by exciting the rotational movement of the permanent electrical dipoles between the water molecules that are delayed from the wave electric field. Thus, water in the ice state is hardly heated by low-frequency microwaves, accrediting the technique as favorable for the application in the retention of solids in food solutions (TANAKA; SATO, 2007; AIDER; DE HALLEUX, 2008; AIDER; DE HALLEUX; MELNIKOVA, 2008; AIDER; OUNIS, 2012).

5.2. Total phenolics content

Figure 10 illustrates the behavior of the TPC for samples of aqueous extract of *M. citrifolia* leaves applied in both cryoconcentration methods. The analytical data together with the statistical analysis of the data are shown in Table 5.

Figure 10 - Total phenolics content present in the concentrated and ice fractions for both methods of cryoconcentration used: a) CCG and b) CCM.

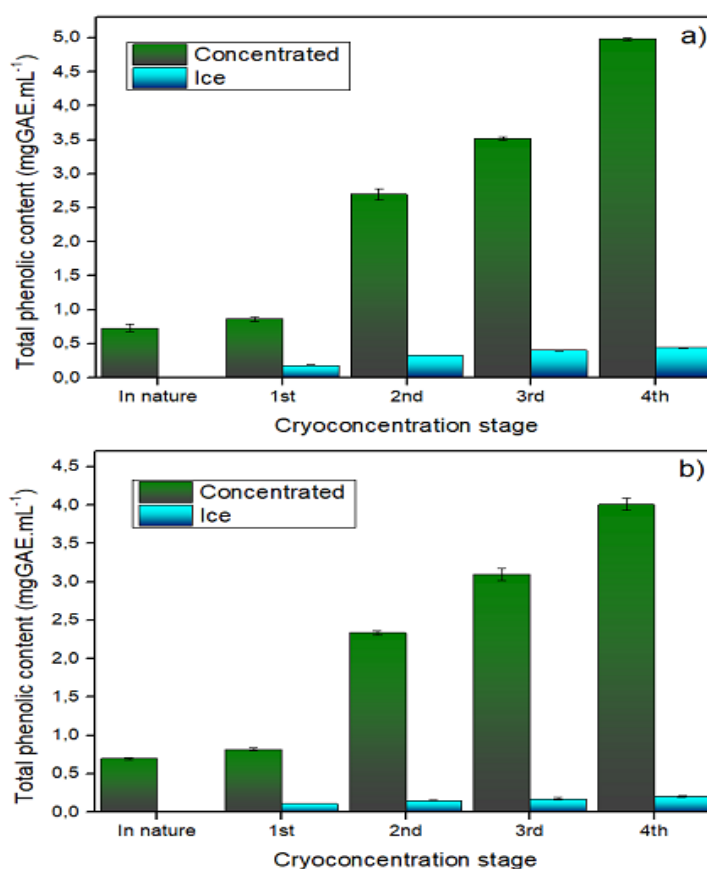


Table 5 - Total phenolics content for the cryoconcentrated and ice fractions of the aqueous extract of *M. citrifolia* leaves in both cryoconcentration methods used.

Sample/ Cryoconcentration method	Total phenolics content (mgGAE.mL ⁻¹)	
	Gravitational	Microwave-assisted
<i>In natura</i>	0.73 ^{bc} ± 0.06	0.70 ^b ± 0.02
CC1	0.86 ^c ± 0.03	0.82 ^b ± 0.02
G1	0.18 ^a ± 0.01	0.11 ^a ± 0.00
CC2	2.70 ^d ± 0.08	2.33 ^c ± 0.03
G2	0.33 ^{ab} ± 0.00	0.15 ^a ± 0.01
CC3	3.52 ^c ± 0.03	3.10 ^d ± 0.08
G3	0.40 ^{ab} ± 0.00	0.17 ^a ± 0.02
CC4	4.98 ^f ± 0.02	4.01 ^e ± 0.08
G4	0.44 ^{abc} ± 0.00	0.21 ^a ± 0.01

Note: Data are expressed as mean ± SD (n = 4). Values followed by the same letter do not differ (ANOVA, followed by Tukey's test; $p < 0.05$). Different symbols indicate significant differences ($P < 0.05$) for each stage of cryoconcentration analyzed in each method separately.

It is noted that for both cryoconcentration methods performed, freezing resulted in the preservation of phenolic compounds and, consequently, promoted an increase ($p < 0.05$) in TPC in all cryoconcentrated samples during the process when compared to the extract *in natura*. According to Adorno et al. (2017), the maintenance of phenolic compounds during the process is helped due to the use of low temperatures. The behavior described in Figure 10 for both methods used shows, as previously discussed, an increase in dry matter, consequently causing an increase in TPC, thus suggesting the preservation of these compounds.

Figure 11 illustrates the percentage efficiency (η) of TPC retention in aqueous extracts of *M. citrifolia* leaves, for each stage of both cryoconcentration methods used. These process parameters are aided by data referring to TPC, which consequently showed a similar behavior between treatments to the solids content. Finally, Figure 12 shows the concentration factor for the accumulation of TPC in all thawing steps in both cryoconcentration methods performed.

Figure 11 - Efficiency in the accumulation of TPC in both methods of cryoconcentration used.

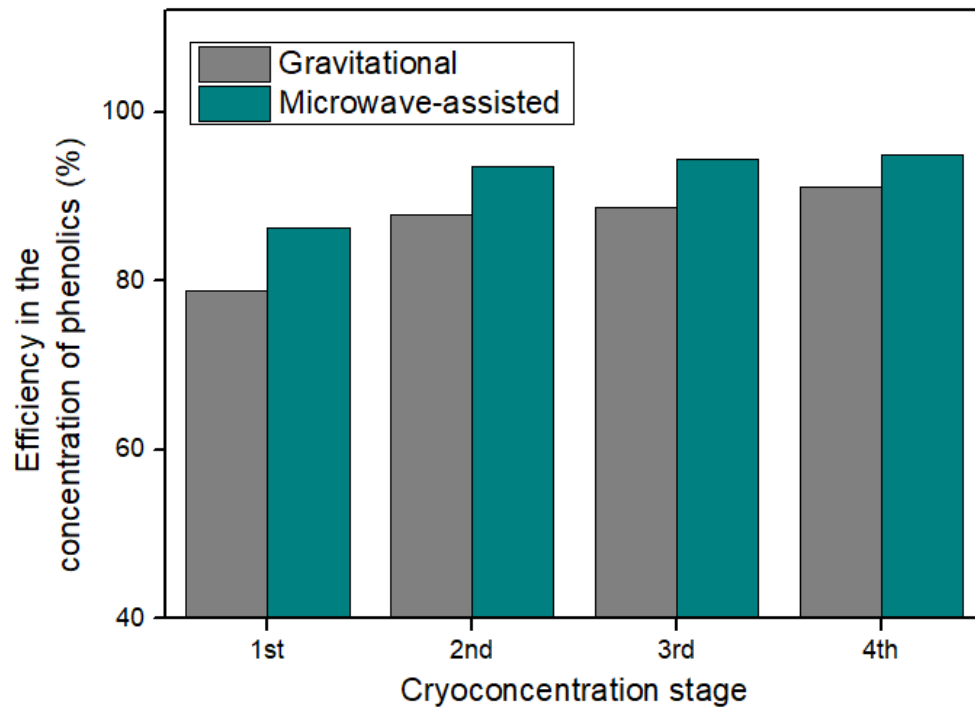
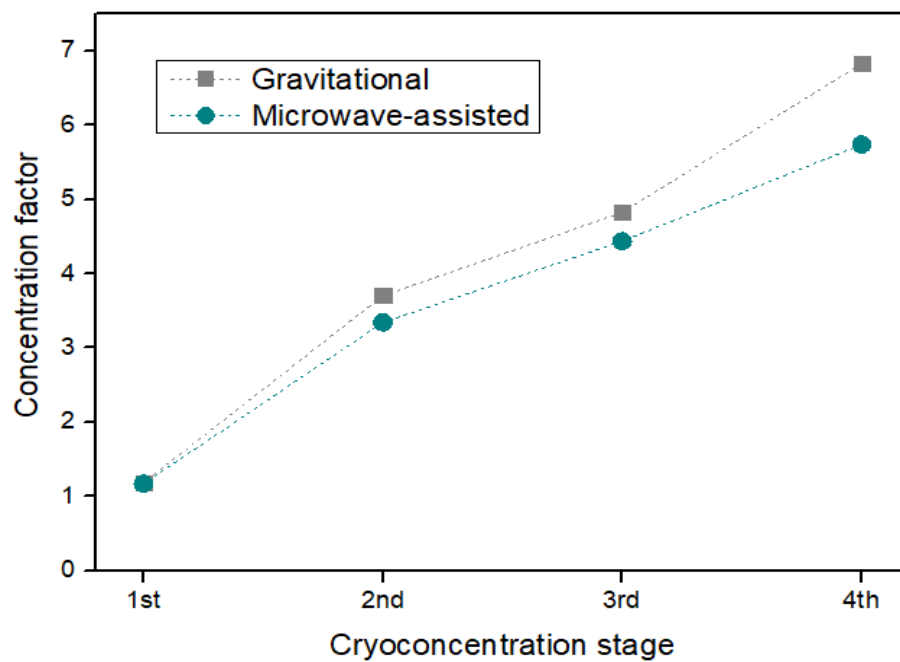


Figure 12 - Behavior of the concentration factor for the TPC for both methods of cryoconcentration used.



Considering the CCG method, the retention process of phenolic compounds was very effective, where TPC increased as the stages of the process progressed. There was a statistically significant difference between the values obtained ($p < 0.05$), with TPC ranging from 0.86 mgGAE.mL⁻¹ for CC1 to 4.98 mgGAE.mL⁻¹ for CC4, with TPC referring to the sample *in natura* 0.73 mgGAE.mL⁻¹, thus representing an increase in TPC of 6.83 times in relation to the initial phenolic content (Figure 12).

Regarding CCM method for retention of TPC, the results obtained were similar to gravitational treatment. The TPC increased significantly during the cryoconcentration stages ($p < 0.05$), thus favoring the retention of phenolic compounds associated with the increase in the total solids content already mentioned. The values varied from 0.70 mgGAE.ml⁻¹ for the sample *in natura*, 0.82 mgGAE.ml⁻¹ for CC1 finished with 4.01 mgGAE.ml⁻¹ in the last stage of the process. Although the TPC associated with CC4 of the microwave-assisted process was satisfactory, we can infer that the gravitational method for thawing was slightly superior to the microwave-assisted technique in the retention of phenolic compounds. The accumulation of TPC in the last stage of cryoconcentration via CCM method represented a C_f of 5.74 times higher than the sample *in natura* (Figure 12).

Regarding the residual ice fractions resulting from both cryoconcentration methods, it is noted that there was no significant difference in the TPC in both methods performed. This fact shows the effectiveness of the cryoconcentration process in both methods, as it is clear that almost all of the TPC in the studied samples was directed to the concentrated samples (CC1 to CC4), resulting in greater purity in the ice samples. A similar effect is noted in the study by Petzold et al. (2016), in the process of cryoconcentration of wine.

In fact, the increase in the TPC concentration factor for samples of the aqueous extract of leaves of *M. citrifolia* for both cryoconcentration methods used refers to another variable that may be associated with the significant effect of retention of both TPC and TSC. This variable refers to the efficiency of the cryoconcentration process in the accumulation of TPC, as shown in Figure 11.

Note that the percentage values for efficiency in the TPC retention process for the CCG method started at 78.87% for the first stage of the process, reaching values of up to 91.15% in the fourth thawing stage. Although the value is higher than the initial one,

when analyzing the behavior of Figure 11 for the gravitational method, it is noticed that there was no significant variation in the efficiency of the process between steps 2, 3, and 4 of the process ($p < 0.05$). In addition, although there was a significant increase in η from the first to the other thawing steps, this increase was not accentuated.

For the CCM, the results regarding the efficiency in the retention of TPC were quite similar to that found in the CCG method, although the point values were slightly higher for the CCM method. Note that for the first cryoconcentration stage for the microwave-assisted method, $\eta = 86.30\%$ was obtained, increasing to 93.47%; 94.40% culminating in 94.86%. As in the gravitational method, the values of n in the microwave-assisted method did not show significant differences for steps 2, 3, and 4 of the process, with a significant increase only from step 1 for the other thawing phases ($p < 0.05$).

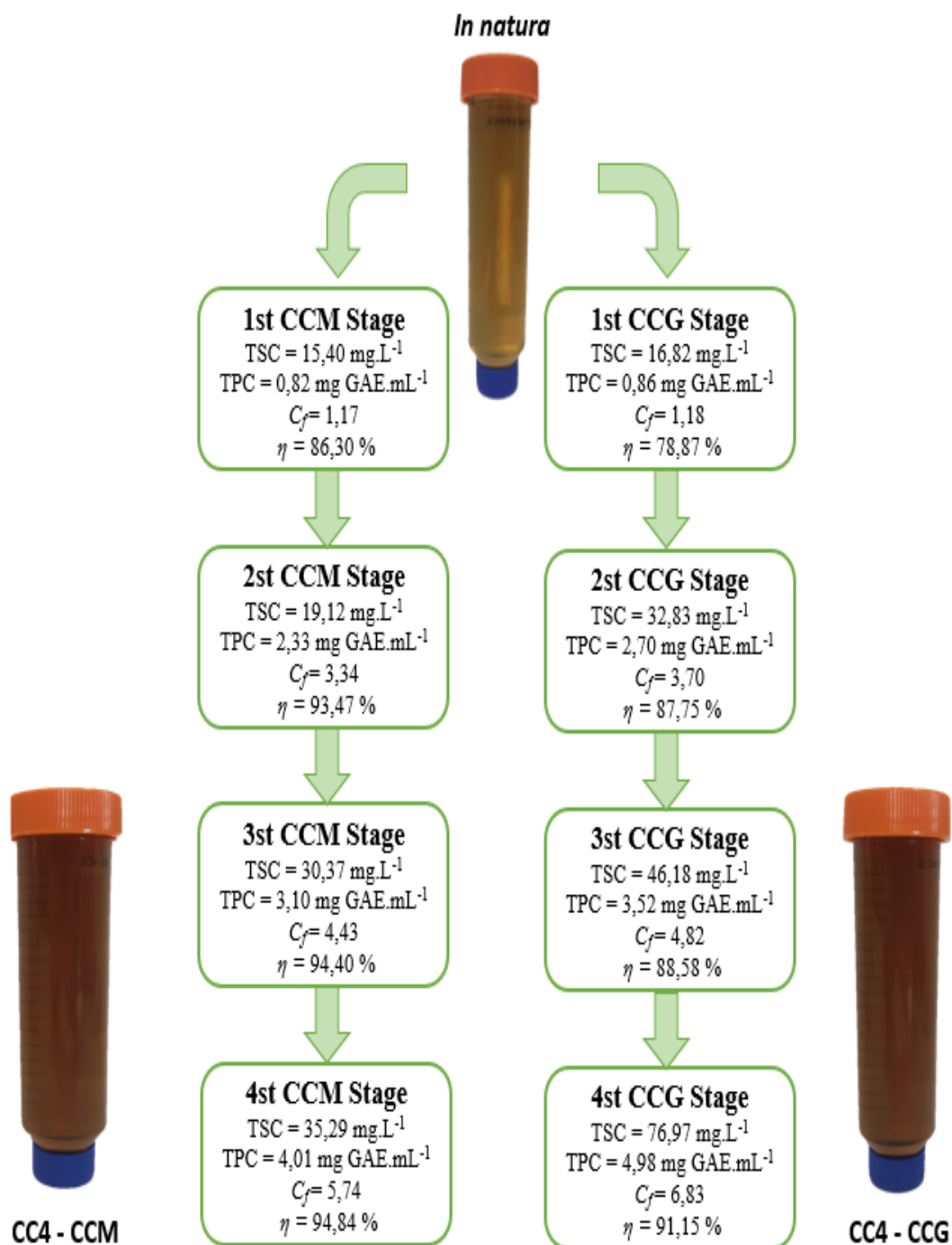
As already described, the CCM cryoconcentration process analytically obtained efficiency values slightly higher than the CCG method. This fact is possibly related to the effect, of greater speed and energy control that the microwave technique causes in the defrosting process. Furthermore, in the microwave process, water in the ice state is hardly heated when exposed to a low frequency of incident resonant radiation, since the electric dipoles exhibit substantial directional inertia due to the rigid network of water molecules present in the sample. This fact corroborates not only faster defrosting but also better percentage efficiency in the process of retaining solids (TANAKA; SATO, 2007; AIDER; DE HALLEUX, 2008).

Another important factor is to consider the fact that in both methods used, the non-significant variation of n in steps 2, 3, and 4 may be related, although quite small, to the deposition of solutes in the residual ice. This fact is explained by Zielinski et al. (2019) and Orellana-Palma; González and Petzold, (2019), who reported that in the cryoconcentration process, each stage of development removes some of the water in the samples, increasing the levels of bioactive compounds. However, efficiency may not vary significantly with the use of several stages, as there is greater solute retention in the remaining ice. This is also reflected in the increase in viscosity at the interface (solute-ice), consequently resulting in greater difficulty of mass transference.

Finally, Haas et al. (2022) mention that another important physicochemical parameter associated with the quality and effectiveness of the cryoconcentration process is the color of the final extracts obtained. Although, in this study, the presentation of this

subtle difference in the color aspect is fully qualitative, it is evident, as shown in Figure 13, the differences in color between the *in natura* sample and the samples referring to the last cryoconcentration stage, indicating, as already described, the retention of larger amounts of solids in more concentrated samples.

Figure 13 - Visual comparison and summary of the properties of TSC, TPC, concentration factor and percentage efficiency of the phenolic retention process between the extracts *in natura* and after the last stage of cryoconcentration for both the CCG and CCM methods employed.



5.3. FTIR Spectroscopy

The dry samples corresponding to the concentrated extracts of *M. citrifolia* leaves in both cryoconcentration methods were analyzed by FTIR to identify the possible functional groups present in the biomolecules of the extracts responsible, among other functions, for the biological activity of the leaf extract. The FTIR spectra are shown in Figure 14. Tables 6 and 7 present a summary of the main peaks obtained in the FTIR spectrum for both cryoconcentration methods used: gravitational and microwave-assisted, respectively.

In summary, the transmittance (%) for the FTIR spectra in both cryoconcentration methods was quite similar, as expected. Theoretically, when we increase the concentration of the aqueous extract of *M. citrifolia* leaves, there is a greater deposition of biochemically active compounds. Another important fact refers to the similarity between the FTIR peaks representative of the CC4 samples, which was also expected since these peaks are attributed to the same samples from the same defrosting stage; however, submitted to different cryoconcentration methods.

The peak similarity for the CC4 samples of both cryoconcentration methods involves values of 3419.2 cm^{-1} and 3385.0 cm^{-1} (gravitational and microwave-assisted, respectively). Such peaks are associated with the stretching vibrations of -OH, and the number of hydroxyl groups to the antioxidant activity of polysaccharides present in extracts (Yuan et al., 2019). In addition, these peaks are possibly related to -OH groups of residual crystallization in the samples (SILVERSTEIN; WEBSTER; KIEMLE, 2006).

Figure 14 - FTIR spectroscopy for the concentrated fractions of both cryoconcentration methods used: a) gravitational and b) microwave-assisted.

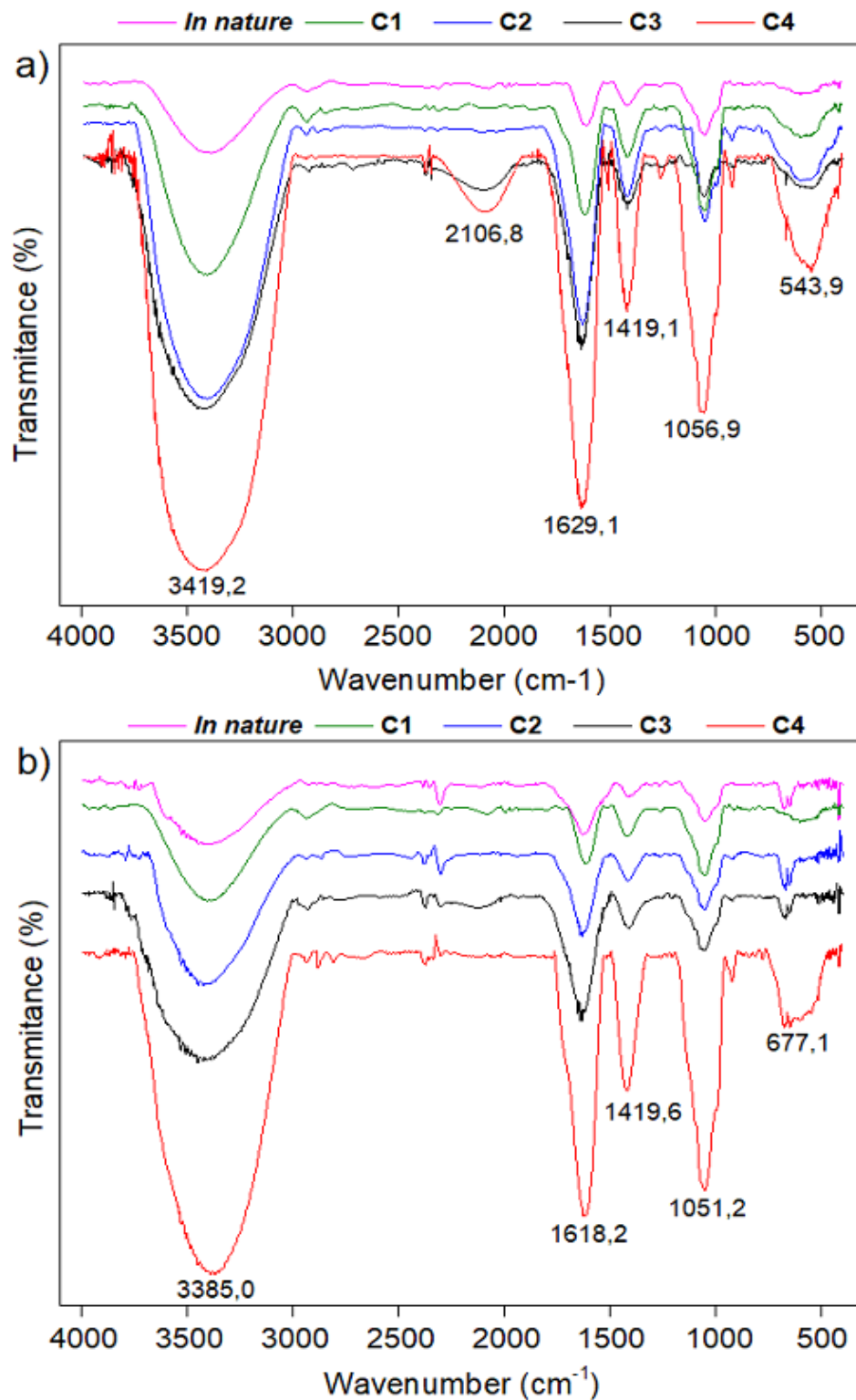


Table 6 - FTIR spectra and their respective functional groups found in the samples of the aqueous extract of cryoconcentrated *M. citrifolia* leaves by the CCG method.

Gravitational method			
Functional group	Detected wavelength (cm ⁻¹)	Referential wavelength (cm ⁻¹)	Reference
Hydrogen-bonded O-H (intermolecular), OH of water of crystallization.	3419.2	3420-3370	Silverstein; Webster and Kiemle (2006); Shimanouchi (1973); Socrates (2001)
Monosubstituted alkynes, -C≡CH and R³-SiCH=C=O	2106.8	2140-2100	Silverstein; Webster and Kiemle (2006); Shimanouchi (1973); Socrates (2001); Vahur et al. (2016)
Conjugated dienes with an aromatic ring. Vinyl ether. -O-CH=CH₂; Vinylidenes (Sat.)₂C=CH₂	1629.1	1625-1630	Silverstein; Webster and Kiemle (2006); Shimanouchi (1973); Socrates (2001); Vahur et al. (2016)
Amides CH₃NH-CO- and thioamides; Secondary alcohols; CH₃NH-CS-; ArNH-. NH₂, Halogen, and -SO-CH₃ groups and =N-CH₃ (amides)	1419.1	1460-1410	Silverstein; Webster and Kiemle (2006); Shimanouchi (1973); Socrates (2001); Vahur et al. (2016)
Ethyl groups; EtO- (ethers) and EtO·CO- (esters)	1056.9	1080-1050	Silverstein; Webster and Kiemle (2006); Shimanouchi (1973); Socrates (2001)
Dibranched alkanes not possessing CH₃ or C₂H; Straight-chain alkanes and Isopropyl benzene.	543.9	555-535	Silverstein; Webster and Kiemle (2006); Shimanouchi (1973); Socrates (2001)

The peaks referring to the values of 1419.1 cm⁻¹ and 1419.6 cm⁻¹ are mainly attributed to the possible presence of nitrogen groups, such as amides, thioamides, and secondary alcohols. According to De Souza et al. (2005), the eventual presence of amides and thioamides may indicate possible reactions of formation of chemical groups with a thiazoline nucleus: an important class of heterocyclic compounds that present a broad spectrum of biological activity, such as anticancer and antibacterial activities.

Similar to both cryoconcentration methods, the spectrum contained an absorption band arising from the glycosidic linkage (C–O–C) stretch vibration at approximately 1056.9 cm^{-1} and 1051.2 cm^{-1} (gravitational and microwave-assisted, respectively). Such peaks are associated with the presence of ethyl and ether groups, which encompass a huge range of bioactive compounds such as flavonol glycosides (SANG et al., 2001a; SOCRATES, 2001; YUAN et al., 2019).

Table 7 - FTIR spectra and their respective functional groups found in the samples of the aqueous extract of cryoconcentrated *M. citrifolia* leaves by the microwave-assisted method.

Microwave-assisted method			
Functional group	Detected wavelength (cm^{-1})	Referential wavelength (cm^{-1})	Reference
Hydrogen-bonded O-H (intermolecular); OH of water of crystallization	3385.0	3420-3370	Silverstein; Webster and Kiemle (2006); Shimanouchi (1973); Socrates (2001)
Conjugated; Vinyl ether; -O-CH=CH₂; Vinylidenes (Sat.)₂C=CH₂ and CH₂=CH-C≡C-	1618.2	1675-1610	Kang et al. (2007); Vahur et al. (2016); Shimanouchi (1973)
Amides CH₃NH-CO- and thioamides CH₃NH-CS-; Secondary alcohols; ArNH-, NH₂, Halogen, and -SO-CH₃ groups and =N-CH₃ (amides)	1419.6	1475-1410	Silverstein; Webster and Kiemle (2006); Shimanouchi (1973); Socrates (2001); Vahur et al. (2016)
Ethyl groups; EtO- (ethers) and EtO·CO- (esters)	1051.2	1080-1050	Silverstein; Webster and Kiemle (2006); Shimanouchi (1973); Socrates (2001)
Vinyls and Vinylenes cis-CH=CH- (hydrocarbons); -CH=CH₂; (Unsat)₂-C=CH₂ and Metal azides or azide ion	677.1	750-630	Silverstein; Webster and Kiemle (2006); Shimanouchi (1973); Socrates (2001)

In summary, for both methods of cryoconcentration used in the samples of the extract CC4 of leaves of *M. citrifolia* we found representative peaks for hydrocarbons,

such as vinyl groups; and mainly saturated and unsaturated hydrocarbons associated with aromatic rings; in addition to carbonyl radicals (see Tables 6 and 7).

Compared to some representative studies such as those carried out by Sang et al. (2001a, b); Deng; West and Jensen (2008), and Singh & Singh (2013); the detection of the chemical groups mentioned above suggests the presence of a wide range of bioactive compounds. They belong majorly to the class of flavonols and iridoids glycosides; anthraquinones and aglycones; in addition to coumarin compounds.

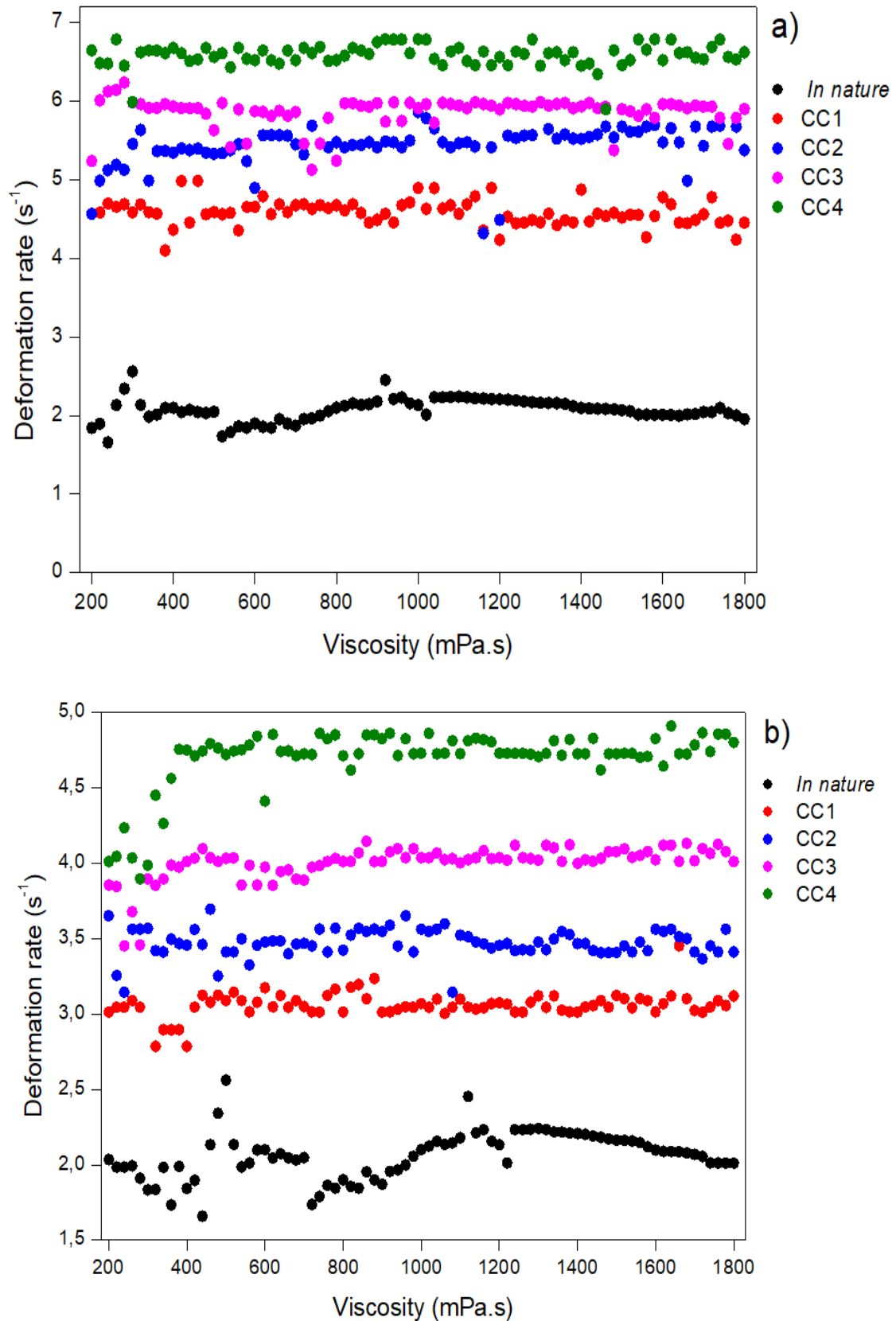
5.4. Rheological analysis of cryoconcentrate extracts

Figure 15 shows the viscosity versus shear rate graphs for samples of aqueous extract of *M. citrifolia in natura* and cryoconcentrated leaves (CC1 to CC4). It was taken into account the viscosities present in the range of the shear rate of 200 s^{-1} and 1800 s^{-1} , due to equipment instability.

It appears that the viscosity remains constant with the increase in the shear rate in all cases. Such behavior is considered characteristic of Newtonian fluids, whose viscosity is constant and follows Newton's Law of viscosity, where the behavior of shear stress and the local velocity gradient is defined through a linear relationship. Examples of typical Newtonian fluids are water, coffee, beer, carbonated drinks, most kinds of honey, sugar syrup, milk, filtered juices, orange juice, and wines (BOURNE, 2002; SCHRAMM, 2006). Nevertheless, for higher concentrations (CC4, for example), the viscosity values are higher, as expected.

It is important to note that the viscosity presented by the cryoconcentrated samples corresponds to a crucial factor in the process. It is associated with the effectiveness of the retention of solids in the concentrated fractions, as already presented in this study, when evaluating parameters such as TSC and the efficiency in the TPC retention process, for example. It was found that the TSC increased as the cryoconcentration steps progressed, as well as that η for both applied cryoconcentration methods did not show significant differences ($p < 0.05$) in steps 2, 3, and 4 of the process (check Figures 8 and 11).

Figure 15 - Apparent viscosity versus shear rate for each stage of both cryoconcentration methods used in the aqueous extract of *M. citrifolia* leaves: a) CCG and b) CCM.



The increase in the total solids content in the concentrated samples is expected to cause an increase in the viscosity of the solutions (PETZOLD et al., 2015). The viscosity presented in the concentrated fractions also presents an important relationship regarding the efficiency in the retention of TPC. The increase in viscosity of the concentrated solutions during the cryoconcentration process resulted in no significant variation in the efficiency of the process in steps 2, 3, and 4 in both methods performed. Aider; De Halleux and Melnikova (2008) explain that this phenomenon is possibly due to a quantity, albeit small of solids retained at the ice-solute interface. Thus, viscosity influences the properties of the crystallization phenomenon (SÁNCHEZ et al., 2009).

Tables 8 and 9 show the adjusted models for the cryoconcentrated samples (CC1 to CC4) for the aqueous extracts of *M. citrifolia* leaves studied via the gravitational and microwave-assisted methods, respectively. The Power Law and Newton models were evaluated for their ability to describe the typical rheological behavior of the samples studied for each defrost stage. It is possible to observe that the models describe the rheological behavior in a satisfactory and characteristic way for the type of fluid studied.

Table 8 - Rheological parameters obtained by adjusting the data to the Power Law model and adjusting data to the Newton model, for the aqueous extract of cryoconcentrated *M. citrifolia* leaves by the CCG method.

Samples	Power law			Newton model		
	K (Pa.s ⁿ)	n	R ²	μ (Pa.s)		R ²
<i>In nature</i>	0.0019	0.97	0.96	1.483 ^a ± 0.20		0.95
CC1	0.0028	1.07	0.94	3.128 ^c ± 0.08		0.94
CC2	0.0023	0.99	0.97	4.801 ^b ± 0.34		0.94
CC3	0.0010	1.03	0.94	5.001 ^{bd} ± 0.28		0.94
CC4	0.0013	1.00	0.95	5.203 ^d ± 0.11		0.95

Note 1: Data are expressed as mean ± SD (n = 3). Values followed by the same letter do not differ (ANOVA, followed by Tukey's test; $p < 0.05$). Different symbols indicate significant differences ($p < 0.05$) for each rheological model separately analyzed.

Note 2: μ is the absolute or dynamic viscosity (Pa.s); **K** the consistency index (Pa.sⁿ); **n** the behavior index (dimensionless) and R² is the correlation coefficient.

In summary, both models tested, for both methods of cryoconcentration, have a good

fit with the data obtained experimentally. However, based on the statistical treatment of these data, it is concluded that the Power Law model was the most suitable, as it presents the best adjustments (highest R^2 values). In addition, the Power Law model applied to both treatments (gravitational and microwave-assisted), presented values for fluid behavior index (n) close to 1, this aspect is consistent with a characteristic behavior typical of a fluid with Newtonian behavior for the analyzed samples.

Table 9 - Rheological parameters obtained by adjusting the data to the Power Law model and adjusting data to the Newton model, for the aqueous extract of cryoconcentrated *M. citrifolia* leaves by the CCM method.

Sample	Power law			Newton model		
	K (Pa.s ⁿ)	n	R^2	μ (Pa.s)		R^2
<i>In nature</i>	0.0018	0.96	0.98	1.4813 ^a ± 0.20		0.95
CC1	0.0021	0.99	0.99	2.014 ^{ac} ± 0.48		0.91
CC2	0.0014	1.00	0.95	3.101 ^{cb} ± 0.28		0.95
CC3	0.0006	1.12	0.96	3.450 ^b ± 0.14		0.95
CC4	0.0003	1.17	0.96	4.001 ^d ± 0.07		0.95

Note 1: Data are expressed as mean ± SD ($n = 3$). Values followed by the same letter do not differ (ANOVA, followed by Tukey's test; $p < 0.05$). Different symbols indicate significant differences ($p < 0.05$) for each rheological model separately analyzed.

Note 2: μ is the absolute or dynamic viscosity (Pa.s); K the consistency index (Pa.sⁿ); n the behavior index (dimensionless) and R^2 is the correlation coefficient.

According to Moura et al. (2016), in their study involving the physical and rheological properties of fruit-based products, it was verified via rheological analysis that the Law of Potency model was applied and the adjustment to the model indicated that, for all samples, the values of “ n ” were less than 1. This result for “ n ” concludes that the samples had their rheological behavior classified as being of a pseudoplastic fluid; unlike the rheological behavior presented here.

5.5. HPLC-DAD-MS assays

M. citrifolia is widely known due to its nutritional character, where about 200 biochemical compounds with bioactive properties have already been identified and

isolated from different parts of this plant (Almeida, de Oliveira, & Hotza, 2017). It is also important to note that the biochemical composition of these compounds differs not only in terms of quantity according to the structure of the plant, but also concerning the place of origin and harvest time of these structures (CHAN-BLANCO et al., 2006). Such differences in the content of bioactive compounds according to the place of origin of *M. citrifolia* are exposed by Deng, West, & Jensen (2010). The phenolic compounds identified and their respective amounts isolated from the sample *in natura* and the cryoconcentrated samples from CCG and CCM methods are shown in Tables 10 and 11 respectively. Figures 16 and 17 present the representative HPLC-DAD-MS chromatograms of the phenolic compounds identified and quantified in the extracts of *M. citrifolia* leaves.

The detection of phenolic compounds made use of a validated method in which it presented low detection limits (0.0104 mg·g⁻¹; 0.0269 mg·g⁻¹; 0.0345 mg·g⁻¹; 0.01395 mg·g⁻¹; 0.0105 mg·g⁻¹; 0.0090 mg·g⁻¹; 0.0082 mg·g⁻¹; 0.0042 mg·g⁻¹; 0.0075 mg·g⁻¹; 0.0028 mg·g⁻¹; according to the listing of compounds in Table 4 identified from 1 to 10 respectively). The analytical curves showed linear behavior from the limit of quantification up to 26 mg·g⁻¹, with models without lack of adjustment ($P < 0.05$) and distribution of random residues. A standard deviation ranging from 0.29% to 4.95% was calculated, considering the three levels (limit of quantification, an intermediate point, and maximum curve). Satisfactory values were obtained as recommended by the International Union of Pure and Applied Chemistry (IUPAC), as well as demonstrated by Thompson, Ellison, & Wood (2002).

According to Tables 12 and 13, the levels of phenolic compounds increased proportionally to the cryoconcentration stages. Total phenolic contents of 47.89 mg·g⁻¹ and 27.93 mg·g⁻¹ were reached for all species detected at the end of the last stage of the CCG and CCM process respectively. These values represent an increase of ~12.70 times the total content present in the *in natura* sample or 1070.3% ± 0.04 in relation to the initial content for the CCG method. For the CCM method, the increase in total phenolic content concerning the *in natura* sample was ~7.4 times greater, or 640.8% ± 0.03 comparing to the initial content (Tables 12 and 13). As explained by Lin, Chang, Yang, Tzang, & Chen (2013), phenolic acids are the main polyphenolic components present in noni juice. In this study, gallic acid, vanillic acid, caffeic acid, p-coumaric acid, and ferulic acid were detected, with respective quantitative increases caused by the CCG

method of 8.75; 22.22; 70.0; 95.83, and 6.5 times compared to the initial amounts *in natura* samples (Table 12). Via the CCM method, the same components already described: gallic acid, vanillic acid, caffeic acid, p-coumaric acid and ferulic acid respectively had quantitative increases of 4.48; 2.70; 39.86; 56.58 and 3.75 times in relation to the initial amounts in the *in natura* samples (Table 13). Such significant increases denote a potential phytotherapeutics effect present in the concentrated fractions.

Figure 16 - Chromatogram containing the identification of the main phenolic species present in the sample *in natura* and in the cryoconcentrated samples of the aqueous extracts of the leaves of *M. citrifolia* by CCG method. The wavelengths, the retention time, and the identification of each compound are detailed in Table 10.

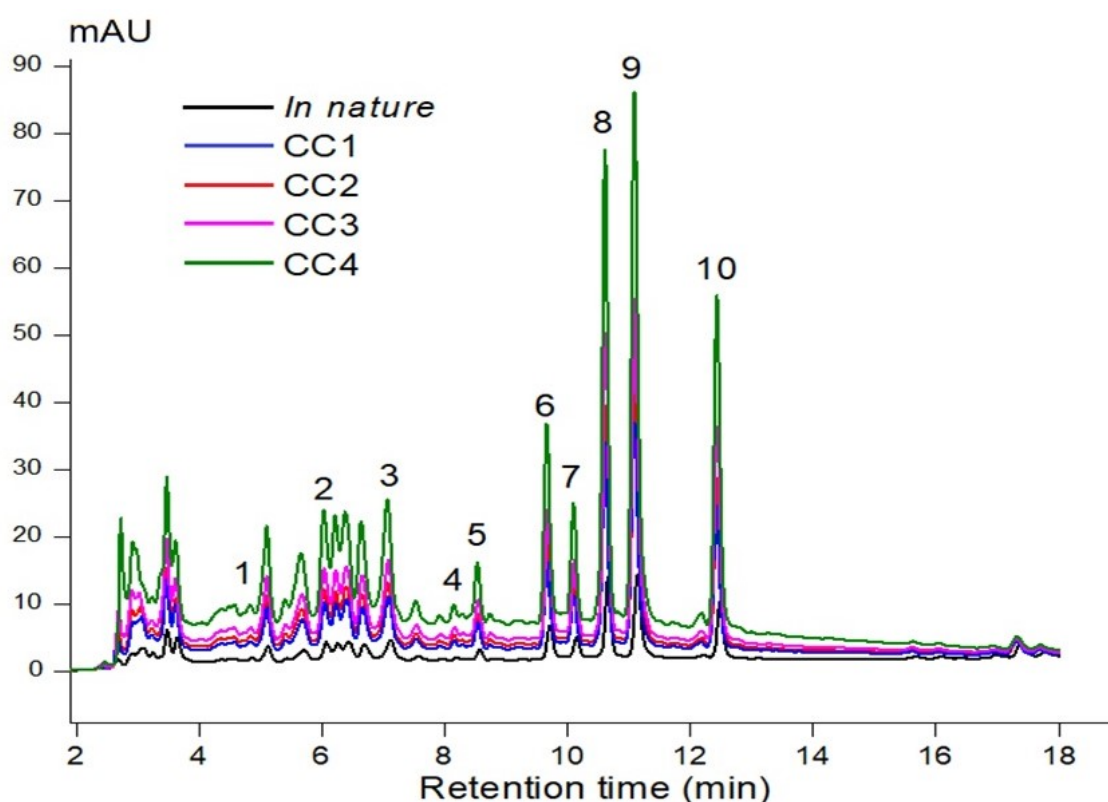


Table 10 - Major phenolic compounds identified via HPLC-DAD-MS assays for *in natura* and cryoconcentrated samples by CCG method.

Phenolic compounds (mg/g)	ID	Wavelength (nm)	Retention time (min)	<i>In natura</i> extract		CC1		CC2		CC3		CC4	
Gallic acid	1	272	4.42	0.06450 ± 0.006 ^a	0.16162 ± 0.011 ^b	0.18616 ± 0.017 ^c	0.31527 ± 0.054 ^d	0.56007 ± 0.139 ^e					
Vanillic acid	2	279	5.94	0.05373 ± 0.002 ^a	0.05796 ± 0.001 ^b	0.07249 ± 0.008 ^c	0.10172 ± 0.007 ^d	0.17849 ± 0.004 ^e					
Catechin	3	279	7.34	2.17775 ± 0.950 ^a	6.94806 ± 1.159 ^b	8.38906 ± 0.396 ^c	13.38955 ± 2.008 ^d	24.07127 ± 5.758 ^e					
Epicatechin	4	324	8.08	0.06293 ± 0.018 ^a	1.37835 ± 0.019 ^b	1.56198 ± 0.041 ^c	2.46959 ± 0.398 ^d	4.24123 ± 1.000 ^e					
Caffeic acid	5	262	8.28	0.00756 ± 0.002 ^a	0.17340 ± 0.009 ^b	0.22844 ± 0.084 ^{bcd}	0.30582 ± 0.045 ^{cd}	0.52516 ± 0.124 ^e					
p-coumaric acid	6	310	9.92	0.01260 ± 0.001 ^a	0.38342 ± 0.025 ^b	0.50584 ± 0.077 ^c	0.64275 ± 0.113 ^d	1.15072 ± 0.251 ^e					
Quercetin	7	370	11.09	0.00833 ± 0.002 ^a	0.04235 ± 0.011 ^b	0.12861 ± 0.006 ^c	0.61191 ± 0.010 ^d	0.94325 ± 0.012 ^e					
Ferulic acid	8	323	10.78	1.29075 ± 0.248 ^a	2.79151 ± 0.109 ^b	3.39623 ± 0.185 ^c	4.97643 ± 0.792 ^d	8.40516 ± 1.881 ^e					
trans-Resveratrol	9	306	10.10	0.00025 ± 0.000 ^a	0.00142 ± 0.000 ^b	0.00173 ± 0.001 ^c	0.00218 ± 0.003 ^{cd}	0.00251 ± 0.001 ^{de}					
Myricetin	10	372	12.42	0.09935 ± 0.047 ^a	2.56549 ± 0.081 ^b	3.42174 ± 0.044 ^c	4.60049 ± 0.731 ^d	7.81549 ± 1.813 ^e					

Data are expressed as mean ± SD (n = 3). Different superscript letters indicate a significant difference ($p < 0.05$) between the *in natura* extract and the cryoconcentrated samples of each cryoconcentration stage.

Figure 17 - Chromatogram containing the identification of the main phenolic species present in the sample *in natura* and in the cryoconcentrated samples of the aqueous extracts of the leaves of *M. citrifolia* by CCM method. The wavelengths, the retention time and the identification of each compound are detailed in Table 11.

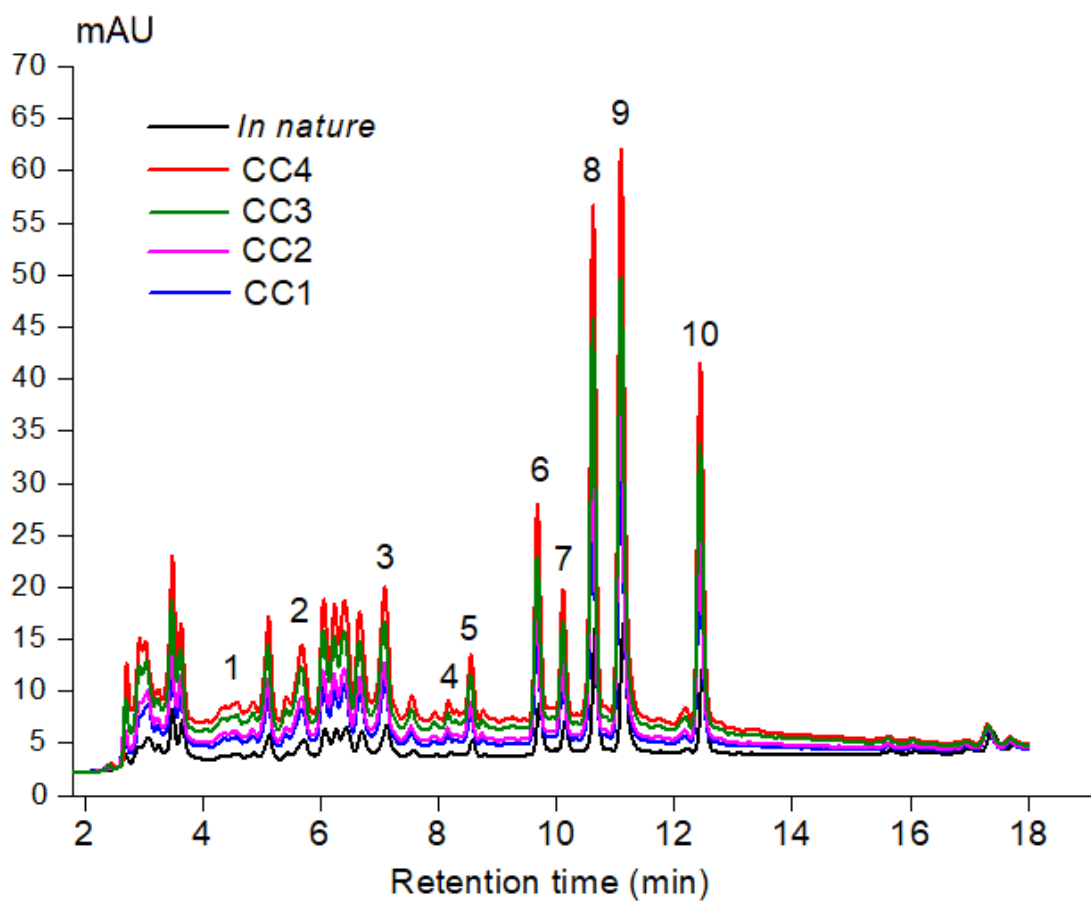


Table 11 - Major phenolic compounds identified via HPLC-DAD-MS assays for *in natura* and cryoconcentrated samples by CCM method.

Phenolic compounds (mg/g)	ID	Wavelength (nm)	Retention time (min)	<i>In natura</i> extract		CC1		CC2		CC3		CC4	
Gallic acid	1	272	4.42	0.06450	± 0.006 ^a	0.13598	± 0.005 ^b	0.19262	± 0.032 ^c	0.23379	± 0.044 ^{cd}	0.28732	± 0.017 ^{de}
Vanillic acid	2	279	5.94	0.05373	± 0.002 ^a	0.06805	± 0.004 ^b	0.07625	± 0.002 ^c	0.09437	± 0.008 ^d	0.14398	± 0.009 ^c
Catechin	3	279	7.34	2.17775	± 0.950 ^a	5.78805	± 0.387 ^b	8.33166	± 0.291 ^c	12.09118	± 0.982 ^d	13.66010	± 0.469 ^c
Epicatechin	4	324	8.08	0.06293	± 0.018 ^a	1.24557	± 0.238 ^b	1.53587	± 0.228 ^{bcd}	1.88334	± 0.356 ^{cd}	2.77438	± 0.252 ^c
Caffeic acid	5	262	8.28	0.00756	± 0.002 ^a	0.16188	± 0.027 ^b	0.20026	± 0.011 ^c	0.24636	± 0.029 ^d	0.29992	± 0.022 ^c
P-coumaric acid	6	310	9.92	0.01260	± 0.001 ^a	0.31061	± 0.001 ^b	0.40979	± 0.003 ^c	0.57371	± 0.006 ^d	0.67908	± 0.004 ^c
Quercetin	7	370	11.09	0.00723	± 0.002 ^a	0.03132	± 0.010 ^b	0.11881	± 0.005 ^c	0.60091	± 0.009 ^d	0.92036	± 0.012 ^c
Ferulic acid	8	323	10.78	1.29075	± 0.248 ^a	2.70986	± 0.823 ^{bc}	3.33964	± 0.173 ^c	4.03448	± 0.410 ^d	4.85555	± 0.154 ^c
<i>trans</i> -Resveratrol	9	306	10.10	0.00020	± 0.000 ^a	0.00102	± 0.000 ^b	0.00153	± 0.001 ^c	0.00191	± 0.003 ^{cd}	0.00221	± 0.001 ^{de}
Myricetin	10	372	12.42	0.09935	± 0.047 ^a	1.98116	± 0.044 ^b	2.77894	± 0.376 ^c	3.84101	± 0.232 ^d	4.31124	± 0.123 ^c

Data are expressed as mean ± SD (n = 3). Different superscript letters indicate a significant difference ($p < 0.05$) between the *in natura* extract and the cryoconcentrated samples of each cryoconcentration stage.

5.6. Biological activity of cryoconcentrate extracts

5.6.1. Antioxidant activity via ABTS, DPPH and ORAC methods

As discussed by Mandukhail; Aziz and Gilani (2010), the antioxidant activity shown by the biochemical components present in the leaves of *M. citrifolia* is remarkable. The analyses of the antioxidant potential via ABTS, DPPH, and ORAC methods were evaluated to verify if the cryoconcentration caused an increase in the antioxidant activity values of the studied extracts. Table 12 shows a comparison between the effect of radical scavenging activity via ABTS and DPPH assays, respectively, for both methods of cryoconcentration performed on aqueous extracts of *M. citrifolia* leaves.

Based on the results presented via ABTS and DPPH methods, there were significant differences ($p < 0.05$) in the different concentrated fractions (CC1 to CC4) in both cryoconcentration methods. In both methods, which are reduced by antioxidants of the samples, either by electron transfer or hydrogen transfer, the radical scavenging activity increased as the cryoconcentration steps progressed.

As also mentioned by Zielinski et al. (2019) in a similar study involving the cryoconcentration of apple juice, there is a strong indication that the increase in antioxidant activity is related to the increase in the TPC of cryoconcentrate extracts. This makes perfect sense since the potential antioxidant is also attributed to the content of biochemically active compounds with the ability to interact in the scavenging of free radicals. However, the Folin-Ciocalteu method, for example, is based on electron transfer, but the reducing power against this compound is not restricted to phenolic compounds (CAMEL; STAGNARO; MARCHIONNI, 2015; CORREA; RUIZ; MORENO, 2018).

Based on the analytical results referring to antioxidant activity via ABTS test; for the gravitational cryoconcentration method, the increase in antioxidant activity was significant for both methods ($p < 0.05$). It is noted values of $0.35 \text{ mgGAE.mL}^{-1}$ for the sample *in natura*, increasing to $0.40 \text{ mgGAE.mL}^{-1}$, ending with $1.44 \text{ mgGAE.mL}^{-1}$ in the last step of the process, a value 4 times higher in the antioxidant activity via ABTS for CC4 compared to the *in natura* sample. ABTS analysis for the microwave-assisted method showed similar behavior in terms of increased antioxidant activity. There was no significant difference between the values corresponding to the sample *in natura* and CC1 ($p < 0.05$), $0,13 \text{ mgGAE.mL}^{-1}$ and $0,18 \text{ mgGAE.mL}^{-1}$ (Table 14). However, at the

last cryoconcentration stage, the antioxidant activity via DPPH increased to 0.60 mgGAE.mL⁻¹, a value 4.6 times higher when compared to the *in natura* sample.

Table 12 - Summary of the results of the analysis of antioxidant activity via ABTS and DPPH methods for the cryoconcentrated and ice fractions in both cryoconcentration methods for the aqueous extract of *M. citrifolia* leaves.

Sample/ Cryoconcentration method	Antioxidant activity via the ABTS method (mgGAE.mL ⁻¹)	
	Gravitational	Microwave-assisted
<i>In natura</i>	0.35 ^b ± 0.03	0.13 ^{ab} ± 0.02
CC1	0.40 ^b ± 0.02	0.18 ^{ab} ± 0.01
G1	0.14 ^a ± 0.00	0.05 ^a ± 0.01
CC2	0.77 ^c ± 0.01	0.25 ^b ± 0.06
G2	0.15 ^a ± 0.00	0.08 ^a ± 0.01
CC3	1.06 ^d ± 0.04	0.46 ^c ± 0.03
G3	0.15 ^a ± 0.00	0.13 ^{ab} ± 0.00
CC4	1.44 ^c ± 0.06	0.60 ^d ± 0.04
G4	0.04 ^a ± 0.00	0.15 ^{ab} ± 0.00

Sample/ Cryoconcentration method	Antioxidant activity via the DPPH method (mgGAE.mL ⁻¹)	
	Gravitational	Microwave-assisted
<i>In natura</i>	0.99 ^b ± 0.07	0.87 ^f ± 0.01
CC1	1.21 ^c ± 0.01	1.28 ^e ± 0.01
G1	0.10 ^a ± 0.01	0.11 ^a ± 0.00
CC2	1.92 ^d ± 0.01	1.72 ^b ± 0.00
G2	0.11 ^a ± 0.00	0.10 ^a ± 0.00
CC3	2.16 ^c ± 0.03	1.80 ^c ± 0.00
G3	0.12 ^a ± 0.00	0.11 ^a ± 0.00
CC4	2.35 ^f ± 0.05	1.90 ^d ± 0.01
G4	0.15 ^a ± 0.00	0.12 ^a ± 0.00

Note: Data are expressed as mean ± SD (n = 4). Values followed by the same letter do not differ (ANOVA, followed by Tukey's test; $p < 0.05$). Different symbols indicate significant differences ($p < 0.05$) for each stage of cryoconcentration analyzed in each method separately.

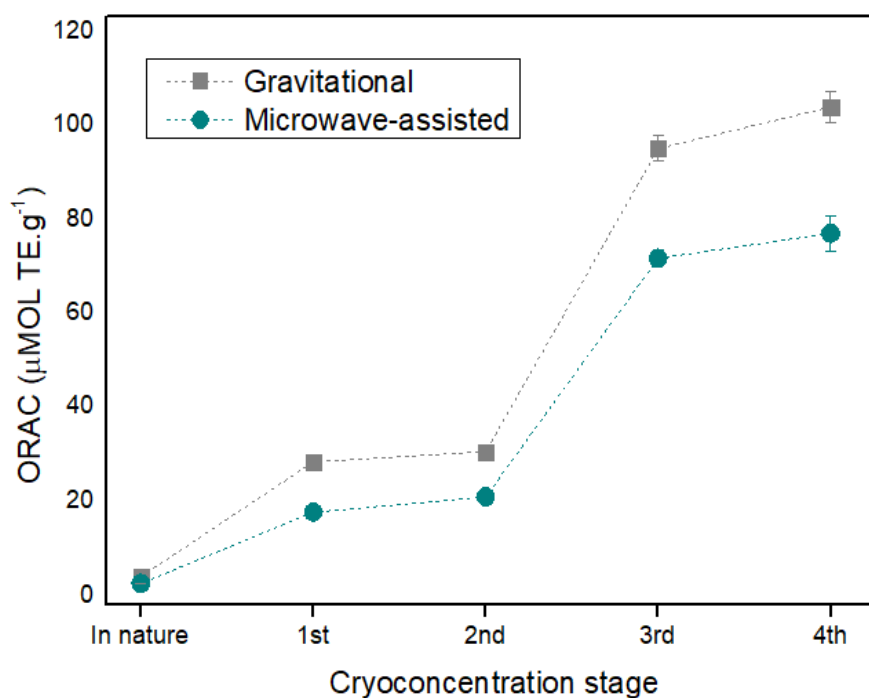
In the case of DPPH tests, there is an increase in antioxidant activity for each stage of the cryoconcentration process in both defrosting methods used. In summary, for all stages of the process, whether gravitational or microwave-assisted, the growth was significant ($p < 0.05$) for the analysis in DPPH (Table 12). An important fact is that for both cryoconcentration methods used, the antioxidant activity exposed via the DPPH method showed higher values than in the analysis via ABTS.

In general, the antioxidant activity increased with the advance of the

cryoconcentration steps for both methods used, thus showing the efficiency of the method to increase the antioxidant activity of the aqueous extracts of *M. citrifolia* leaves. According to Adorno et al. (2017), although the behavior is similar for analyses via ABTS and DPPH, it is difficult to compare the results obtained by different methods of determining antioxidant activity. These differences are related to the different mechanisms involved during the reaction, encompassing the most diverse types of biochemical species in the extract that can alter the antioxidant potential of the sample as a whole.

The third test used to determine the antioxidant activity in aqueous extracts of cryoconcentrated *M. citrifolia* leaves is based mainly on a radical initiator to generate the peroxy radical, and its mechanism of action is hydrogen atom transfer (OU et al., 2002). Figure 18 illustrates the effect of antioxidant activity via the ORAC method for cryoconcentrate extracts in both thawing methods. At first, the antioxidant activity was higher for the gravitational method when compared to the microwave-assisted method.

Figure 18 - Antioxidant activity via the ORAC method verified in the concentrated extracts of leaves of *M. citrifolia* in each stage for both cryoconcentration methods used.



In summary, the behavior of antioxidant activity via the ORAC method was similar in both thawing methods (Figure 18). It can be noticed that both in the gravitational and

microwave-assisted method, there is a significant difference in the antioxidant activity in relation to the sample *in natura* when compared to CC1 ($p < 0.05$). However, there was no significant difference between steps 1 and 2 in both methods of cryoconcentration. Subsequently, the values of antioxidant activity increased as we proceed to step 3 of the process. Finally, the values of $103 \pm 3 \text{ uMOL TE.g}^{-1}$ and $76 \pm 3 \text{ uMOL TE.g}^{-1}$ of the antioxidant activity for the gravitational and microwave-assisted methods respectively, presented in the last cryoconcentration stage did not show significant differences in relation to the values obtained from the thawing step 3 ($p < 0.05$).

Such response is similar to the results presented by Arend et al. (2017) and Adorno et al. (2017). Both works suggested that in an industrial process, cryoconcentration could be interrupted in the third stage, if we consider this method of obtaining antioxidant activity, thus reducing the processing time and the consumption of energy.

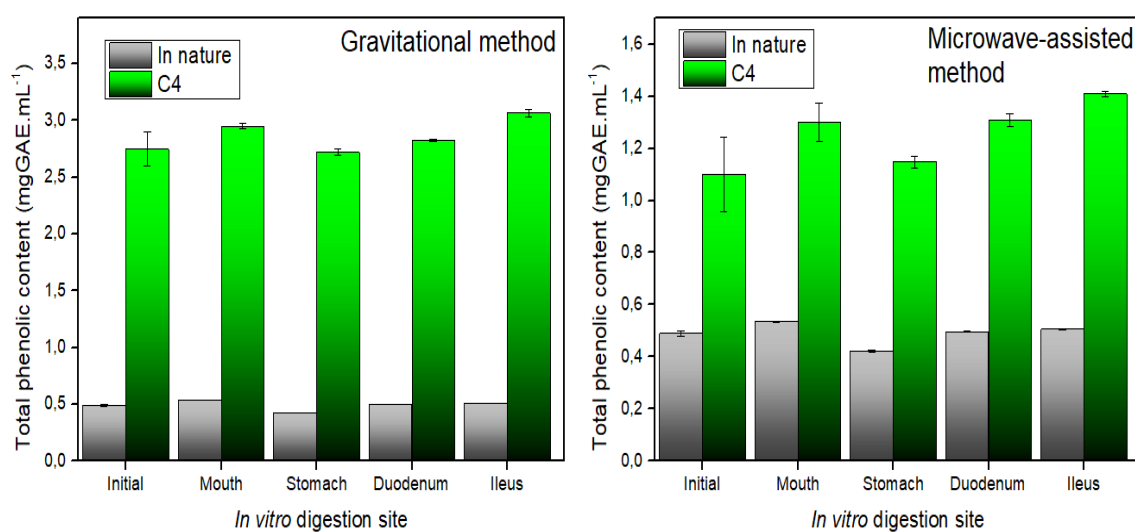
5.6.2. *In vitro* assays of simulation of gastrointestinal digestion

Figures 19 and 20 illustrate the behavior of TPC and antioxidant activity via ABTS, respectively, of samples *in natura* and samples referring to the last stage of cryoconcentration (CC4) submitted to the *in vitro* process of simulation of gastrointestinal digestion in both methods of cryoconcentration used for samples of aqueous extract of *M. citrifolia* leaves. One of the most important considerations to be carried out in the analysis of the behavior of such variables submitted to the simulated digestion process is the fact that the evaluation of the parameters in each cryoconcentrated and ice sample, will be centered mainly on how much the TPC and the antioxidant activity it is susceptible to sudden changes in pH (YUAN et al., 2019).

Considering the behavior of TPC during *in vitro* digestion in different gastrointestinal digestion sites in both thawing methods, it is noted that statistically the TPC values were not affected by the enzymatic attack promoted by simulated digestion ($p < 0.05$). Table 13 illustrates the analytical values for the TPC. As shown in Figure 19, the TPC for samples referring to the last stage of CCG method remained much higher when compared with samples *in natura*. The TPC content for the concentrated samples was $2.75 \text{ mgGAE.mL}^{-1}$ CC4 without the enzymatic attack; $2.95 \text{ mgGAE.mL}^{-1}$ for the region corresponding to the mouth; $2.72 \text{ mgGAE.mL}^{-1}$ for the region corresponding to

the stomach; 2.82 mgGAE.mL⁻¹ for the region corresponding to the duodenum and 3.06 mgGAE.mL⁻¹ for the region corresponding to the ileum.

Figure 19 - Behavior of TPC in the *in vitro* simulation of gastrointestinal digestion for extracts of leaves of *M. citrifolia* cryoconcentrated in both studied methods. Note that the cryoconcentrated fractions (samples) evaluated were those corresponding to the last executed cryoconcentration stage (CC4). The analysis was performed by comparing the concentrated samples with the fresh samples for each portion (region) of the simulated digestion.



Considering the microwave-assisted cryoconcentration process, the behavior of TPC for samples *in natura* and CC4 during simulated digestion *in vitro*, was quite similar to what occurred with samples cryoconcentrated by the CCG method. In summary, there were significant differences in relation to the enzymatic attack that simulated digestion in different portions of the gastrointestinal tract, mainly those related to digestion in the stomach and the CC4 sample without passing through the digestive process (Table 13). However, the TPC values for cryoconcentrated samples remained much higher when compared to samples *in natura* even submitted to the digestive process. For CC4 samples from microwave-assisted cryoconcentration, TPC showed values of 1.10 mgGAE.mL⁻¹ before simulated digestion; 1.30 mgGAE.mL⁻¹ for digestion referring to the mouth; 1.15 mgGAE.mL⁻¹ for stomach digestion; 1.31 mgGAE.mL⁻¹ for digestion referring to the duodenum region and 1.41 mgGAE.mL⁻¹ for digestion referring to the

ileum region (Table 13).

Table 13 - Behavior of TPC and antioxidant activity via ABTS method during *in vitro* simulation of gastrointestinal digestion for CC4 samples extracts of leaves of *M. citrifolia* cryoconcentrated in both studied methods.

Gastrointestinal region/ Cryoconcentration method	Behavior of TPC (mgGAE.mL ⁻¹)	
	Gravitational	Microwave-assisted
Initial	0.49 ^a ± 0.01	0.49 ^a ± 0.01
Mouth	0.53 ^a ± 0.00	0.53 ^a ± 0.00
Stomach	0.42 ^a ± 0.00	0.42 ^a ± 0.00
Duodenum	0.50 ^a ± 0.00	0.50 ^a ± 0.00
Ileus	0.51 ^a ± 0.00	0.51 ^a ± 0.00
CC4 Initial	2.75 ^b ± 0.15	1.10 ^b ± 0.14
CC4 Mouth	2.95 ^b ± 0.02	1.30 ^{bcd} ± 0.07
CC4 Stomach	2.72 ^b ± 0.30	1.15 ^{bc} ± 0.02
CC4 Duodenum	2.82 ^b ± 0.01	1.31 ^{cd} ± 0.03
C4 Ileus	3.06 ^b ± 0.03	1.41 ^d ± 0.01

Gastrointestinal region/ Cryoconcentration method	Behavior of antioxidant activity via ABTS (mgGAE.mL ⁻¹)	
	Gravitational	Microwave-assisted
Initial	0.04 ^a ± 0.00	0.04 ^{abc} ± 0.00
Mouth	0.05 ^a ± 0.00	0.05 ^{bc} ± 0.00
Stomach	0.01 ^a ± 0.00	0.01 ^a ± 0.00
Duodenum	0.01 ^a ± 0.00	0.01 ^{ab} ± 0.00
Ileus	0.21 ^b ± 0.00	0.21 ^f ± 0.00
CC4 Initial	0.34 ^c ± 0.00	0.15 ^{de} ± 0.00
CC4 Mouth	0.40 ^d ± 0.02	0.17 ^{ef} ± 0.01
CC4 Stomach	0.18 ^b ± 0.01	0.07 ^c ± 0.01
CC4 Duodenum	0.33 ^{cd} ± 0.03	0.13 ^d ± 0.01
C4 Ileus	0.83 ^e ± 0.02	0.47 ^g ± 0.02

Note: Data are expressed as mean ± SD (n = 4). Values followed by the same letter do not differ (ANOVA, followed by Tukey's test; $p < 0.05$). Different symbols indicate significant differences ($p < 0.05$) for each stage of cryoconcentration analyzed in each method separately.

We can conclude that the enzymatic attack under different pH values that simulated the *in vitro* digestion process did not affect the TPC and the cryoconcentrated fractions in both thawing methods used. In other words, theoretically, the TPC would remain intact at the end of the digestion of the CC4 samples. The significant difference ($p < 0.05$) verified in the CC4 cryoconcentrated sample via microwave-assisted method when subjected to simulated digestion in the stomach region, suggests that the cryoconcentration method affects the significant variation of the CPT for this region of

the gastrointestinal tract. However, considering that, as already mentioned in this study, the content of TPC was higher in cryoconcentrated samples via the gravitational method, this technique used for the retention of phenolics in samples of aqueous extract of leaves of *M. citrifolia* was more satisfactory in maintaining these bioactive compounds when they were submitted to a complete simulation of gastrointestinal digestion. A similar result was found by Ryu & Koh (2018), who carried out an *in vitro* digestion process to verify the stability of the anthocyanin content *Rubus occidentalis* L.. It was found that during simulated digestion, digestion in the stomach did not significantly affect the content total anthocyanins.

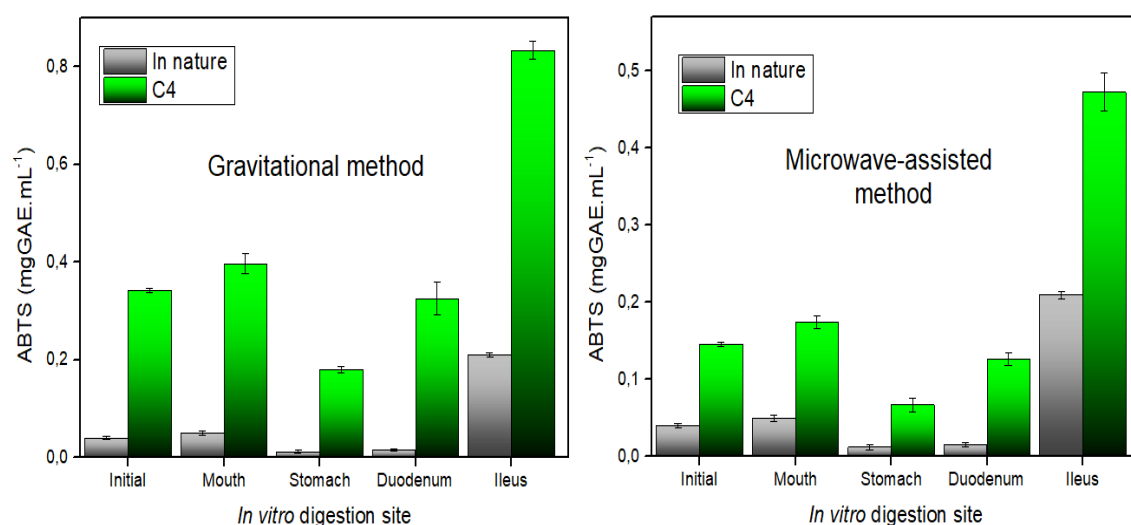
Figure 20 illustrates the behavior of antioxidant activity via ABTS of samples *in natura* and for CC4 cryoconcentrated samples by the CCG and CCM method, submitted to the *in vitro* simulated digestion process. The numerical values of the antioxidant activity can be seen in Table 15. It is noticed that the antioxidant activity in both cryoconcentration methods used was significantly affected in the different *in vitro* digestion sites ($p < 0.05$). In both cryoconcentration processes, the highest values of antioxidant activity via ABTS, were found in the ileum region, 0.83 mgGAE.mL⁻¹ for the gravitational method and 0.47 mgGAE.mL⁻¹ for the microwave-assisted method (Table 13).

Considering the effect of antioxidant activity via ABTS for CC4 samples from both cryoconcentration processes submitted to the *in vitro* digestion process, it is clear that the region corresponding to digestion in the stomach was the one that most affected radical capture activity via ABTS, when compared to other *in vitro* digestion sites. The antioxidant activity values for CC4 after digestion in the stomach were 0,18 mgGAE.mL⁻¹ and 0,07 mgGAE.mL⁻¹ for the gravitational and microwave-assisted thawing processes.

Such reduction in antioxidant activity by ABTS in the digestion region corresponding to the stomach may be related to how the pH influences the principle of the antioxidant reaction, where the compound has the ability to supply electrons or hydrogen (LEE et al., 2018). As previously described in that study, the antioxidant activity values via ABTS increased as the cryoconcentration steps progressed. Consequently, such an increase was, among other factors, due to the presence or the capacity to retain bioactive substances that the cryoconcentration process has on these compounds. Such results indicated that the aqueous extract of cryoconcentrated *M.*

citrifolia leaves had antioxidant activity and that this activity was closely related to the concentration.

Figure 20 - Behavior of antioxidant activity via ABTS method in the *in vitro* simulation of gastrointestinal digestion for extracts of leaves of *M. citrifolia* cryoconcentrated in both studied methods. Note that the cryoconcentrated fractions (samples) evaluated were those corresponding to the last executed cryoconcentration stage (CC4). The analysis was performed by comparing the concentrated samples with the fresh samples for each portion (region) of the simulated digestion.



According to Lee et al. (2018), the principle of the antioxidant reaction is that the compound has the ability to supply electrons or hydrogen. However, the antioxidant mechanism of the bioactive compounds present in the different structures of *M. citrifolia* is not yet fully understood due to their high molecular weight, complicated constituents, and structure (THOO et al., 2013). However, based on the study developed by Yuan et al. (2019) the low pH value exerted by simulated *in vitro* digestion in the stomach region, can contribute precisely to the ability to supply electrons to capture free radicals that such bioactive compounds have, thus compromising the reduction of antioxidant activity.

6. CONCLUSIONS OF PART I

The option to use block cryoconcentration techniques via CCG and CCM methods was quite satisfactory and efficient in the retention process of bioactive compounds present in *M. citrifolia* leaf extracts. Given these methods, the use of robust and expensive equipment is not necessary, with easy process execution and high performance in the recovery of the final product.

Both cryoconcentration methods allowed the retention of a large amount of solids and phenolic compounds in the concentrated fractions, with high concentration factors in the retention of solutes and high efficiency in the concentration of phenolic compounds. Although the use of the CCG technique resulted in a greater accumulation of solids and retained phenolic compounds; both methods are considered efficient for this purpose.

The FTIR spectroscopy for the concentrated fractions of the aqueous extract of leaves of *Morinda citrifolia* allowed us to verify the evidence of the presence of biochemically active compounds with verified phytotherapeutic properties. Such a result leads to the conclusion that the extracts corresponding to the last stage of cryoconcentration for both methods used can be processed and applied as a product with a potential phytotherapeutic effect.

The higher viscosity values found in the extracts referring to the last stage of cryoconcentration in both methods studied are due to the high effectiveness of accumulation of solids in the concentrated samples. This presents an effect on mass transfer at the solute-ice interface, thus having a direct effect on the efficiency parameters in the retention of solids during the defrosting process.

Antioxidant activity via ABTS, DPPH, and ORAC methods increased as the stages of the cryoconcentration process progressed. We may conclude that the concentrated samples had a higher antioxidant effect when compared to the *in natura* samples.

The *in vitro* simulation process of gastrointestinal digestion did not affect the total phenolics content in any sample referring to the cryoconcentrated fractions, revealing that the TPC remains intact without significant reduction at the end of the simulated digestive process. In contrast, the antioxidant activity via the ABTS method was reduced during the simulated digestion process, mainly in the region referring to

digestion in the stomach, possibly due to the low pH value in this region, which leads to a reduction in antioxidant activity.

The results are very promising; however, more in-depth studies are needed, especially concerning the recovery of residual solids in the ice fractions. In addition, the concentrated products resulting from the bioactive retention techniques produced a product with potential for phytotherapeutic use.

PART II

Nanobiotechnology and food science connection: biosynthesis of silver nanoparticles by cryoconcentrated extracts of *M. citrifolia*

Conceptual diagram of Part II

Why?

- Among the different living systems harnessed for the synthesis of metal nanoparticles, plants have found predominant application in the synthesis process, as the use of plants for the biosynthesis of metal nanoparticles can be beneficial compared to other biological agents such as microorganisms.
- Plants are better synthesizers than other biological methods due to the abundant availability of plant resources when compared to other forms of biological resources. Furthermore, plants provide a better platform for nanoparticle synthesis as they are non-toxic chemicals and provide natural bioreduction agents.
- In addition to containing high amounts of bioactive compounds with relevant nutraceutical properties, *Morinda citrifolia* leaf extracts provide large amounts of biologically active agents in the process of forming silver nanoparticles, making this plant species an excellent supplier of raw material for bioconversion.

What has already been done?

- Studies such as those of Pai et al. (2015) and Morales-Lozoya et al. (2021) already make use of the application of leaf extracts of *M. citrifolia* in the synthesis of silver nanoparticles. However, there is nothing described in the literature if the use of extracts with greater deposition of bioactive due to the cryoconcentration process allows the obtaining nanoparticles with improved physicochemical properties. The novelty of this part of the study is centered on verifying this possibility.

Study hypotheses:

- If the cryoconcentration of extracts from *M. citrifolia* leaves promotes increased retention of bioactive compounds, and these same bioactive compounds are the main components responsible for the biosynthesis of silver nanoparticles in a colloidal medium, the use of concentrated extracts in the biosynthesis will result in nanoparticles with even more improved physicochemical properties?

Experimental methods:

- Physicochemical characterization of the nanoparticles obtained through the determination of the average size, stability in colloidal medium by zeta potential, determination of the chemical nature of the nanoparticles by UV-Vis spectroscopy, FTIR and Atomic Absorption with Flame and electron microscopy assays.
- Study of the interference of the variation of biosynthesis parameters on the size and stability of nanoparticles.

Responses:

- Silver nanoparticles from cryoconcentrated extracts with smaller average size and greater functional stability against the same nanoparticles from the non-cryoconcentrated stratum.

1. INTRODUCTION

Nanotechnology, an emerging and fascinating field of science, allows for advanced research in many areas, and recent nanotechnological discoveries can open up new applications in the field of biotechnology and agriculture. Particularly, nanotechnology has contributed to chemical sensing, water cleaning and disease prevention as well as conversion of agricultural and food waste into energy and other useful by-products through enzymatic nanobioprocessing, (AL-WHAIBI; FIROZ; AL-KHAISHANY, 2015; NASH; SHOSEYOV, 2016).

The search for new biosynthesis routes has dictated the pace of new research in the field of biosynthesis of nanometals with functional properties (ZHANG; HU; DENG, 2016). Meeting this demand, nanoparticles (NPs), an indispensable product of nanotechnology, and especially metallic nanoparticles, enter the scene (ZHANG et al., 2011; TANAKA; CHUJO, 2014). Engineered metal nanoparticles are produced by various physical and chemical methods. However, these methods are harmful as the chemicals used are often toxic, flammable, and not easily disposable due to environmental issues, expensive, and have a low production rate. Then, new and sustainable methodologies of the so-called “green nanotechnology” emerge, which were recently developed for the synthesis of NPs (EL-SHERBINY; SALIH, 2018). New biochemical routes of natural precursors have been analytically studied for the design and synthesis of nanoparticles with the desired size, shape, and functionality (SINGH et al., 2018).

The use of microorganisms (fungi and bacteria), as well as natural products (fruit juices, polysaccharides, and plant extracts) containing abundant hydrogen atoms for the biosynthesis of NPs, is more advantageous when compared to conventional methods of synthesis in terms of biocompatibility, low production, cost and natural bioreducing chemical atmosphere (LI et al., 2011; EL-SHERBINY; SALIH, 2018). These synthetic pathways do not use toxic solvents, chemical precursors, and additional reducing agents (EL-RAFIE; EL-RAFIE; ZAHRAN, 2013). The green synthesis of metallic nanoparticles also employs amino acids, phytochemicals, polysaccharides, polyphenols, and vitamins as precursor components of biotransformation (MITTAL et al., 2014). Notably, there is an immense need to develop better methodologies and approaches using green nanotechnology to increase the suitability of the biosynthesis of nanometals, one of these approaches is via the use of plant extracts, apparently,

appropriation of new mechanisms and pathways that make it possible to increase the yield. of bioproduction through the use of plants, is characterized as a new tool in the acquisition of an innovative method/technology.

The ability of plant extracts to reduce metal ions has been known since the early 1900s. The literature indicates that NPs present in soil impact plant growth, cell structure, and physiological and biochemical functions (RICO; PERALTA-VIDEA; GARDEA-TORRESDEY, 2015). However, when considering the bioreductive property inherent to plant extracts, the nature of the reducing agents involved is not well understood yet. Nevertheless, due to their simplicity, the use of live plants or extracts of whole plants and plant tissues to reduce metallic salts to nanoparticles has attracted considerable attention in the last 30 years (NAGRA et al., 2020).

The synthesis mediated by plant extracts is a growing focus of attention, the already highlighted simplicity of performing biosynthesis assays is combined with the ease of scaling up, non-aggressive environment and low cost of operation (SARATALE et al., 2018). Furthermore, plant extracts can act as both reducing and stabilizing agents in the synthesis of nanoparticles, of which the source of the plant extract is known to influence the characteristics of nanoparticles. This is because different extracts contain different concentrations and combinations of organic reducing agents, that is, the vast presence of biochemically active compounds in plant extracts are primarily responsible for the biosynthesis mechanism (MITTAL; CHISTI; BANERJEE, 2013; PERALTA-VIDEA et al., 2016; NAIKOO et al., 2021).

The biosynthesis of nanometals through the use of plants involves the direct participation of phytochemical components in the bioproduction mechanism. Moreover, the concentration of bioactive in food liquids, mainly of plant origin, covers the increase in the content of biochemical components of these foods. Thus, we have the possibility of obtaining a new dynamic and innovative tool that promotes the compilation of the technique of concentration of bioactive from food liquids of plant origin, and the use of these biomolecules in the synthesis of nanometals with functional properties.

The objective of this part of the study will be precisely the application of concentrated fractions of *M. citrifolia* leaves obtained by cryoconcentration methods presented in this study, in the synthesis of NPs, with emphasis on the bioproduction of silver nanoparticles (AgNPs). Such investigation will make use of methods that include

clean, low-cost and high-performance technologies, integrating the use of residues from the food industry with high biological value. The originality of this part of the study is related to the use and comparison of extracts concentrated in the physicochemical properties of the AgNPs obtained. Finally, we hope that combining the cryoconcentration technique with metal biosynthesis results in the generation of stable nanoparticles in a colloidal system, with improved functional properties.

2. AIMS

2.1. General aim

The general objective of this part is to promote the biosynthesis of silver nanoparticles (AgNPs) through the use of cryoconcentrated extracts from *Morinda citrifolia* leaves obtained in part 1 of this study.

2.2. Specific aims

- Compare the aspects of size and stability of AgNPs obtained from extracts concentrated by the CCG and CCM methods.
- Evaluate the control of the size of silver nanoparticles under different biosynthesis conditions.
- Verify the stability of silver nanoparticles, including their agglomeration and dispersion aspects, via zeta potential analysis under different biosynthesis conditions.
- Characterize chemically and structurally silver nanoparticles via UV-Vis, FTIR, and Electron Microscopy.

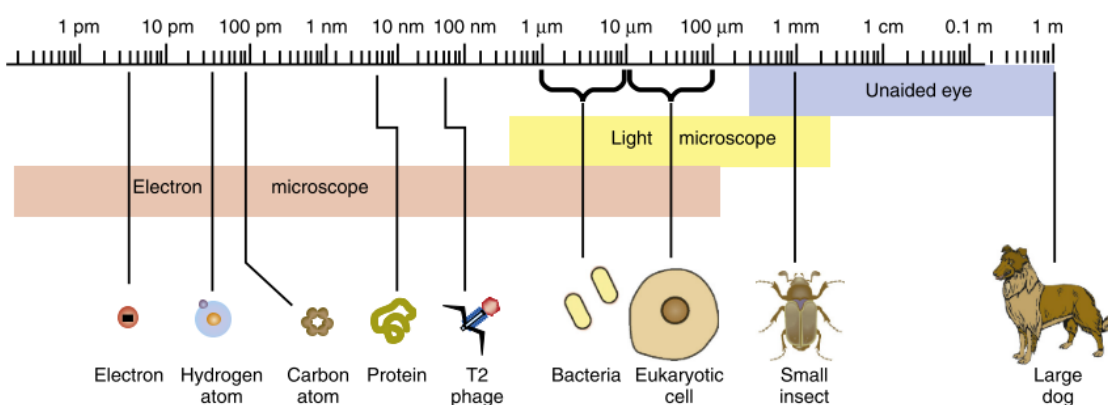
3. LITERATURE REVIEW

3.1. Nanotechnology inspired by living organisms

Nanotechnology works centered on the processing of separation, assimilation, and deformation of materials by an atom or a molecule” was well established by Professor Norio Taniguchi, from Tokyo Science University, for the term “nanotechnology”. Professor Taniguchi's words were blunt: “this is the branch of science of manipulating matter on an atomic or molecular scale.” Since then, nanotechnology has advanced as a scientific innovation in the 21st century, comprising an interdisciplinary area that comprises the construction, handling, and use of these materials with a scale smaller than 100 nm. In short, nanotechnology treats matter at the molecular level and has indeed entered the domain of a vast area of applications (DE MORAIS et al., 2014; NAIKOO et al., 2021).

Once it focuses on the synthesis and manipulation of particle size structures with dimensions smaller than 100 nm, Figure 21 seeks to illustrate a scale comparison of sizes where nanotechnology is approached. Nanotechnology combines principles with physical and chemical procedures to generate nanosized particles with a specific function. However, there is a great stimulus on the part of researchers, who increasingly seek to support nanotechnology in the life sciences, especially in biomedical devices and medicine. Nanoparticles exhibit completely new or improved properties based on specific characteristics such as size, shape, and orientation (JAIN, 2011; NAIKOO et al., 2021).

Figure 21 - Size comparisons where objects range in size from 1 meter to 1 picometer.



Adapted from Clark and Pazdernik (2016)

Taking into account that the internal components of biological cells are on the same scale as those studied by nanotechnology. Thus, the main practical objective of what can now be called nanobiotechnology is to use biological components to perform tasks at the nanoscale (SINGH et al., 2018).

The biological synthesis of nanoparticles is an economic and ecological method and can replace physical and chemical methods, as these methods are commonly toxic and expensive. Consequently, nanomaterials have been synthesized using microorganisms and plant extracts. The use of plant extracts for nanoparticle synthesis is potentially advantageous over microorganisms due to the ease of scaling up biological hazards and the elaborate process of maintaining cell cultures.

Biological methods can employ microorganism cells or plant extracts to produce nanoparticles. Nanoparticle biosynthesis is an exciting recent addition to the large repertoire of nanoparticle synthesis methods, and now, nanoparticles have entered a period of commercial exploitation. Au, Ag, Zn and Cu produced by medicinal plants are the most pharmacologically active, possibly due to the fixation of several pharmacologically active residues (SARATALE et al., 2018).

3.2. Nanotechnology and the principle of sustainable and green chemistry

Globally, many marked changes in agricultural production patterns are taking place today. Such changes were only possible through the application of modern labor-saving technologies to intensive farm mechanization, irrigation, post-harvest management, and use of improved crop varieties. While this remarkable progress is indeed remarkable, food insecurity still exists, leading to poverty in many developing countries (HUSEN; SIDDIQI, 2014).

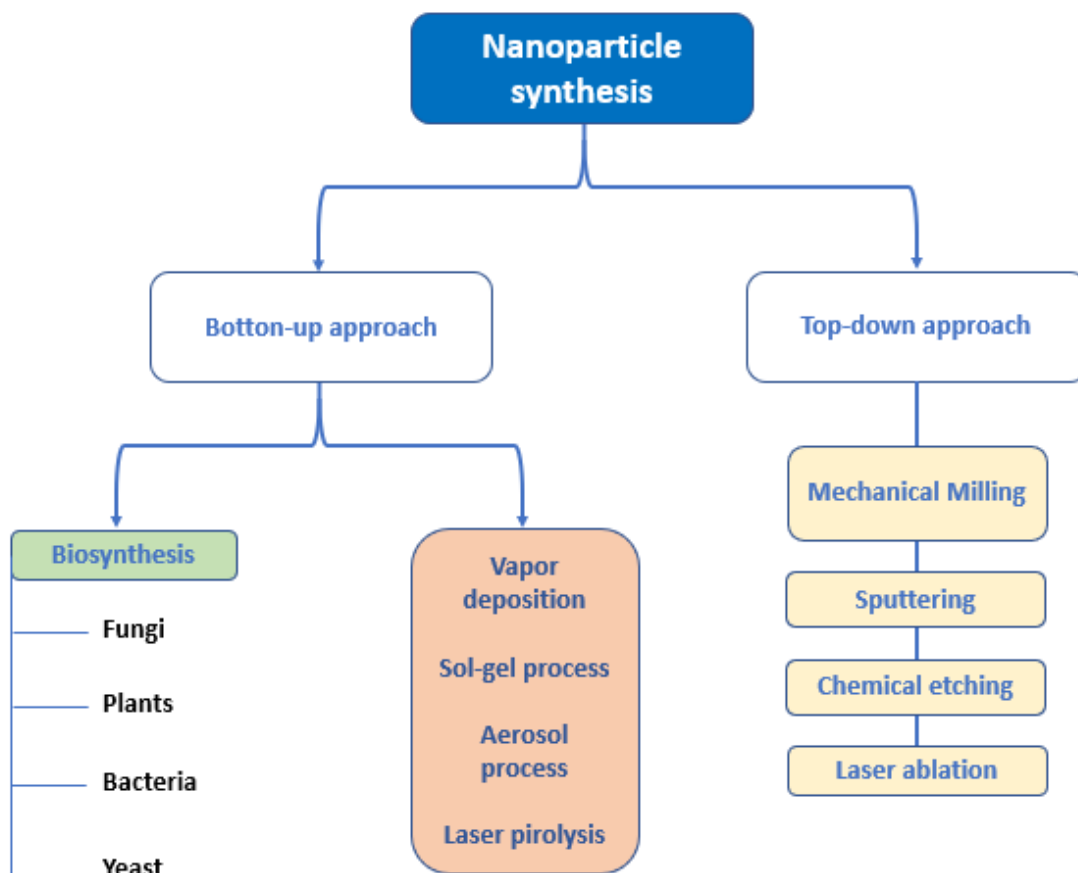
A huge global problem is to increase food production with limited resources and minimal and efficient use of fertilizers and pesticides without polluting the environment. Since the generation of food waste of plant origin is a recurring problem in the food industry, nanotechnology emerges as a potential tool to mitigate this problem (DAWSON, 2008). Plants are capable of accumulating metals on a nanometer scale, up to concentrations hundreds of times higher than those found in non-metal accumulating plants (HUSEN; SIDDIQI, 2014). Since plant residues from the food industry comprise a large accumulation of tailings, leaves, and stalks, for example, they

appear as excellent raw materials in the acquisition of nanometals. Taking into account that the proposed biosynthesis of metals by plants includes a methodology that discards the use of reagents and materials harmful to the environment, the biochemical route of synthesis can be considered sustainable, being then considered an environmentally friendly chemical principle, popularly called "green chemistry" (RAJAN et al., 2015).

The selection of a green or ecological solvent, a good reducing agent, and safe material for stabilization are the most important requirements for the synthesis of nanoparticles. Extensive synthetic pathways have been used to make nanoparticles, with physical, chemical, and biosynthetic routes being the most common. Chemical procedures are generally very expensive and involve the use of dangerous and poisonous chemicals that pose a variety of environmental hazards (NATH; BANERJEE, 2013). A biosynthetic pathway is a green approach to producing nanoparticles for biomedical purposes that is safe, biocompatible, and ecologically beneficial. Fungi, algae, bacteria, plants, and other organisms can be used to carry out this synthesis. Due to the presence of phytochemicals in their extract that act as a stabilizer and reducing agent, some plant parts such as leaves, fruits, roots, stems, and seeds have been used in the synthesis of various nanoparticles. Numerous biological and physicochemical mechanisms for nanoparticle formation can be divided into two categories: bottom-up and top-down approaches. Figure 22 depicts the creation of nanoparticles using several biological and physicochemical methods.

Among the different living systems harnessed for the synthesis of metal nanoparticles, plants have found predominant application in the synthesis process, as the use of plants for the biosynthesis of metal nanoparticles can be beneficial compared to other biological agents (KUMAR; CHISTI; CHAND, 2013). In the case of plant systems, the elaborate process of maintaining cell cultures is eliminated. In the current scenario of nanotechnology, plants are better synthesizers than other biological methods due to the abundant availability of plant resources when compared to other forms of biological resources. Furthermore, plants provide a better platform for nanoparticle synthesis as they are non-toxic chemicals and provide natural covering agents. In addition, the use of plant extracts also reduces the cost of isolation of microorganisms and culture media, increasing the cost-competitive viability in relation to the synthesis of nanoparticles by microorganisms (PRASAD, 2014; AL-WHAIBI; FIROZ; AL-KHAISHANY, 2015).

Figure 22 - Main methods of nanoparticles synthesis via biological and physicochemical approaches.



Adapted from Naikoo et al. (2021).

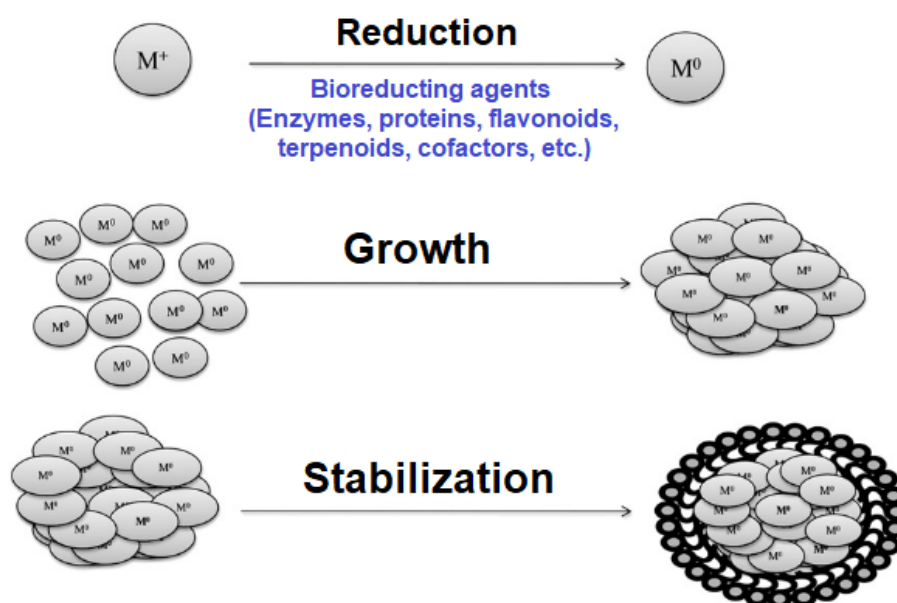
3.2.1. Biosynthesis of nanometals by plants

Methods for generating nanoparticles can generally be classified as “top down” or “bottom up”, as seen in Figure 22. The top-down synthesis produces nanoparticles by reducing the size of a suitable starting material. Physical and chemical treatments are used to reduce the size of the object. Because the surface chemistry and other physical attributes of nanoparticles are heavily dependent on the surface structure, top-down production methods create defects in the product's surface structure, which is a severe restriction (NAGRA et al., 2020).

In bottom-up syntheses, nanoparticles are synthesized from smaller entities, for example, joining smaller atoms, molecules, and particles (KUMAR; CHISTI; CHAND, 2013). The nanostructured building blocks of nanoparticles are produced first, then

assembled to make the final particle in bottom-up synthesis. Chemical and biological methods of synthesis are used predominantly in bottom-up synthesis. The bottom-up mechanism for the synthesis of nanometals by plant extracts is the most well-established in the literature (PERALTA-VIDEA et al., 2016; EL-SHERBINY; SALIH, 2018). Figure 23 depicts the possible mechanism of nanoparticle creation using a bottom-up approach.

Figure 23 - Bottom-up mechanisms of nanoparticle synthesis (M^+ - Metal ions).



Adapted from Kumar; Chisti and Chand (2013).

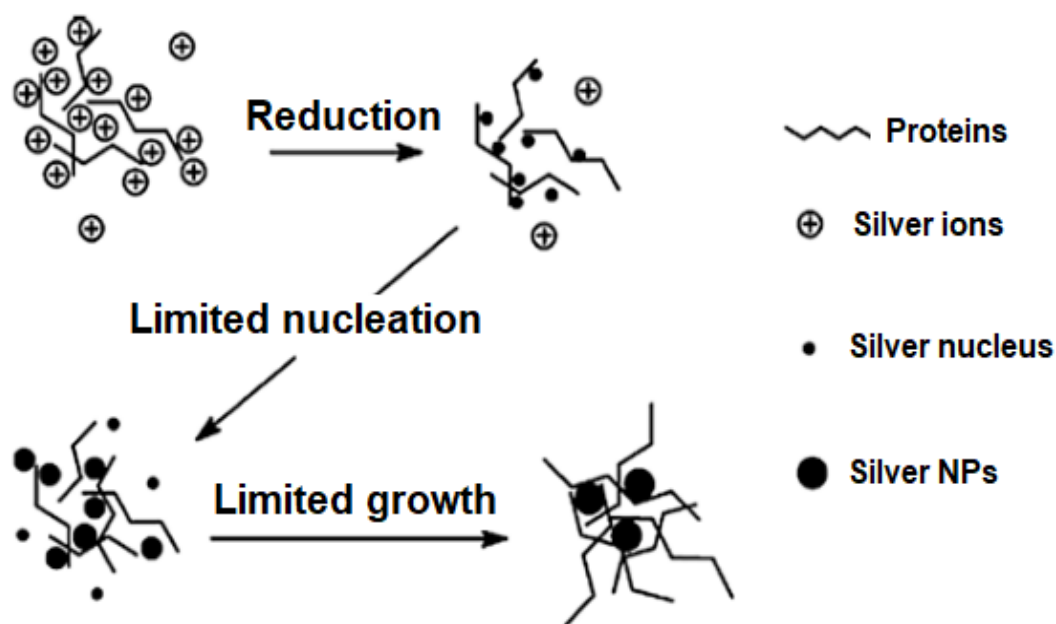
In the production of nanoparticles using plant extracts, the extract is simply mixed with a solution of metallic salt at room temperature (PAI et al., 2015; SYAFIYUDDIN et al., 2017; MORALES-LOZOYA et al., 2021). The reaction takes only a few minutes to complete. This method was used to create nanoparticles of silver, gold, and a variety of other metals. The nature of the plant extract, its concentration, the concentration of the metallic salt, pH, temperature, and contact duration are all known to have an impact on the creation rate, quantity, and other properties of nanoparticles (KUMAR; CHISTI; CHAND, 2013).

The exact mechanism and components responsible for plant-mediated synthetic nanoparticles remain to be elucidated. It has been proposed that proteins, amino acids,

organic acids, vitamins, as well as secondary metabolites such as flavonoids, alkaloids, polyphenols, terpenoids, heterocyclic compounds, and polysaccharides, have significant roles in the reduction of metallic salts and, in addition, act as covering agents and stabilization for synthesized nanoparticles (PERALTA-VIDEA et al., 2016). El-Kassas & El-Sheekh (2014), for example, showed that the hydroxyl functional group of polyphenols and the carbonyl group of proteins from *Corallina officinalis* extract could assist in the formation and stabilization of gold nanoparticles.

Philip et al. (2011), showed the synthesis and stabilization of silver and gold nanoparticles by binding biomolecules in *Murraya koenigii* leaf extract. According to the research, there are different mechanisms to synthesize nanoparticles in different plant species. Singh et al. (2016), adds that dicotyledonous plants contain many secondary metabolites that may be suitable for the synthesis of nanoparticles. Figure 24 presents a schematic illustration of the biosynthesis mechanism of silver nanoparticles using *Capsicum annum* extract used by Li et al. (2007). In this study, according to the authors, the silver ions undergo electrostatic interaction with the proteins present in the plant extract, which leads to the formation of the silver complex.

Figure 24 - Schematic representation of the mechanism of synthesis of AgNPs.



Adapted from Li et al. (2007).

3.2.2. Biosynthesis of nanometals by *Morinda citrifolia*

As previously described, among the various living beings with the potential for the synthesis of metallic nanoparticles, plants have a predominant role in the synthesis process. Its use can be beneficial compared to other biological agents since with the use of plants in the biosynthesis of nanometals, the process of maintaining cell cultures is eliminated (MITTAL; CHISTI; BANERJEE, 2013). The relevant biosynthesis property of metallic nanoparticles includes *Morinda citrifolia*. Table 14 briefly explores some examples of the potential that noni presents in the biosynthesis of metallic nanoparticles.

Table 14 - Summary of some studies involving the biosynthesis of nanometals by *M. citrifolia*.

Metal NP	Plant structure	Size (nm)	Characterization	Biological property	Reference
Ag	Leaves	100	UV-Vis and DLS	Antimicrobial	(PAI et al., 2015)
	Root	30 to 55	FTIR, XRD, FE-SEM e TEM	Cytotoxic	(SUMAN et al., 2013)
	Leaves	9 to 69	UV-Vis, EDS, FTIR e FE-SEM	Antimicrobial	(SYAFIUDDIN et al., 2017)
	Leaves	10 to 60	UV-Vis, FTIR, SEM and TEM	Antimicrobial	(SATHISHKUMAR et al., 2012)
	Leaves, Fruits e Seeds	3 to 11	UV-Vis, FTIR and TEM	Antimicrobial	(MORALES-LOZOYA et al., 2021)
AgCl	Leaves	12	UV-Vis, FTIR, DRX and TEM	Antimicrobial	(ASHOK KUMAR; PALANICHAMY; ROOPAN, 2014)
Al	Root	Not informed	FAAS	Uninformed	(TONTRONG; KHONYOUNG; JAKMUNEE, 2012)
Au	Root	12 to 38	XRD, FTIR, FE-SEM, EDS and TEM	Uninformed	(SUMAN et al., 2014)
TiO ₂	Root	20 to 39	XRD, FTIR, EDS and FE-SEM	Larvicide	(SUMAN et al., 2015)
	Leaves	15 to 19	XRD, FTIR, UV-Vis, EDS and SEM	Antimicrobial	(SUNDRARAJAN et al., 2017)

Abbreviations: UV-Vis (ultraviolet visible spectroscopy); FTIR (Fourier transform infrared spectroscopy); DLS (dynamic light scattering); XRD (X-ray diffraction); EDS (energy scattering X-ray spectroscopy); FE-SEM (field emission transmission electron

microscopy); SEM (Scanning electron microscopy); TEM (Transmission Electron Microscopy); FAAS (Flame atomic absorption spectrometry).

A new hydrothermal method developed by Sundrarajan et al. (2017), promoted the biosynthesis of titanium dioxide nanoparticles from the ethanolic extract of *Morinda citrifolia* leaves. To promote photosynthesis, 0.1 M TiCl_4 was added to the extract, then the solution was transferred to a Teflon-coated stainless-steel autoclave at 120 °C for 8 hours. The characterization of the extract by X-ray diffraction (XRD) identified the main peak at 27.3° corresponding to TiO_2 in the tetragonal rutile phase. The TiO_2 nanoparticles had a spherical shape with an average size ranging between 15 and 19 nm. TiO_2 nanoparticles also showed antimicrobial properties against *E. coli*, *S. aureus*, *Bacillus subtilis*, *Candida albicans*, *Pseudomonas aeruginosa*, and *Aspergillus niger*. In another similar work promoting TiO_2 biosynthesis from the aqueous extract of *M. citrifolia* root, larvicidal properties against *Anopheles stephensi*, *Aedes aegypti*, and *Culex quinquefasciatus* were identified in the extract (SUMAN et al., 2015).

Among the metallic nanoparticles biosynthesized by *M. citrifolia*, perhaps silver (Ag) is the most desired nanometal in the synthesis process. Syafiuddin et al. (2017) promoted the biosynthesis of silver nanoparticles (AgNPs) from aqueous extracts of leaves of various plants, including *Morinda citrifolia*. Biosynthesis was possible due to the reduction of silver ions by adding AgNO_3 to the aqueous extract. The biosynthesis process included the centrifugation of the extract containing AgNO_3 followed by its characterization. AgNPs had a spherical shape with sizes up to 69 nm, in addition to antimicrobial properties against *Bacillus cereus* and *E. coli*.

It was identified that silver nanoparticles (AgNPs) biosynthesized using aqueous extract of *M. citrifolia* root have a highly significant cytotoxic effect on HeLa cells. The cytotoxic effect was possible through the treatment with different concentrations of the extract containing the AgNPs in cells seeded in tissue culture plates. The MTT cytotoxicity analysis by the reduction of the dye [3-(4,5-dimethylthiazol-2yl)-2,5-diphenyl tetrazolium] bromide confirmed the cytotoxic effect of AgNPs (SUMAN et al., 2013).

3.3. State of the art considerations

In fact, nanotechnology is an emerging and fascinating new field of science, it allows advances in many areas, and new nanotechnological discoveries can open up new applications in the field of biotechnology and agriculture. New and sustainable methodologies on the so-called “green nanotechnology” were recently developed for the synthesis of nanoparticles. Since the aforementioned methodology does not use toxic solvents, chemical precursors and additional reducing agents. The green synthesis of metallic nanoparticles also employs amino acids, phytochemicals, polysaccharides, polyphenols and vitamins as precursor components of biotransformation. It is notable that there is an immense need to develop methodologies and approaches using green nanotechnology to increase the suitability of the biosynthesis of nanometals, one of these approaches is via the use of plant extracts, of which the appropriation of new mechanisms and pathways that make it possible to increase the yield of bioproduction through the use of plants, characterizing itself as a new tool in the acquisition of an innovative method/technology.

The objective of this part of the study is focused on the use of concentrated extracts of *M. citrifolia* via CCG and CCM, in the acquisition of silver nanoparticles with subsequent physical-chemical characterization of the product obtained and its comparison with the nanoparticles obtained using the *in natura* extract.

4. MATERIALS AND METHODS

4.1. *Plant extract used in biosynthesis*

Based on the principle previously established by Naikoo et al. (2021), in which the bioactive compounds present in plant leaf extracts promote both the bioreduction and the colloidal stability of NPs, it was decided to use leaf extracts as raw material for the biosynthesis of AgNPs. of *M. citrifolia* referring to the last step of both cryoconcentration methods obtained in Part 1 of this study (CC4-CCG and CC4-CCM). To compare the physicochemical properties of AgNPs, the extract referring to the *in natura* sample of *M. citrifolia* leaves was also included.

4.2. *Methodology for biosynthesis of AgNPs*

The production of silver nanoparticles will follow the principle of the bioreduction mechanism of metallic ions added to a solution containing the plant extract under study. The basic methodology to promote biosynthesis will follow the assays described by Syafiuddin et al. (2017) and Morales-Lozoya et al. (2021) with few adaptations.

In this study, we will first try to separate the biosynthesis assays and subsequent characterization into two groups, in the Group 1, the plant extract that will be used will be the cryoconcentrated fraction referring to the last stage of the CCG (gravitational cryoconcentration), that is, the CC4 fraction. In Group 2, the plant extract used will be the CC4 fraction from the CCM (microwave-assisted cryoconcentration) process.

In both groups, biosynthesis will follow two protocols: in Protocol 1, an aqueous solution of 1 mM AgNO₃ will be prepared for the synthesis of silver nanoparticles. The reaction mixture will be added from 5 mL of the cryoconcentrated plant extracts (CC4-CCG and CC4-CCM) to 95 mL of 1 mM aqueous solution of AgNO₃ in 250 mL Erlenmeyer flasks. The reaction mixture will be kept in a light-free environment at a controlled room temperature of 28 °C under gentle agitation in an incubator for 24 hours. For the control, a solution of 100 mL of AgNO₃ with the same concentration without leaf extract will also be prepared. The colloidal solutions will be obtained by centrifuging the reaction medium for 10 min at 4000 rpm, then the solution will be vacuum filtered with a 0.2 µm nylon membrane. The suspensions will be stored in falcon tubes in a dark environment.

The first stage of AgNPs biosynthesis was carried out through the use of cryoconcentrated extracts of noni. Protocol 2 will follow the study of variations in the main parameters involved in biosynthesis, to assess their effect on the size and stability of AgNPs. For this, the concentration of the metallic precursor was varied (1 mM, 2 mM, and 4 mM), keeping constant the amount of extract, and treatment temperature (5 mL and 28 °C respectively). Likewise, to determine the effect of extract composition, the amount of extract will be varied (10 mL, 15 mL, and 20 mL of extract in 100 mL of aqueous solution), keeping the amount of metallic precursor and temperature constant (1 mM and 28°C respectively). The variation of the treatment temperature (40 °C, 50 °C and 60 °C) was also evaluated, keeping constant the concentration of the metallic precursor and the volume of cryoconcentrate used. Finally, we evaluated the shelf-life of AgNPs by varying the storage period (30 days, 45 days, and 60 days), keeping the other biosynthesis parameters as described in Protocol 1. biosynthesis will be applied to sample CC4 in both cryoconcentration processes applied in this study (CCG and CCM method).

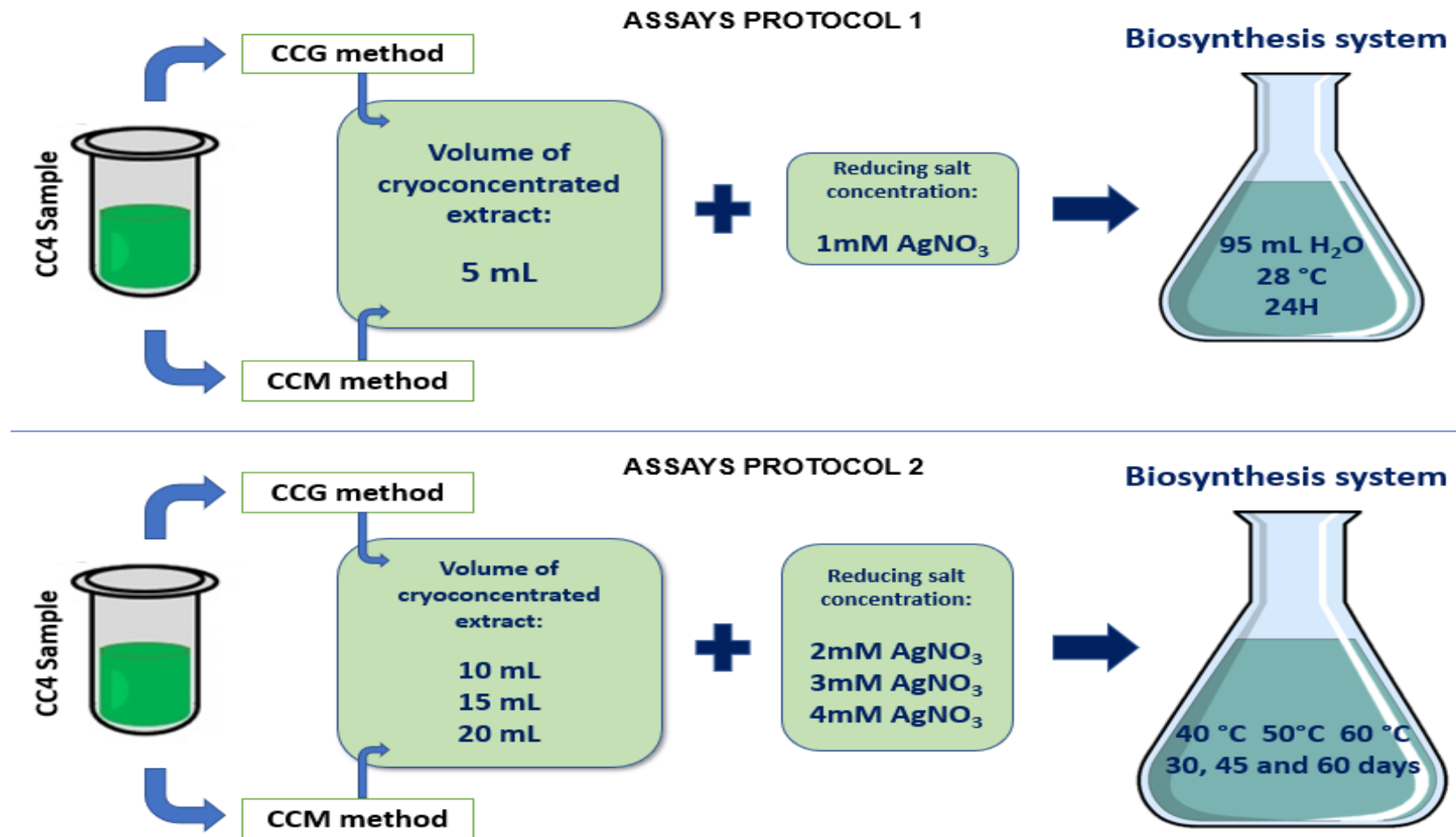
All characterization assays applied in this study also include extract *in natura* samples from *M. citrifolia* leaves. Table 15 presents a detailed summary of the methodology adopted for the biosynthesis of AgNPs. For purposes of illustration, Figure 25 also presents a general schematic outline of the AgNPs biosynthesis methodology.

Table 15 - Summary of process variables in the AgNPs Biosynthesis methodology from *M. citrifolia* extracts concentrated by the CCG and CCM method (CC4-CCG and CC4-CCM).

ASSAYS PROTOCOL 1						
Analysis group	<i>M. citrifolia</i> extract used	Extract volume (mL)	AgNO ₃ concentration (mM)	Treatment temperature (°C)	Storage time (days)	Characterization tests
1	CC4-CCG	5	1	28	1	DLS, Zeta Potential, UV-Vis and FTIR spectroscopy, FAAS, SEM-EDS and TEM
2	CC4-CCM	5	1	28	1	DLS, Zeta Potential, UV-Vis and FTIR spectroscopy, FAAS, SEM-EDS and TEM
ASSAYS PROTOCOL 2						
Analysis group	<i>M. citrifolia</i> extract used	Extract volume (mL)	AgNO ₃ concentration (mM)	Treatment temperature (°C)	Storage time (days)	Characterization tests
1	CC4-CCG	10	2	40	30	DLS, Zeta Potential and UV-Vis spectroscopy
		15	3	50	45	
		20	4	60	60	
2	CC4-CCM	10	2	40	30	
		15	3	50	45	
		20	4	60	60	

Abbreviations: UV-Vis (Ultraviolet visible spectroscopy); FTIR (Fourier transform infrared spectroscopy); DLS (dynamic light scattering); EDS (energy scattering X-ray spectroscopy); SEM (Scanning electron microscopy); TEM (Transmission electron microscopy); FAAS (Flame atomic absorption spectrometry).

Figure 25 - Summary of process variables in the AgNPs Biosynthesis methodology from *M. citrifolia* extracts concentrated by the CCG and CCM method (CC4-CCG and CC4-CCM).



4.3. Characterization of the silver nanoparticles

4.3.1. Dynamic light scattering

The size configuration of the silver nanoparticles will be determined by electrical light distribution (DLS) in a Nano-flex MicrotracS3000/S3500 Series - Particle Metrix equipment.

For an experimental run made of the size of AgNP, about 10 mL of the surroundings, from which the thoughts will be delivered to a 50 mL beaker. Then, the component containing the laser light source is immersed in the sample. The analysis of the frequency of light incident on how the particle will be applied by the equipment software generates a cumulative distribution and size of the nanoparticles. The DLS assays were carried out at the Interdisciplinary Laboratory for the Development of Nanostructures (LINDEN/UFSC).

4.3.2. Zeta potential

The determination of the stability of the nanoparticles was carried out through the evaluation of the zeta potential of the colloidal solutions coupled with a DLS equipment (Nano-flex Stabino, Particle Metrix).

The experimental execution proceeds with the transfer of 10 mL of the colloidal samples containing the AgNPs to a cylindrical Teflon cell, after which the solution was stirred. The mV value of the instantaneous zeta potential (ZP) and the pH of the sample is quickly determined and this ZP value was assigned as the initial zeta potential. Subsequently, the equipment was adjusted to measure the zeta potential under the effect of different pH values of the sample, always varying from an acid pH via HCl titration to an alkaline pH via NaOH titration (3.0 to 10.0 respectively). The result is computerized, and this results in a graph of the PZ variation as a function of the pH of the samples. The ZP assays were carried out at the Interdisciplinary Laboratory for the Development of Nanostructures (LINDEN/UFSC).

4.3.3. UV-visible

The solutions containing the AgNPs were analyzed by UV-Vis spectroscopy, in a dual-beam spectrophotometer (Hitachi, Model U 1900), operating at a resolution of 1

nm, with scanning absorption spectra adjusted to a length range of wave between 200 and 600 nm. About 5 mL of the samples containing the colloidal silver nanoparticles were used in quartz cuvettes. The samples were diluted in water so that the absorption peak remained within the wavelength detection range set in the spectrophotometer. The UV-Vis spectroscopy assays were performed at the Laboratory of Mass Transfer (LABMASSA/UFSC).

4.3.4. Fourier transform infrared

The FTIR spectroscopy assays followed the same protocol described in item 4.4.3 of Part 1 of this study.

The proposal for the implementation of these new FTIR assays was to compare the intensity of the transmittance peaks obtained with the CC4 samples obtained via the CCG and CCM method, with the solutions containing the AgNPs obtained by these same cryoconcentrated samples. The results obtained by FTIR are useful in providing evidence of the presence of functional groups present in solutions containing AgNPs. These functional groups make up the biomolecules responsible for the reduction of silver ions in the formation of nanoparticles (Ag^+ to Ag^0) and the stabilization mechanism of AgNPs in colloidal solution. The tests involving the FTIR were carried out at the Process Control Laboratory (LCP/UFSC).

4.3.5. Flame atomic absorption

In this work FAAS analysis was used to determine the presence and amount of silver nanoparticles after biosynthesis by detecting the presence of reduced silver ions in the colloidal dispersions. The analyzes were performed in an equipment (Hitachi Model Z-8230) with a silver hollow cathode lamp, working at an operating current of 2 mA, and a wavelength and spectral bandwidth of 328.1 and 0.2 nm, respectively.

Only the AgNPs obtained through the assays described in Protocol 1 (Table 15) were submitted to FAAS analysis, that is, the AgNPs obtained from the CC4-CCG and CC4-CCM samples. The AgNPs obtained from the extract *in natura* were also subjected to an FAAS assay. All FAAS assays were performed in triplicate. The FAAS assays were performed at the Chemical Analysis Center of the QMC/UFSC.

4.3.6. Electron microscopy and energy-dispersive X-Ray

Scanning (SEM) and transmission electron microscopy (TEM) analyzes of AgNPs were carried out in order to evaluate the shape, size and spatial arrangement aspects of the nanoparticles. Tests with both equipment were performed at LCME/UFSC.

The preparation of the samples of silver nanoparticles for visualization in the SEM-EDS was carried out by diluting the samples by 50% (v/v) followed by dripping them onto small previously cleaned and sterilized aluminum supports called “stubs”. After the dripping, the stubs were taken to a vacuum incubator where they remained for a period of 48 h to promote the drying of the dripped sample. SEM-EDS analyzes were performed (JEOL, model JSM-6390LV) at a voltage of 30.0 kV with a maximum image magnification of 50,000x. The energy dispersion spectrometry (EDS) system coupled to the electron microscope promoted the chemical characterization/elemental analysis of the test material, allowing the identification and confirmation of the presence of silver nanoparticles.

At last, the preparation of AgNPs samples for analysis in TEM, the experimental execution followed from the deposit of a drop of the solution containing the AgNPs on a grid, a type of copper grid with 3 mm in diameter coated with a carbon film with multiple meshes, also known as meshes. After the dripping of the solution containing the AgNPs, the grids were taken to incubation and remained for a period of 48 h to promote the drying of the dripped samples. After drying, the samples were submitted to visualization (TEM, JEOL model JEM-1011) operating at a voltage of 100 kV, with the resolution of the images adjusted in the visualization range between 20-100 nm.

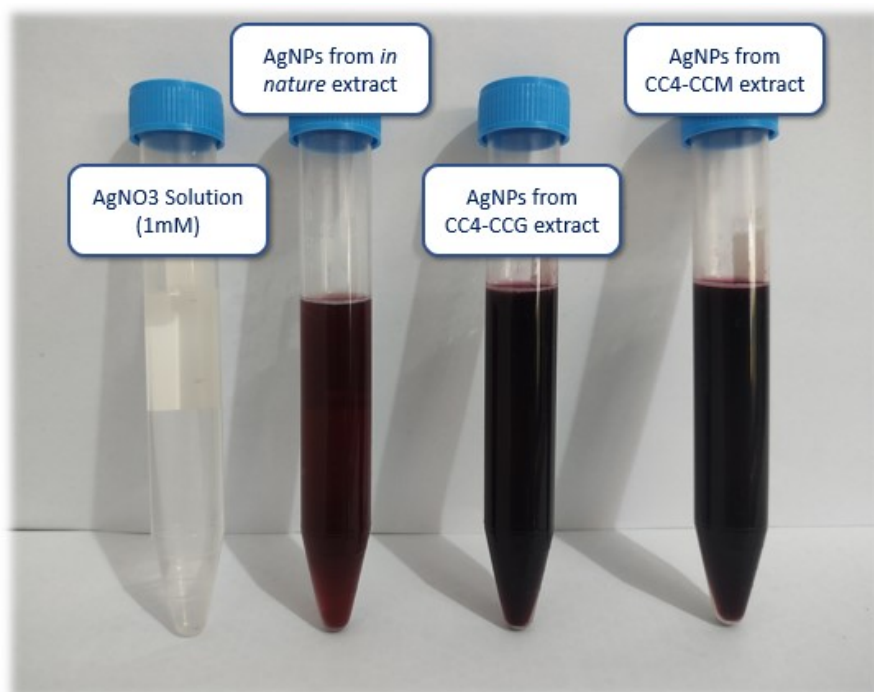
5. RESULTS AND DISCUSSION

5.1. Biosynthesis analysis

5.1.1. Standard conditions: Assays protocol 1

The AgNPs produced from samples of cryoconcentrated extracts from *M. citrifolia* leaves belonging to Assays Protocol 1 (*in natura* extract, CC4-CCG and CC4-CCM) after 24 hours of reaction are illustrated in Figure 26.

Figure 26 - AgNPs produced from extracts *in natura* and from concentrated extracts (CC4-CCG and CC4-CCM) of *M. citrifolia* leaves following Assays Protocol 1.



Because of the surface plasmon resonance (SPR) phenomenon, UV–vis spectroscopy is frequently the primary technique utilized in the characterization of metallic nanoparticles (SMITHA; PHILIP; GOPCHANDRAN, 2009). A collective stimulation of electrons in the conduction band around the nanoparticle surface is known as surface plasmon resonance. Because of particle size and shape, electrons conform to a given vibration mode. Metallic nanoparticles, as a result, have distinct optical absorption spectra in the UV–vis range (SIDDIQUI; AL-WHAIBI; MOHAMMAD, 2015).

The analysis of the surface plasmon resonance increase of the silver ion by UV-Vis spectroscopy for the samples of the extract *in natura*, CC4-CCG, and CC4-CCM, were also evaluated and are shown respectively in Figures 27, 28, and 29. After 48-h reaction, the UV-vis absorption spectra of the silver nanoparticles solution revealed a maximum peak at about 421 nm to AgNPs from CC4-CCG method, which was attributed to the silver nanoparticles' surface plasmon resonance band (SPR).

Although there are small variations in wavelength (nm) for the UV-Vis peaks shown in Figures 26, 27, and 28, it is well established in the literature that such wavelength values are characteristic of AgNPs. Logeswari; Silambarasan and Abraham (2015) described UV-vis spectra for AgNPs produced by five different plant extracts. The results showed maximum absorbance at 420 nm, which increased with the time of incubation of silver nitrate with the plant extract, thus corroborating the results shown in Figures 26, 27, and 28. According to Figures 26, 27, and 28, it is noted that the UV-Vis curve showed an increased absorbance in the studied time intervals and the peaks observed were at 423 nm, 421 nm, and 425 nm (Figures 26, 27, and 28 respectively) corresponding to the characteristic surface plasmon resonance of silver nanoparticles. The differences in absorbance intensity indicate, as described by Tripathy et al. (2010), that the CCG method promoted the production of AgNPs in higher concentration, in relation to the CCM method and the synthesis from the extract *in natura*. The observation of the behavior of the UV-Vis spectroscopy curves of the AgNPs produced via Assays Protocol 1 also indicated that the reduction of Ag⁺ ions occurred extracellularly, as corroborated in the study carried out by Suman et al. (2014).

It is also important to point out that during the biosynthesis process, AgNPs were formed as the shade of the solution varied from a brownish to almost black color (Figures 26, 27, and 28). With time, the mixture became darker and darker but remained highly stable after 24 h of treatment. This color change corroborates the study by Pai et al. (2015), clearly indicating the reduction of Ag⁺ ions, qualitatively confirming the formation of AgNPs. Therefore, as also described by Saratale et al. (2018), from the visual observations it became clear that the plant extract of *M. Citrifolia* was a good Ag⁺ ion reducing agent for silver nanoparticles.

Figure 27 - UV-Vis spectra for the AgNPs produced from the *in natura* extract of *M. citrifolia* leaves. The change in color from brownish to almost black after 48 h of biosynthesis is indicative of the effectiveness of the bioreduction from Ag^+ to Ag^0 .

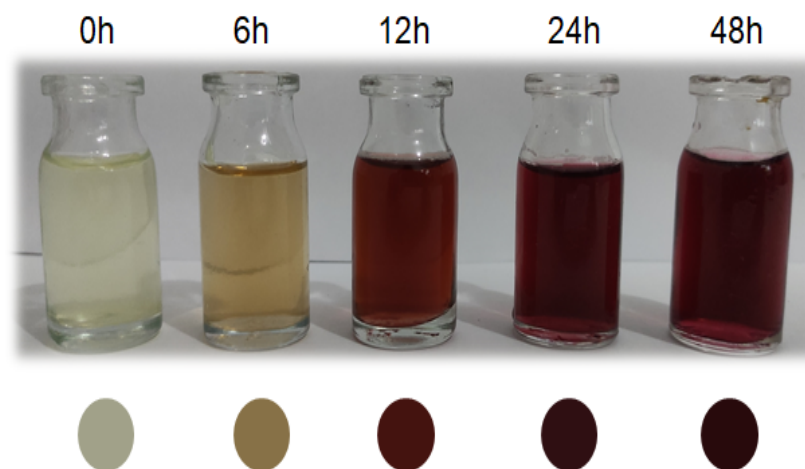
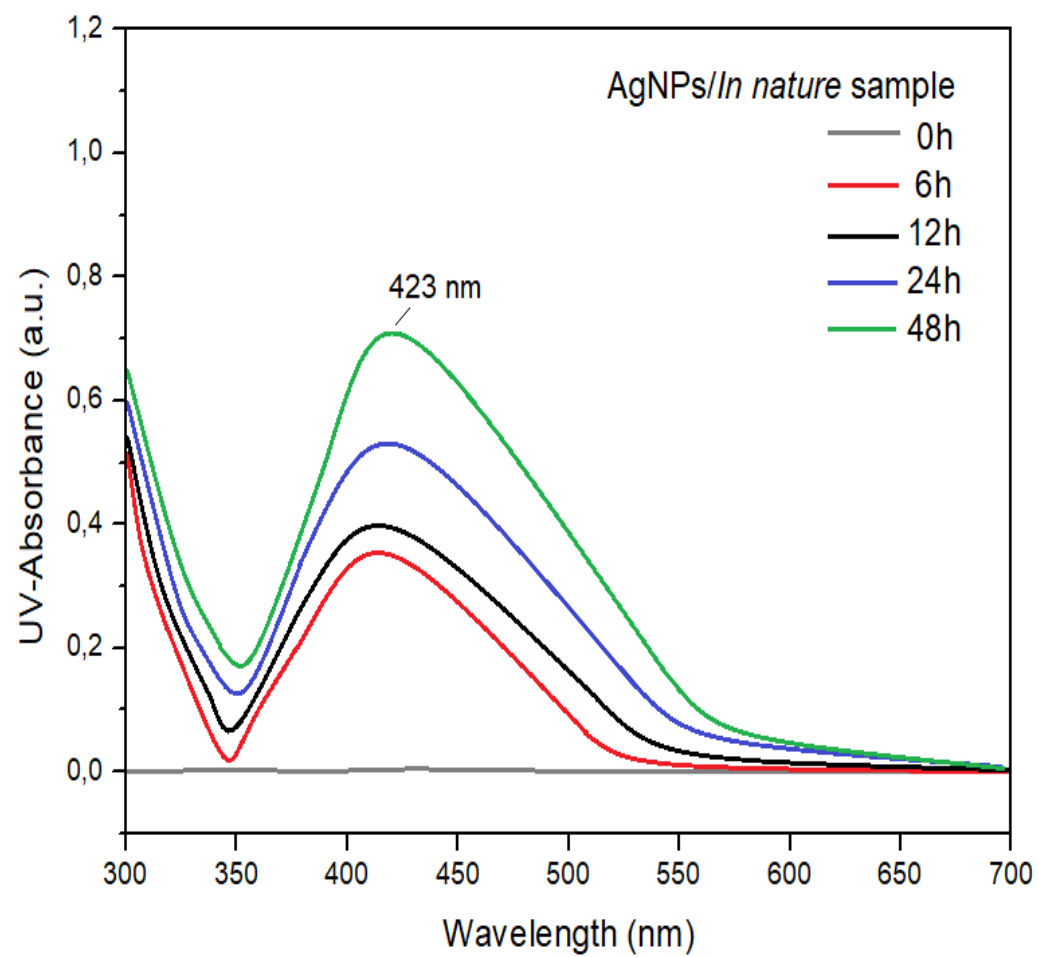


Figure 28 - UV-Vis spectra for the AgNPs produced from the CC4 extract via CCG method of *M. citrifolia* leaves. The change in color from brownish to almost black after 48 h of biosynthesis is indicative of the effectiveness of the bioreduction from Ag^+ to Ag^0 .

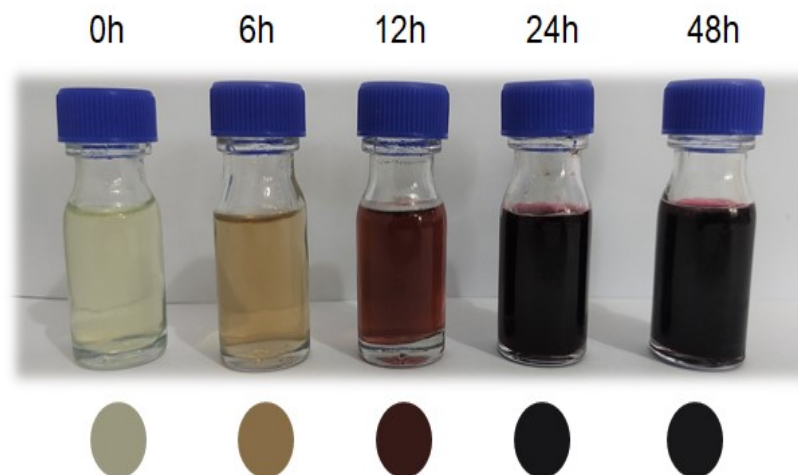
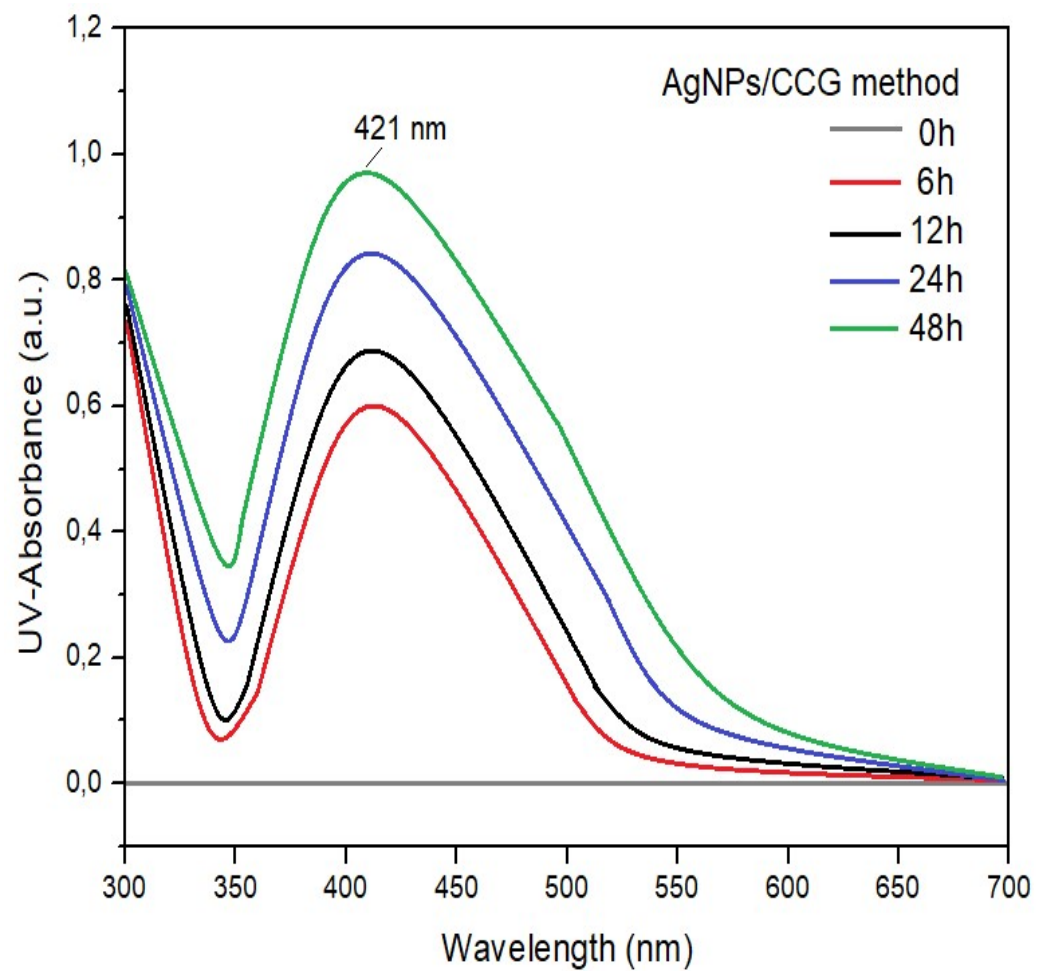


Figure 29 - UV-Vis spectra for the AgNPs produced from the CC4 extract via CCM method of *M. citrifolia* leaves. The change in color from brownish to almost black after 48h of biosynthesis is indicative of the effectiveness of the bioreduction from Ag^+ to Ag^0 .

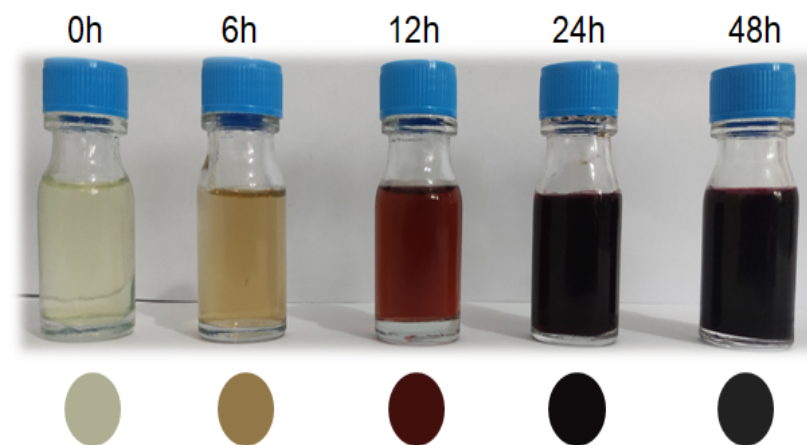
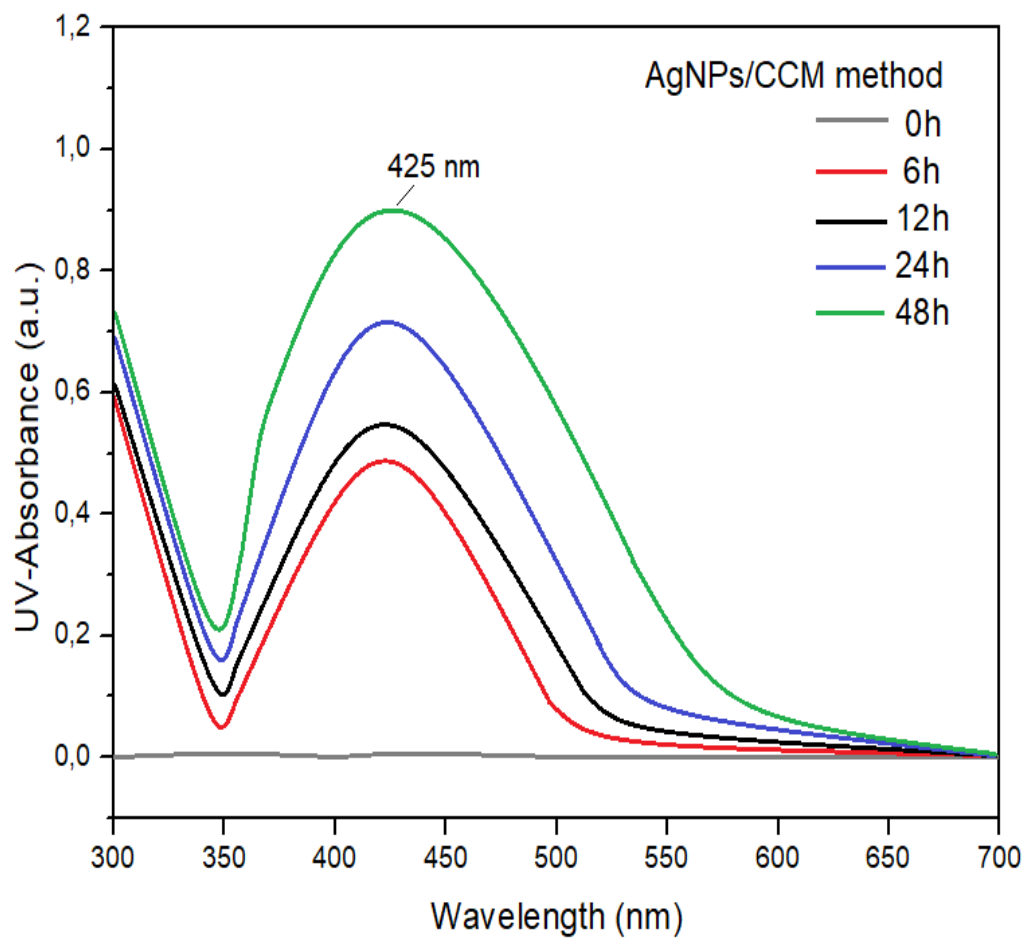


Figure 30 shows the variation of zeta potential (ZP) as a function of pH for the prescribed samples (Assays Protocol 1). Figure 31 shows the cumulative and percentage size distribution of AgNPs biosynthesized using extracts *in natura* and cryoconcentrated by CCG and CCM methods from *M. citrifolia* leaves, both particle size and ZP assays were performed 24 h after the beginning of AgNPs biosynthesis. Table 16 shows the analytical data of the average size of the nanoparticles, as well as the zeta potential and the initial pH of the samples at the time of analysis.

It is observed that the cryoconcentration method caused an effect on the determination of the size of AgNPs, the NPs obtained by the CCG method showed an average size of 23 nm, an average size smaller than the NPs obtained from the *in natura* extracts and from the cryoconcentrated extract by the CCM method, which had an average size of 41 and 34 nm respectively.

As previously described, the bioreduction process in obtaining nanometals from plant extracts is governed by the mechanism described as bottom-up, this approach refers to the build-up of material from the bottom: atom-by-atom, molecule-by-molecule, or cluster-by-cluster (PERALTA-VIDEA et al., 2016). For the use of plants in biosynthesis, leaf extracts contain phytochemicals that play an important role in the formulation and increase of the bioactivity of nanoparticles (KISHEN; MEHTA; GUPTA, 2020). Regarding the behavior of ZP as a function of pH in the biosynthesis of AgNPs, the immediate values of the zeta potential detected after 24 h of the bioreduction period were -9.85, -28.34 and -15.85 mV for the biosynthesized AgNPs by extract *in natura*, and by CCG and CCM methods respectively (Table 16).

The scan to verify the ZP as a function of pH variation was performed with increasing pH values (ranging from acidic to basic pH values). It is verified that the ZP of the AgNPs obtained via the CCG and CCM method decline to values between -25 mV and -35 mV when the pH reaches values close to neutrality and alkaline values, the isoelectric points for the NPs in both prescribed methods were in pH values between 4 and 5 (Figure 30). Such results agree with the generally accepted values for the stability of particles in a colloidal suspension, which prevails when the zeta potential value is less than or equal to -30 mV; or greater than or equal to 30 mV (MIRHOSSEINI et al., 2008).

As previously described, the tests involving CCG resulted in higher amounts of TSC and TPC when compared with the CCM technique and via the use of the extract *in natura* (Figures 8 and 10). Therefore, the smaller particle size and lower ZP values for the AgNPs produced by *M. citrifolia* extracts via the CCG method can be easily explained due to the greater accumulation of bioactive present in the samples obtained by CCG when compared to those obtained by CCM and in the *in natura* sample.

Figure 30 - Variation of zeta potential as a function of pH of AgNPs produced according to Assays Protocol 1 (*in natura* extracts and CCG and CCM method).

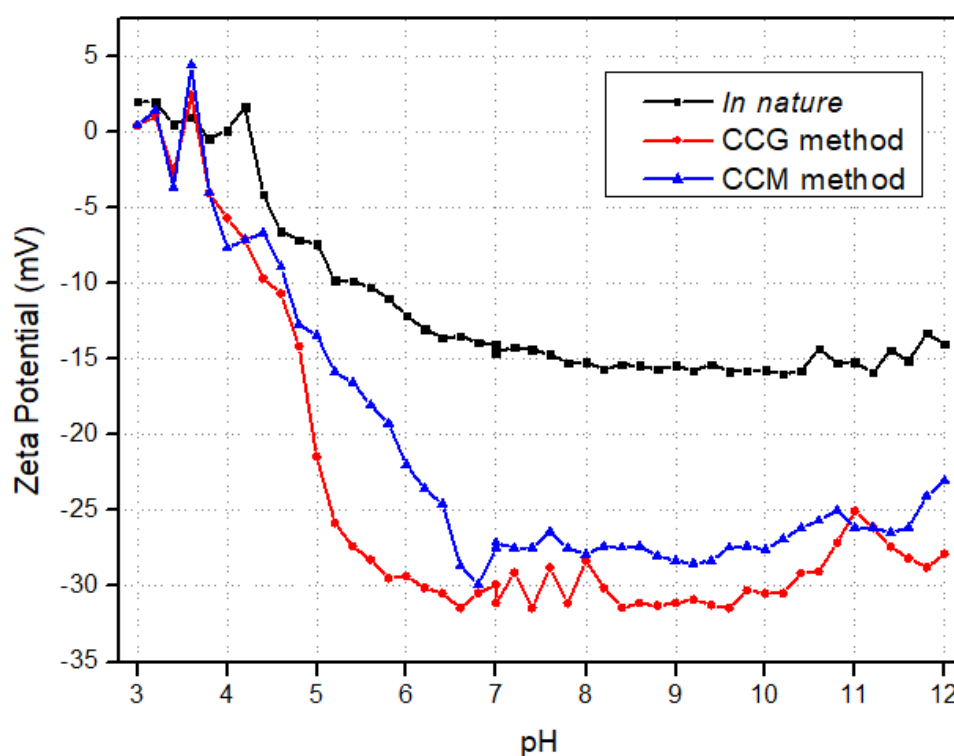
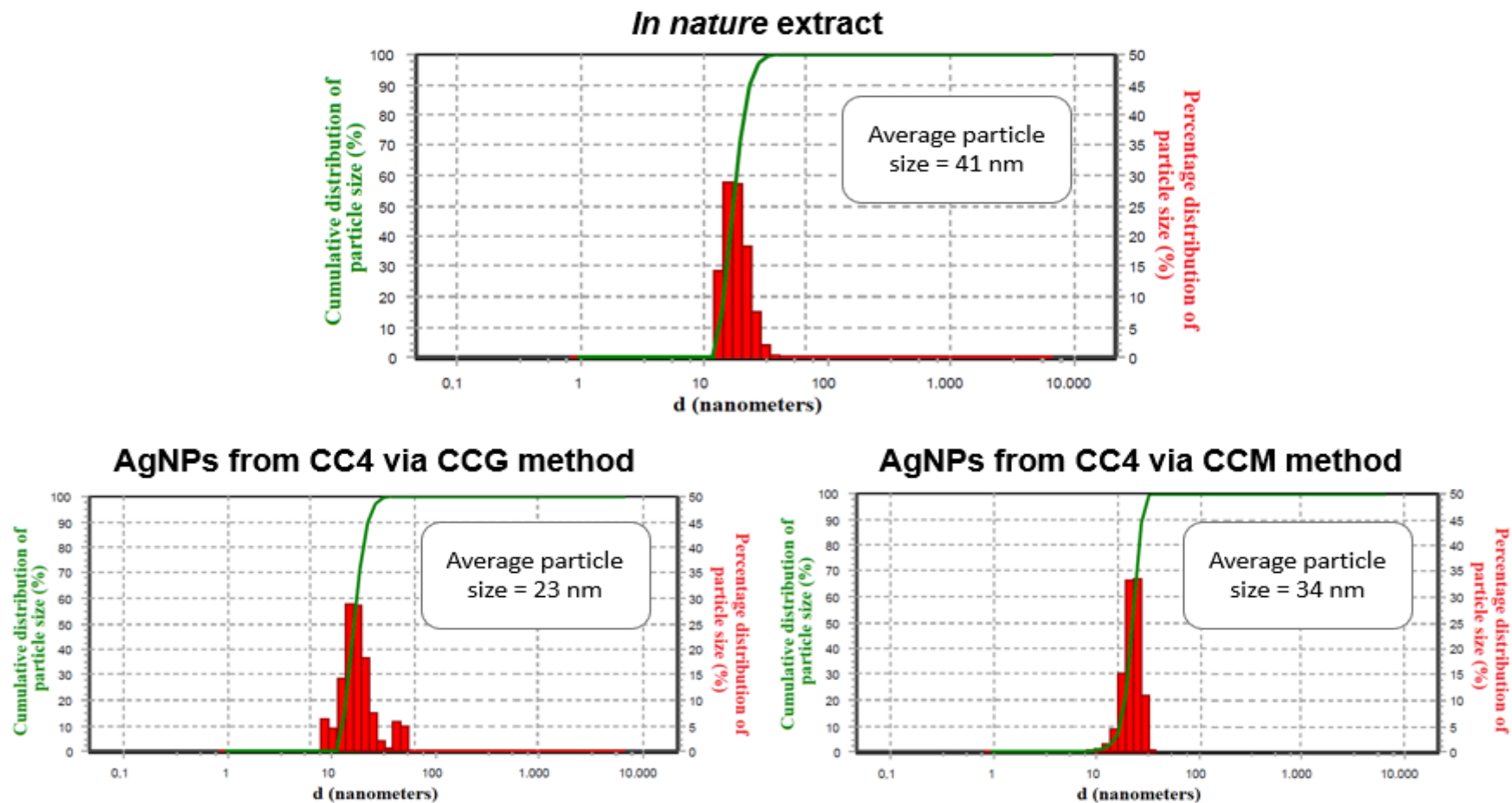


Table 16 Average particle size, zeta potential, and initial pH values for AgNPs for samples developed in Assays Protocol 1.

Type of <i>M. citrifolia</i> extract used in the biosynthesis of AgNPs	Particle size (nm)	Initial zeta potential (mV)	Initial pH
<i>In natura</i>	41	-9.85	5.53
CC4-CCG method	23	-28.34	5.61
CC4-CCG method	34	-15.85	5.29

Figure 31 - DLS assays for particle size detection from the cumulative and percentage distribution of AgNPs produced from the *M. citrifolia* leaves extract *in natura* and via extracts cryoconcentrated by the CCG and CCM methods.



5.1.2. Influence of biosynthesis conditions on the size and stability of AgNPs

5.1.2.1. Effect of the concentration of the metallic precursor

The tests involving the behavior of AgNPs in the face of changes in process variables were developed according to the methodology prescribed in Assays Protocol 2 (Table 15). The first trial involved varying the AgNO_3 concentration between 2 and 4 mM, keeping the other biosynthesis parameters constant, that is, as prescribed in Assays Protocol 1. Figure 32 shows the UV-Vis spectra (a) and b)) and the variation of the ZP as a function of pH (c) and d)) for the AgNPs from the extracts obtained by CCG and CCM, with variation in the concentration of the reducing salt (AgNO_3) in the biosynthesis process.

Figure 32 - Effect of AgNO_3 concentration, on maximum absorbance wavelength (a) and b)) and ZP as a function of pH (c) and d)) on AgNPs.

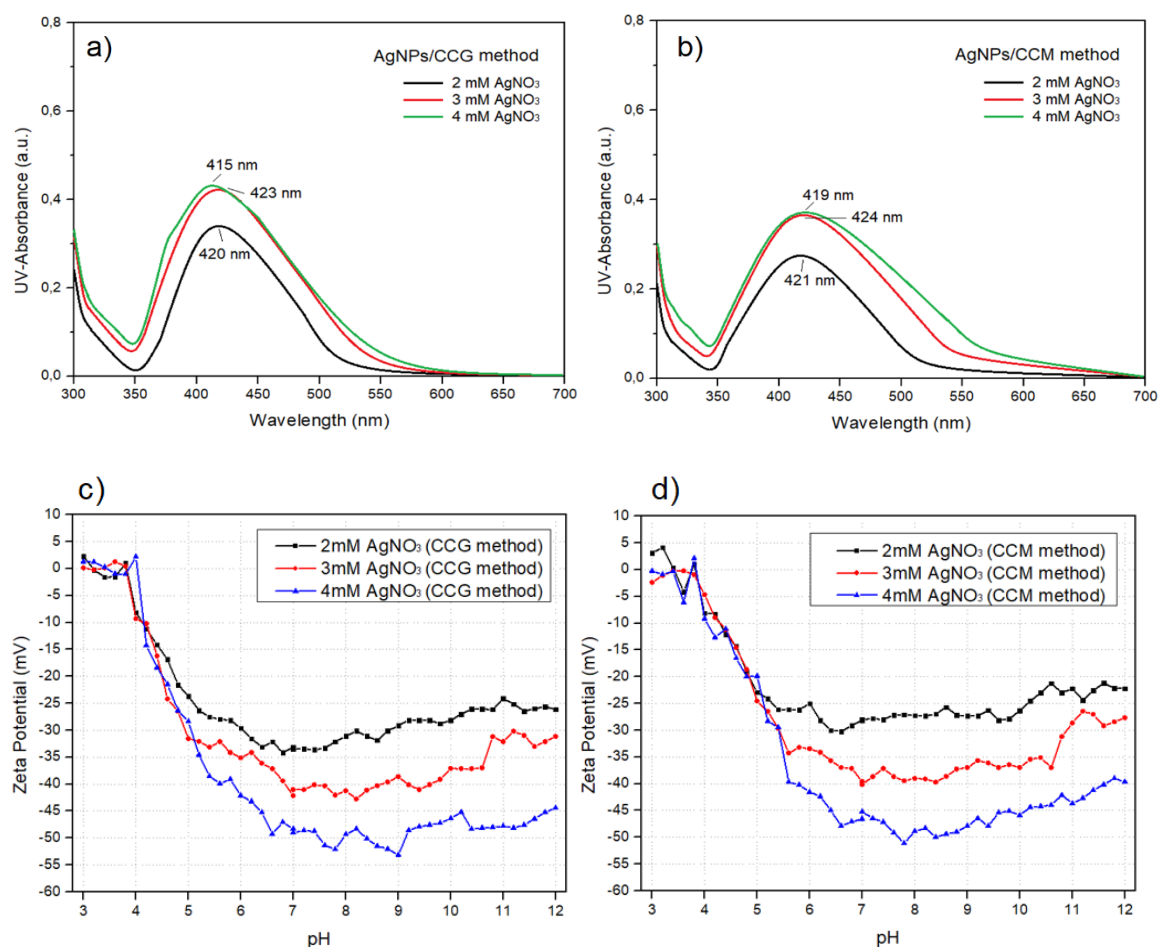


Table 17 shows the analytical data of the average size of the nanoparticles, as well as the zeta potential, the initial pH of the samples, and the wavelength at the peak of absorbance in UV-Vis in the face of changes in AgNO₃ concentration.

Table 17 - Influence of metallic precursor concentration on size, zeta potential and UV-Vis spectrum of AgNPs produced by cryoconcentrated *M. citrifolia* extracts.

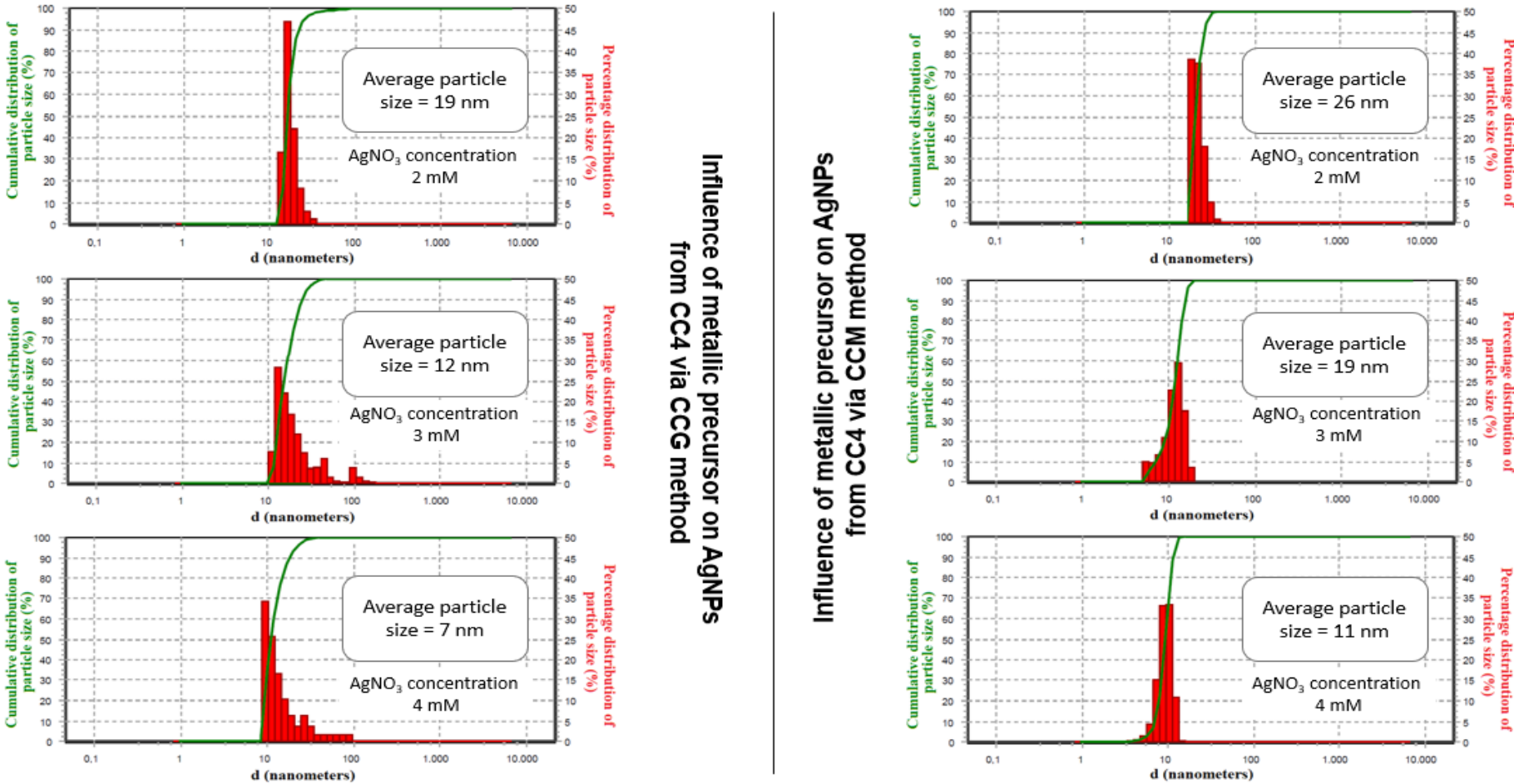
<i>M. citrifolia</i> extract used in the biosynthesis	AgNO ₃ concentration (mM)	Wavelength at maximum absorbance (nm)	Mean size (nm)	Initial pH	Initial zeta potential (mV)
CC4 Cryo Grav	2	420	19	5.91	-21.36
	3	423	12	5.83	-28.12
	4	415	7	5.77	-37.45
CC4 Cryo Micro	2	421	26	5.94	-19.18
	3	424	19	5.76	-24.76
	4	419	11	5.79	-30.39

According to Figure 32 a) and b), it can be seen that the increase in the concentration of the reducing salt caused a shift in the wavelength in the maximum absorbance: from 420 nm, 423 nm, and 415 nm for the AgNPs produced by the CCG method with AgNO₃ concentrations ranging from 2 mM, 3 mM and 4 mM respectively. For the CCM method, the AgNPs behaved similarly with respect to the wavelength at the UV-Vis absorbance peak: 421 nm, 424 nm, and 419 nm with AgNO₃ concentrations ranging from 2 mM, 3 mM and 4 mM, respectively. A subtle decrease in wavelength is observed for the treatment with the highest concentration of the metallic precursor followed. Henglein (1993), makes us know that the band shift, from red (more energetic) to blue (less energetic), depends on morphology, particle size, aggregation state and medium.

Another important aspect to be mentioned is the relationship between the UV-Vis spectrum, ZP, and particle size. Figure 33 shows the interference of the reducing salt

concentration (AgNO_3) on the average size of the AgNPs obtained by the two cryoconcentration methods studied. It can be seen that, when increasing the concentration of the metallic precursor in the reaction medium, the UV-Vis spectrum becomes narrower (Figure 32 a) and b)), indicating a greater polydispersity in the size of the nanoparticles, which reflects in the lower values of ZP as the pH migrates from neutral to alkaline (Figure 32 c) and d)), indicating greater stability of the NPs, finally reflecting a smaller particle size in the treatment with AgNO_3 at 4 mM. Likewise, NPs synthesized with the lowest silver content have a broader spectrum; that is, they will have a smaller dispersion. Therefore, in the histograms of the AgNPs synthesized (Figure 33), the increase in the concentration of silver nitrate caused a behavior inversely proportional to the size of the NPs, with greater polydispersity. Such behavior of AgNPs was also observed in previously developed studies (SUÁREZ-CERDA et al., 2015).

Figure 33 - Percentage and cumulative distribution assays of AgNPs produced from extracts obtained by CCG and CCM with variation in the concentration of the metallic precursor.



Influence of metallic precursor on AgNPs from CCG via CCG method

Influence of metallic precursor on AgNPs from CCM via CCM method

5.1.2.2. Effect of varying the volume of the cryoconcentrated extract

The second test of variation of AgNPs biosynthesis parameters was in relation to the volume of cryoconcentrated extract used in the reaction medium. Figure 34 shows the UV-Vis spectra (a) and b)) and the variation of the ZP as a function of pH (c) and d)) for the AgNPs of the extracts obtained by CCG and CCM, with a variation of the volume of the cryoconcentrated extract in the process of biosynthesis. Table 18 presents the analytical data of the average size of the nanoparticles, as well as the zeta potential, the initial pH of the samples, and the wavelength at the peak of absorbance in UV-Vis in relation to the changes in the volume of the cryoconcentrated extract.

Figure 34 - Effect of volume of the cryoconcentrated extract, on maximum absorbance wavelength (a) and b)) and ZP as a function of pH (c) and d)) on AgNPs.

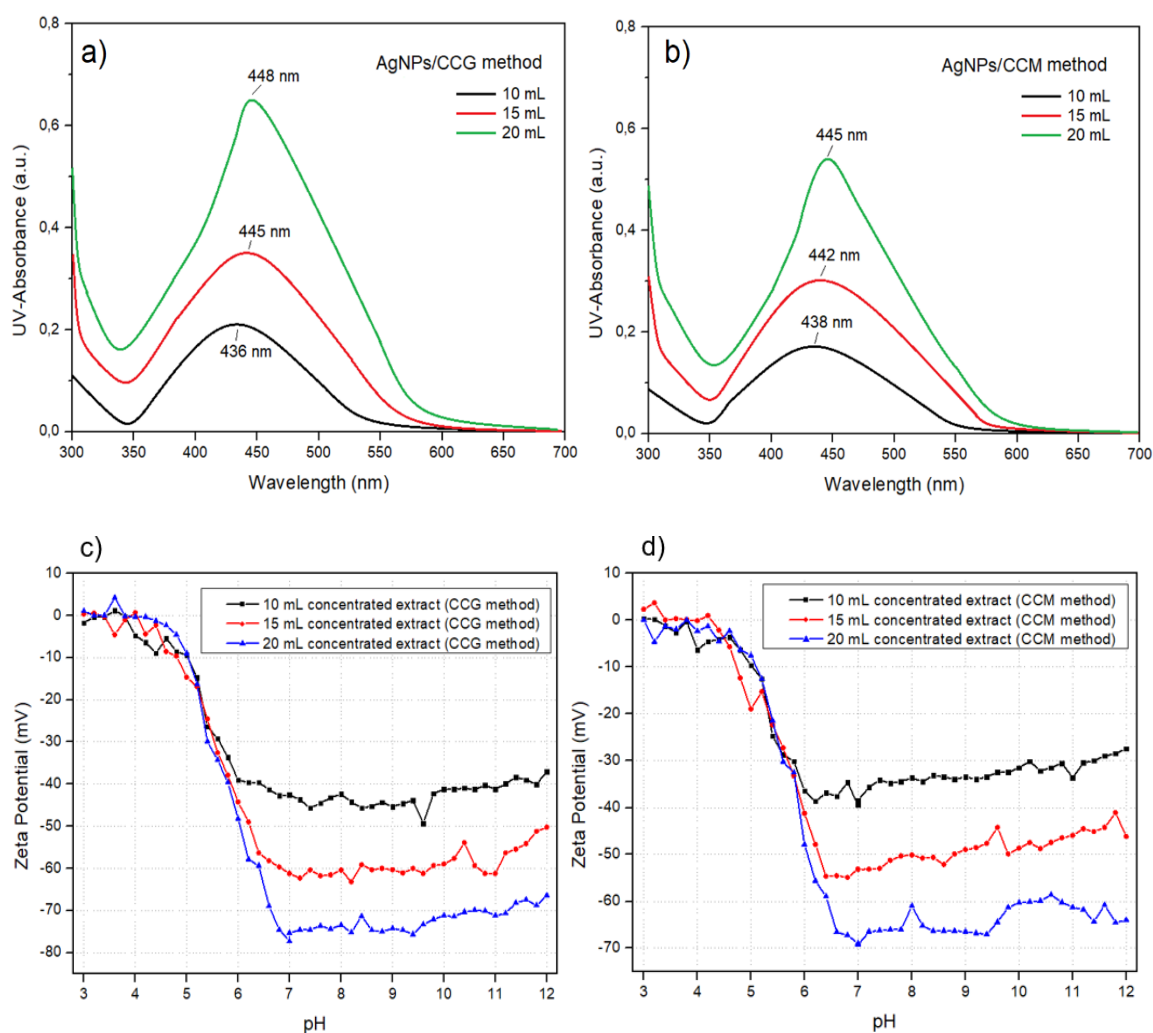


Table 18 - Influence of volume of cryoconcentrated on size, zeta potential and UV-Vis spectrum of AgNPs produced by cryoconcentrated *M. citrifolia* extracts.

<i>M. citrifolia</i> extract used in the biosynthesis	Volume of cryoconcentrated (mL)	Wavelength at maximum absorbance (nm)	Mean size (nm)	Initial pH	Initial zeta potential (mV)
CC4 Cryo Grav	10	436	21	5.33	-21.36
	15	445	32	5.89	-28.12
	20	448	44	5.26	-37.45
CC4 Cryo Micro	10	438	45	5.18	-19.18
	15	442	56	5.63	-24.76
	20	445	63	5.20	-30.39

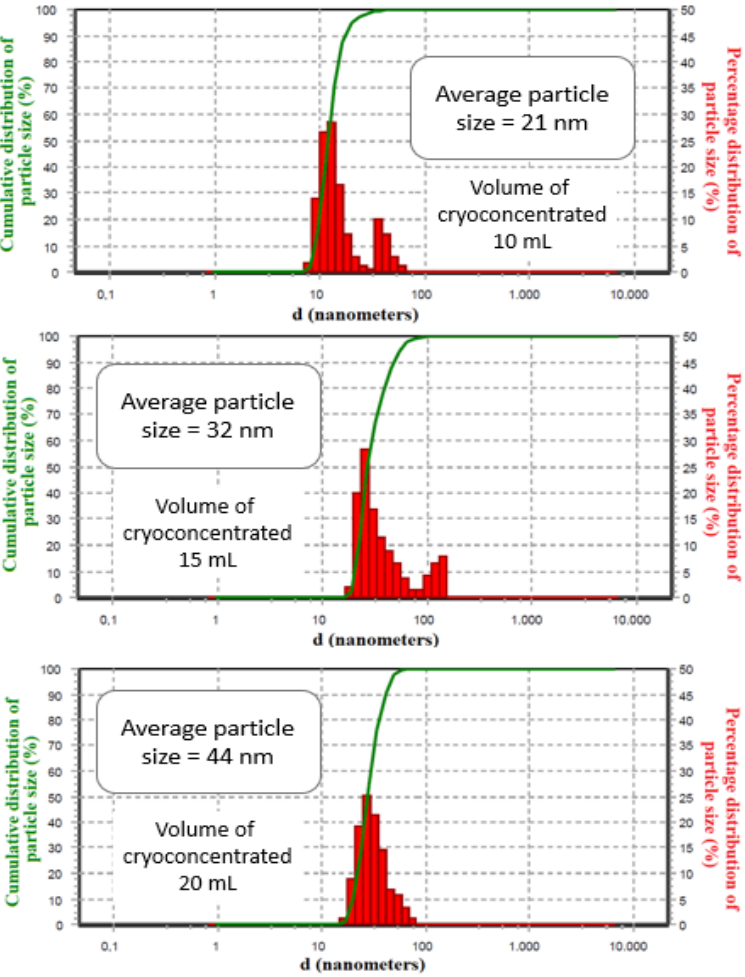
The behavior of AgNPs in the face of changes in the volume of the cryoconcentrated extract can be assured by similar works such as those developed by Tripathy et al. (2010) and Morales-Lozoya et al (2021). According to Figure 34 a) and b), it is noted that for both cryoconcentration methods used (CCG and CCM) the particles increasing the volume of the concentrate caused an increase in the UV-Vis absorbance peak and the wavelength representative (Table 18). According to Syafiuddin et al. (2017), the size of silver nanoparticles depends on the proportion of silver ions in the coating agent/stabilizing agent and the amount of the biosynthesis mediating agent. Small variations in absorbance peaks reflected changes in particle size due to changes in volume ratios of the cryoconcentrated *M. citrifolia* extract and the concentration of the metallic precursor.

Figure 35 shows the variation in particle sizes with the increase in the volume of the cryoconcentrated extract. It can be seen that the increase in the volume of cryoconcentrate for biosynthesis caused an increase in the average particle size, however, even though the size values presented by the AgNPs produced with the extract of the CCG method were smaller than the AgNPs produced with the extract obtained by the CCM method, both cryoconcentration methods promoted the production of AgNPs with an average size below 100 nm.

An interesting fact is a relationship between particle size and ZP when increasing the volume of cryoconcentrated extracts. According to Jadoun et al. (2021), the amount of biomass plays a key role in the bioreduction mechanism of Ag^+ ions to Ag^0 . The increase in the amount of plant biomass in the reaction medium allows a higher release of the bioactive compounds responsible for both the bioreduction process and the stabilization process of silver nanoparticles. It can be seen that in both cryoconcentration methods, their respective biosynthesized AgNPs presented ZP values considered stable as the extract volume was increased. In both methods, CCG and CCM, the ZP of AgNPs reached values between -60 mV and 80 mV for pH between 7 and 10 when the volume of 20 mL of cryoconcentrate was used, which represents excellent stability in colloidal medium (CANO-SARMIENTO et al., 2018). Once again, this fact reinforces the thesis that, under alkaline conditions, the biosynthesis of silver nanoparticles will be more efficient, that is, the generation of stable silver nanoparticles will be successful.(BIRLA et al., 2013). It is also noted that the isoelectric point obtained in this test was between 4 and 5 for pH values (Figure 34 c) and d)).

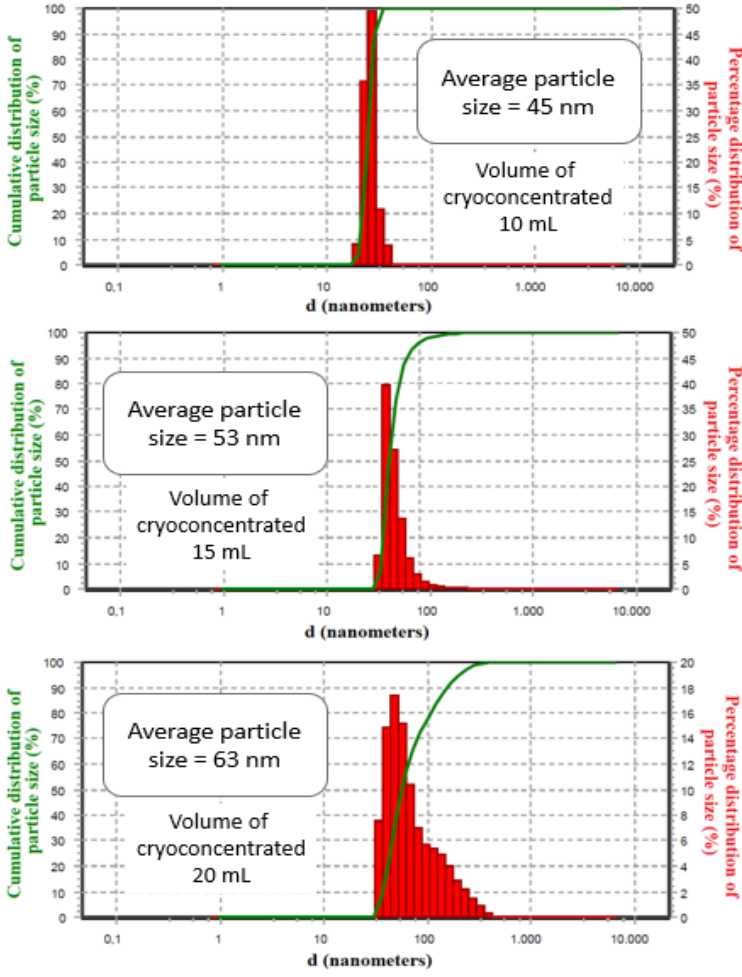
Finally, the fact that increasing the volume of cryoconcentrated extracts causes greater stability of AgNPs, but does not result in a consequent reduction in the size of NPs, can be explained by the study developed by Morales-Lozoya et al. (2021). Since the main components of *M. citrifolia* leaf are anthraquinones, coumarins, carotenoids, flavonoids, iridoids, and organic acids; these bioactive are responsible for promoting the bioreduction of silver salt. However, it can be seen that the increase in the volume of cryoconcentrated extracts, with consequent increases in bioactive compounds, promoted greater stability in the colloidal medium, resulting in lower ZP values. However, we noticed large amounts of bioactive for larger volumes of concentrate with a low concentration of AgNO_3 . This apparent imbalance in the ratio between extract volume/concentration of the metallic precursor probably resulted in the reduction of the polydispersity of AgNPs, with subtle aggregation of NPs.

Figure 35 - Percentage and cumulative distribution assays of AgNPs produced from extracts obtained by CCG and CCM with variation in the volume of the cryoconcentrated.



Influence of volume of cryoconcentrated on AgNPs from CCG via CCG method

Influence of volume of cryoconcentrated on AgNPs from CCM via CCM method



5.1.2.3. Effect of treatment temperature variation

The temperature adopted to promote biosynthesis is one of the most important factors in any chemical and biological reaction, as it directly affects the reaction rate, stability, dispersity, and size of NPs (TRIPATHY et al., 2010; BIRLA et al., 2013). Figure 36 a) and b) shows the UV-Vis spectra of the AgNPs produced by *M. citrifolia* extracts concentrated by the CCG and CCM methods, respectively. The ZP for the AgNPs in both cryoconcentration methods is also shown in Figures 36 (c) and d)). Table 19 presents the analytical data of the average size of the nanoparticles, as well as the zeta potential, the initial pH of the samples, and the wavelength at the peak of absorbance in UV-Vis in relation to the variation of the temperature of biosynthesis of the NPs.

Figure 36 - Effect of treatment temperature variation, on maximum absorbance wavelength (a) and b)) and ZP as a function of pH (c) and d)) on AgNPs.

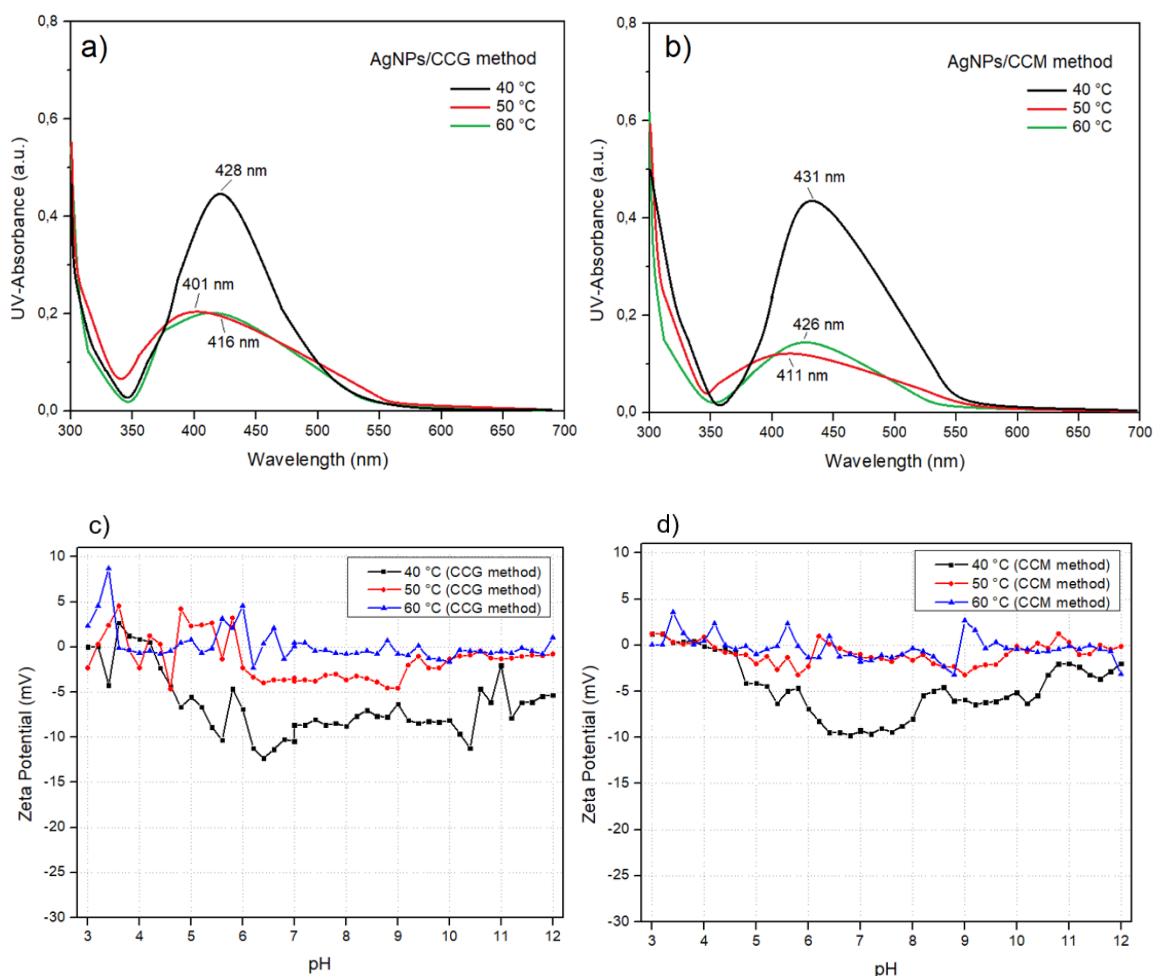


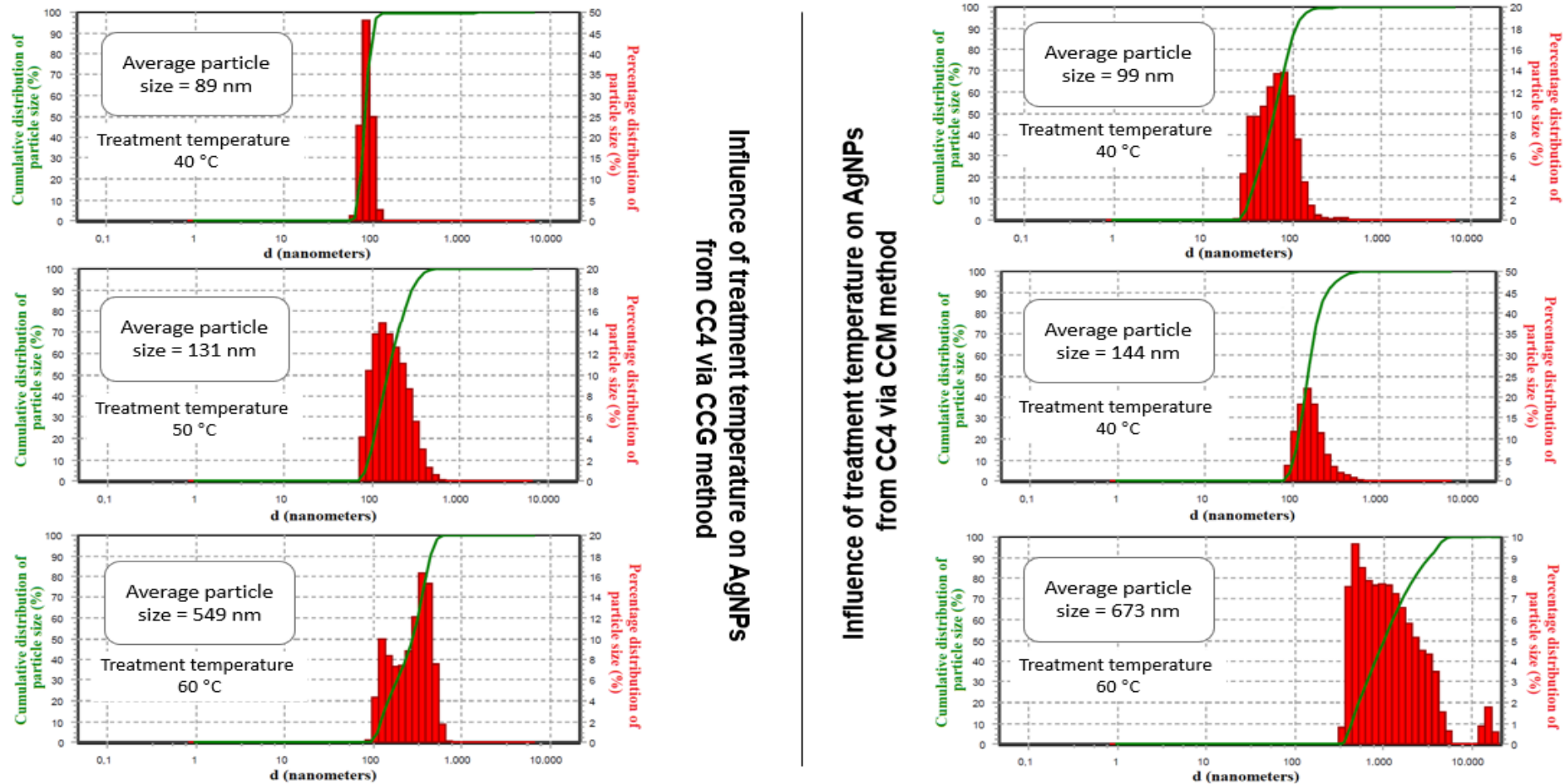
Table 19 - Influence of treatment temperature on size, zeta potential, and UV-Vis spectrum of AgNPs produced by cryoconcentrated *M. citrifolia* extracts.

<i>M. citrifolia</i> extract used in the biosynthesis	Treatment temperature (°C)	Wavelength at maximum absorbance (nm)	Mean size (nm)	Initial pH	Initial zeta potential (mV)
CC4 Cryo Grav	40	428	89	5.51	-9.36
	50	401	131	5.59	-7.45
	60	416	549	5.41	-2.89
CC4 Cryo Micro	40	431	99	5.46	-9.09
	50	411	144	5.29	-6.08
	60	426	673	5.64	-1.45

In short, the relationships between UV-Vis absorbance peaks, stability via ZP, and particle size resulted in an expected result. For both AgNPs produced by extracts obtained via CCG and CCM methods, as the treatment temperature increased, the average size of AgNPs increased abruptly (Table 19), followed by the approximation of ZP values as a function of pH close to zero, ranging from ± 5 mV for treatments at 50 and 60 °C (Figure 36 c) and d)).

Figure 37 shows the particle size distribution histograms produced with extracts from both cryoconcentration methods as a function of the treatment temperature of the reaction medium. It is noted that the treatment at 40 °C, in both the CCG and CCM methods, produced AgNPs with average sizes below 100 nm, but with low stability, as shown by the ZP plots (Figure 36 c) and d)). As already assumed, it is noted again that the treatment in an alkaline medium promotes greater stability in the NPs, and even at 40 °C we obtained ZP values of the AgNPs close to -10 mV at pH between 7 and 10. It did not occur in the treatments at 50 and 60 °C. At this last temperature, we obtained average particle sizes of 549 and 673 nm for the AgNPs synthesized with extracts obtained by CCG and CCM, respectively. Again, as in previous treatments of variation of biosynthesis parameters, the CCG method produced NPs with smaller particle size values and better stability in the colloidal medium.

Figure 37 - Percentage and cumulative distribution assays of AgNPs produced from extracts obtained by CCG and CCM with variation in the treatment temperature.



5.1.2.4. Effect of storage time of AgNPs

The last analysis to evaluate the variation of biosynthesis conditions in the production of AgNPs was verified by comparing the UV-Vis spectra, size, and stability of the nanoparticles after different post-biosynthesis time intervals, that is, varying the age (or storage time) of silver nanoparticles to verify if there would be an abrupt increase in the size and agglomeration of the nanoparticles even after 30 days of the addition of the silver salt in the cryoconcentrated extracts of *M. citrifolia*. The UV-Vis and ZP absorbance peaks of the AgNPs from the extracts concentrated by CCG and CCM are shown in Figure 38. Table 20 presents the analytical data of the average size of the nanoparticles, as well as the zeta potential, the initial pH samples, and the wavelength at the peak of absorbance in UV-Vis concerning the variation of the storage time of NPs.

Figure 38 - Effect of storage time variation of AgNPs, on maximum absorbance wavelength (a) and b)) and ZP as a function of pH (c) and d)) on AgNPs.

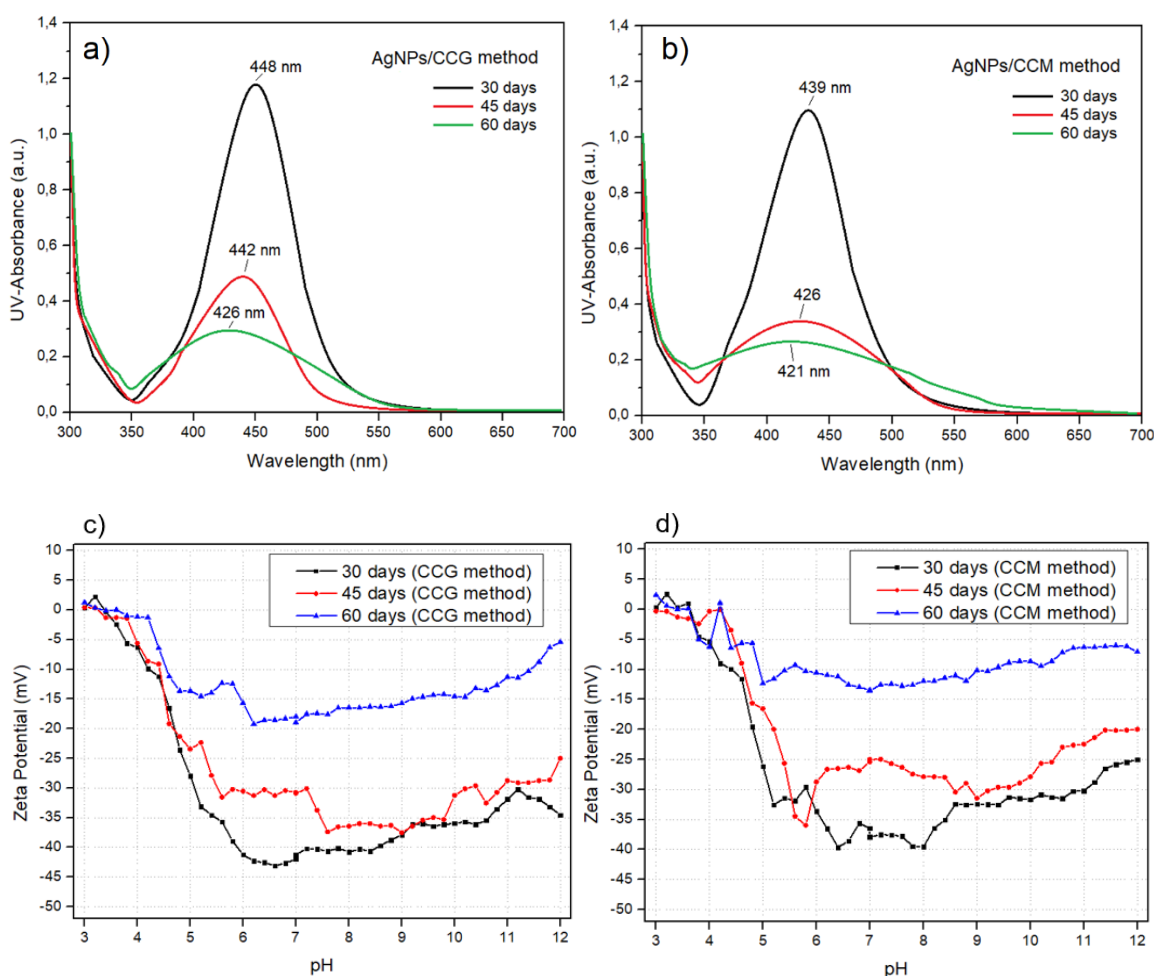


Table 20 - Influence of storage time on size, zeta potential, and UV-Vis spectrum of AgNPs produced by cryoconcentrated *M. citrifolia* extracts.

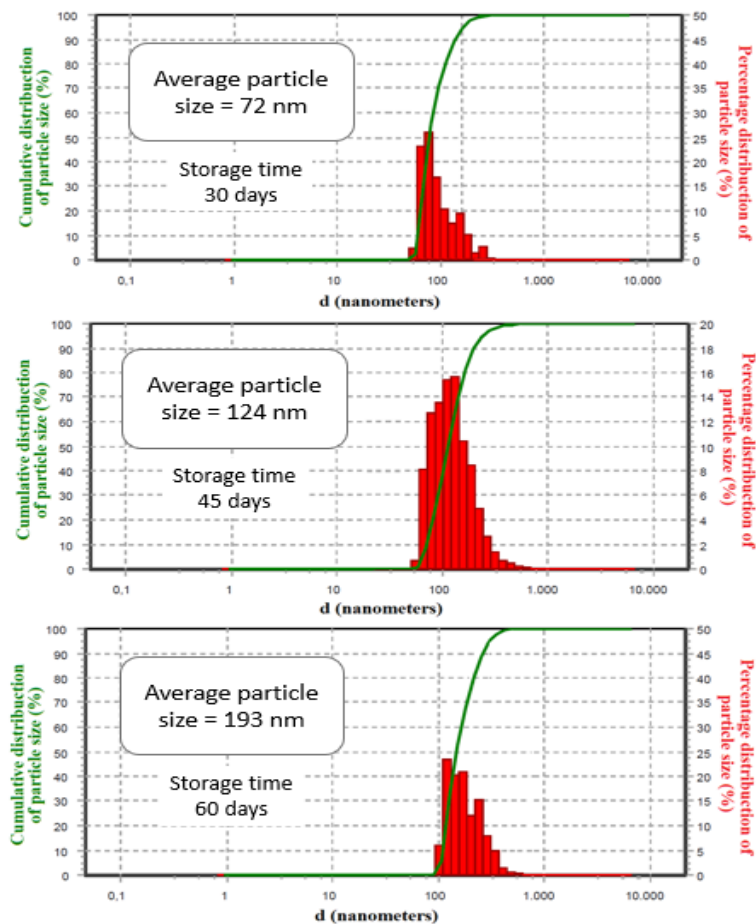
<i>M. citrifolia</i> extract used in the biosynthesis	Storage time (days)	Wavelength at maximum absorbance (nm)	Mean size (nm)	Initial pH	Initial zeta potential (mV)
CC4 Cryo Grav	30	448	72	5.44	-38.64
	45	442	124	5.77	-32.13
	60	426	193	5.81	-14.71
CC4 Cryo Micro	30	439	91	5.23	-32.81
	45	426	144	5.66	-29.18
	60	421	211	5.62	-8.92

Regarding the UV-Vis spectra presented, it is noted that in both cryoconcentration methods, the AgNPs produced after 30 days of storage showed absorption peaks very close to the representative values for AgNPs, as well as those obtained in the Assay Protocol 1. higher UV-Vis absorbance peaks were observed after 30 days of storage, falling sharply as storage time was prolonged. This behavior of the UV-Vis bands seen in shorter storage time is quite similar to that in Figure 32 (a) and b)). In fact, the longer the storage time, the wider the UV-Vis spectrum. In other words, they will have a smaller dispersion, which is corroborated in Figure 39. In this case, after 30 days of storage, the size of AgNPs increased in size more than 100 nm for both biosynthesis with extracts obtained by CCG and CCM.

The ZP aspect of AgNPs in terms of storage time follows a similar pattern. The longer the storage time, the more the ZP values approach the range considered unstable, denoting greater agglomeration and flocculation of the NPs (Figure 38 c) and d)). In both ZP tests for both cryoconcentration methods to obtain NPs, the isoelectric point was obtained with a pH range between 4 and 5, and the best ZP values were again visualized in a pH range ranging between 7 and 10. It is noted again, as in the previous treatments, that the CCG method resulted in NPs with smaller particle sizes and greater stability in the colloidal medium.

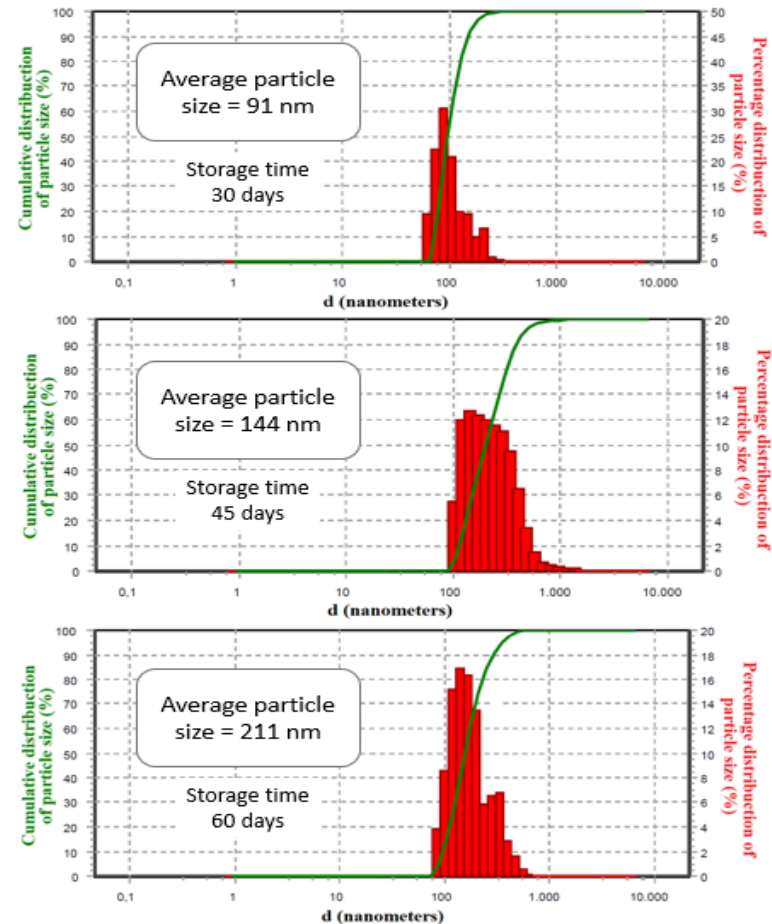
The gradual increase in the average size of AgNPs as the storage time progressed was expected. According to Ledwith et al. (2007) and Rai et al. (2009), the main agents responsible for the stabilization mechanism and consequently repulsion between biological silver nanoparticles are proteins and other biomolecules present in the reaction medium, allowing the nanoparticles to remain separate from one another. others, thus avoiding their agglomeration. Over time, such biomolecules that surround the nanoparticles inevitably lose their activity, thus resulting in the interaction between the nanoparticles and, consequently, increasing their average size. However, in our study, it was possible to obtain NPs with an average size below 100 nm and good stability for up to 30 days.

Figure 39 - Percentage and cumulative distribution assays of AgNPs produced from extracts obtained by CCG and CCM with variation in the storage time of AgNPs.



Influence of storage time on AgNPs from CCG via CCG method

Influence of storage time on AgNPs from CCM via CCM method



5.1.3. Considerations about the size and stability of AgNPs

As previously mentioned, the description of nanotechnology is somewhat controversial when it comes to what can be considered a nanotechnology product or component, but there is a consensus that the dimensions of nanoparticles should be between 1-100 nm. Another consensus is that the physical and chemical properties of nanoparticles vary when on larger size scales, and these base their properties on the thesis that the surface structures involved are much larger compared to the volumes resulting in larger contact areas. In fact, when a nanoparticle decreases in size, a greater proportion of its atoms will be arranged in the surface region of the nanoparticle when compared to the innermost layers. As a practical example, the AgNPs obtained in this study, from which the treatments described in the variations of the biosynthesis parameters, resulted in AgNPs with a size of 30 nm. Such NPs have about 5% of their atoms arranged on their surface; for NPs obtained with a size of 10 nm, as in the treatment with 4 mM of AgNO₃ (Figure 33, CCG method for obtaining the extract), this proportion increases to 20%, reaching up to 50% for a 5 nm nanoparticle. Consequently, it can be deduced that the smaller a nanoparticle, the greater amount of fraction of atoms on its surface when compared to larger nanoparticles (CAO, 2011; SRIVATSAN, 2012; LOWE; LOWE, 2015).

Regarding the ZP assays, Cano-Sarmiento et al. (2018) make us know that NPs from food matrices are electrically charged, interact with each other and with the environment, and are produced through various processes and interface mechanisms. In fact, since the ZP analysis for nanometals of plant origin establishes conditions of stability of the particles in the medium, it is known that for colloidal systems where the medium is of biological origin, the charge arises from the ionization of the surface groups, from the adsorption of material from the active surface.

In our study, the results obtained from ZP reveal that the pH in the slightly basic or alkaline condition favored the colloidal stability of the biosynthesized NPs. According to Akintelu et al. (2021), controlling the pH of biosynthesized nanoparticles could be adopted to regulate the shapes and sizes of nanoparticles. However, the same study revealed that the pH for the formation of nanoparticles only significantly affects the size of the nanoparticles with no significant effect on their shape.

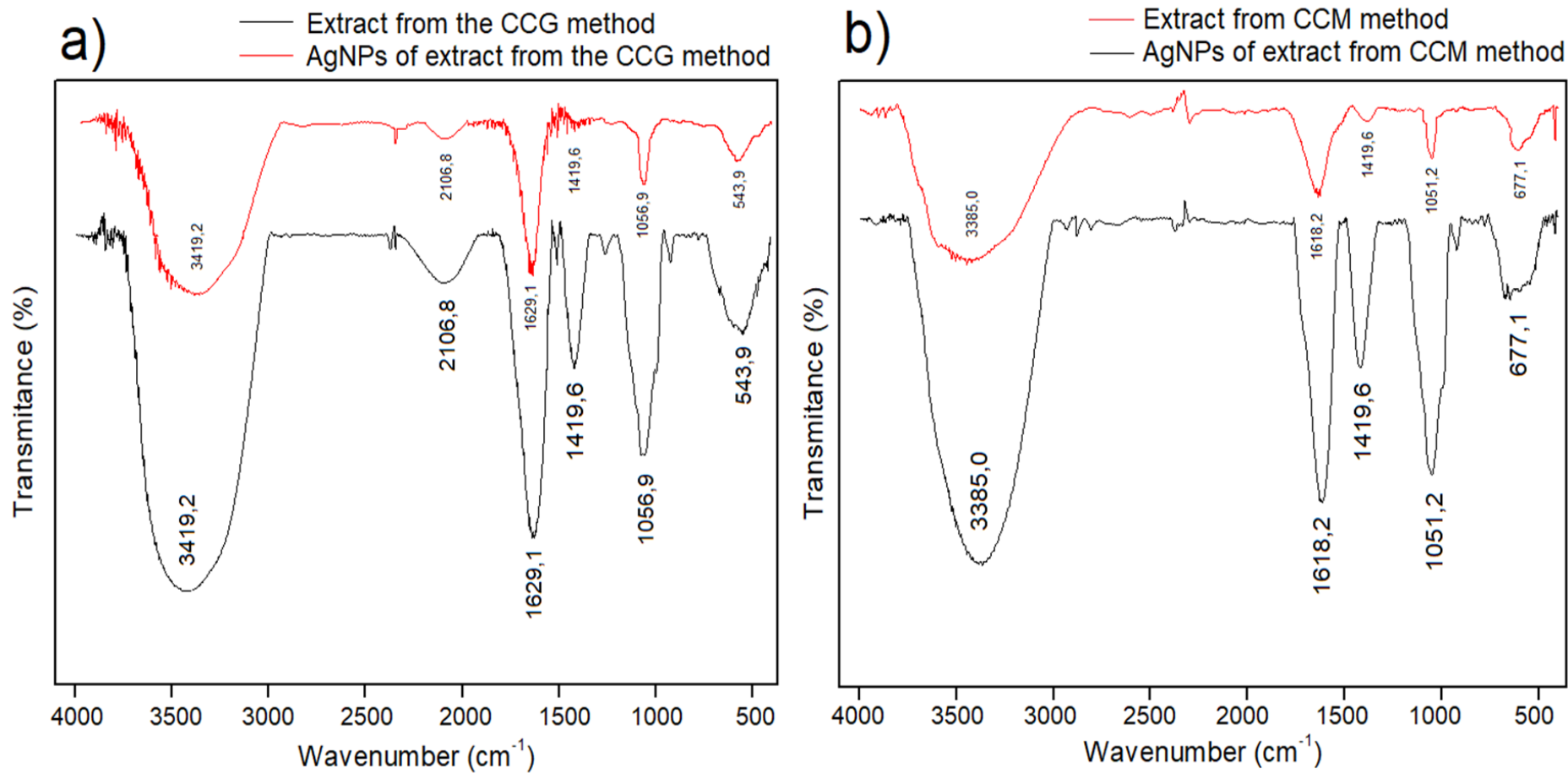
A second important observation is centered on the characteristic pH range for solutions of plant origin in the synthesis of nanoparticles. In this study, it was verified that in all pH measurement tests for solutions containing AgNPs, the pH values after synthesis were in the pH range between 5 and 6. Since the best stability conditions via ZP were obtained at pH varying from neutral to basic, it can be inferred, as corroborated in the study by Tripathy et al. (2010), that the beginning of biosynthesis occurs as a result of a subtle drop in pH. Finally, in this study it was confirmed via HPLC assays that the cryoconcentrate of *M. citrifolia* leaf extract contained elements with an acidic character, such as gallic, vanillic, caffeic acid, and catechins (Tables 10 and 11). It can be inferred that the process of biological reduction in the formation of AgNPs was accompanied by the oxidation of organic acids present in the extract.

5.2. Structure analysis of AgNPs

As previously described, the FTIR spectroscopy assays on cryoconcentrated extracts by the CCG and CCM methods aimed to prescribe functional groups present in the concentrated samples (Tables 6 and 7). Since the biomolecules present in concentrated noni extracts are responsible for promoting biosynthesis, therefore FTIR has become an important tool in understanding the involvement of functional groups in the interactions between metallic particles and biomolecules. Figure 40 presents a comparison between the transmittance spectra (%) FTIR obtained for the samples CC4-CCG (Figure 40 a)), CC4-CCM (Figure 40 b)) and the transmittance spectra (%) FTIR for the AgNPs obtained using the previously mentioned cryoconcentration methods.

It can be seen that in both assays for CCG and CCM, the main FTIR peaks represented hydrogen-bonded O-H (3419.2 nm and 3385.0 nm), conjugated dienes with an aromatic ring (1629.1 nm and 1618.2 nm) and ethyl groups (1056.9 nm and 1051.2 nm). It can be seen that for all FTIR transmittance peaks obtained for both CC4-CCG and CC4-CCM, the same peaks that represented the AgNPs occurred at a lower transmittance intensity (Figure 40).

Figure 40 - Comparison between the FTIR spectra of cryoconcentrated samples and AgNPs produced by the same sample: CC-CCG (a) and CC4-CCM (b).



These results corroborate those obtained by Morales-lozoya et al. (2021), Suman et al. (2013), and Akintelu et al. (2021), which report that these results infer the involvement of metabolites of *Morinda citrifolia* extract in the bioreduction of silver ions and formation of AgNPs. The near disappearance of the band 3419.2 nm and 3385.0 nm suggests that the -OH functional groups play a vital role in the bioreduction and stabilization of Sathishkumar et al. (2012) synthesized AgNPs.

Finally, Morales-lozoya et al. (2021) add that the differences between the FTIR spectra of cryoconcentrated extracts and their respective AgNPs suggest the formation of chelates of Ag ions and -OH groups of free sugars, carboxylic acids, and polysaccharides present in EM. Therefore, we can conclude that the formation of chelates results in the oxidation of hydroxyl groups and, therefore, in the reduction of Ag^{1+} ions to Ag^0 to form AgNPs.

The presence of bioreduced silver ions, as well as their quantity, was detected by FAAS. The analysis was performed on the samples containing the AgNPs obtained from the cryoconcentrated extracts via the CCG and CCM method, as well as on the sample containing the AgNPs obtained from the *in natura* extract of *M. citrifolia* leaves, that is, the same samples that composed the analysis of UV-Vis spectroscopy, particle size, and stability via ZP of Assay Protocol 1. According to FAAS analysis, the presence of bioreduced AgNPs was detected. The quantitative results in mg/L of the silver nanoparticles formed are shown in Table 21.

Table 21 - Concentration of AgNPs determined by FAAS, produced through the use of cryoconcentrated extracts of *Morinda citrifolia* via CCG, CCM method, and by extract *in natura*.

Type of <i>M. citrifolia</i> extract used in the biosynthesis of AgNPs	Amount of AgNPs per FAAS (mg/L)
<i>In natura</i>	6.12 ± 0.06
CC4-CCG	33.24 ± 0.41
CC4-CCM	15.61 ± 0.36

Data are expressed as mean ± SD (n = 4).

In the present study, it is noted that, as well as the CCG method in the recovery of bioactive from *M. citrifolia*, resulted in higher levels of solids (Table 3) and phenolic compounds (Table 5). Moreover, at higher concentrations of bioactive identified by HPLC (Table 10), the AgNPs generated by this extract were also in higher concentration when compared to the CCM method and much higher than the extract *in natura*. This result is clearly due to a condition in which the presence of a greater amount of substrate present in the concentrated extracts resulted in rapid bioreduction and, consequently, in the formation of greater amounts of silver nanoparticles.

5.3. Microstructure analysis of AgNPs

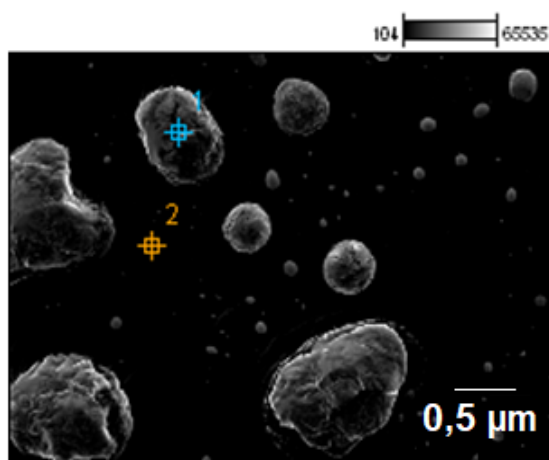
The SEM-EDS assays shown in Figures 41, 42, and 43 provide a semi-qualitative approach to the results obtained since the purpose of using SEM is primarily to visualize the morphological and polydispersity aspects of AgNPs.

The use of EDS coupled with SEM is intended to be a qualitative tool in confirming the formation of AgNPs, thus corroborating the effectiveness of biosynthesis. In SEM-EDS micrographs, a dispersed distribution of AgNPs is observed, both in samples from *in natura* plant extracts and in cryoconcentrated in both concentration methods performed (CCG and CCM).

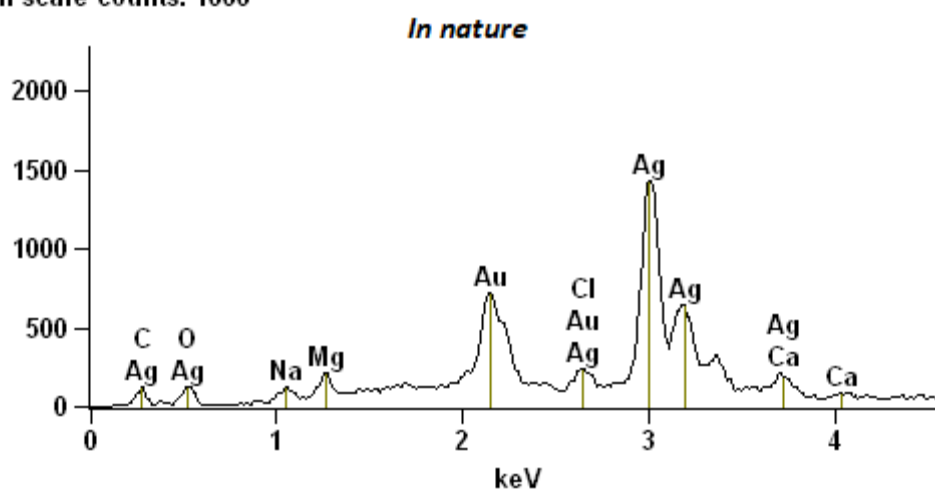
The AgNPs presented themselves as small aggregates at a scale of up to 500 nm, due to the limitations of the equipment. As shown in Figures 41, 42, and 43, it can be inferred that silver nanoparticles have an approximately spherical shape.

In addition, it is possible to perceive the presence of residues of non-reactive organic matter, coming from the plant extract around the AgNPs (Figures 42 and 43). From the SEM-EDS images, a dispersed distribution of AgNPs, as well as small aggregates of them, can be observed. This behavior of NPs is similar to that presented by Morales-Lozoya et al. (2021). The presence of metallic silver was confirmed by analyzing the sample by EDS to determine its composition. The presence of chemical elements such as Cu (sample support), Si, Na, Cl, O, and C (from the extract), are part of the composition of the aqueous sample and corroborate the studies provided by Cvetkovikj et al. (2013) and Samateh et al. (2018). Finally, from the EDS test, the incident energy peak can also be observed, which according to Suman et al. (2014), is characteristic of silver (3.0 keV), as well as its relative abundance at this point.

Figure 41 - SEM-EDS micrograph of AgNPs related to the *in natura* extract of *M. citrifolia* leaves.



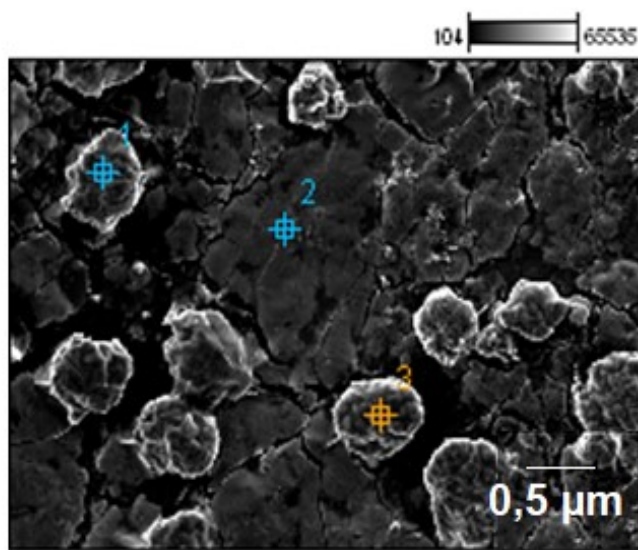
Full scale counts: 1666



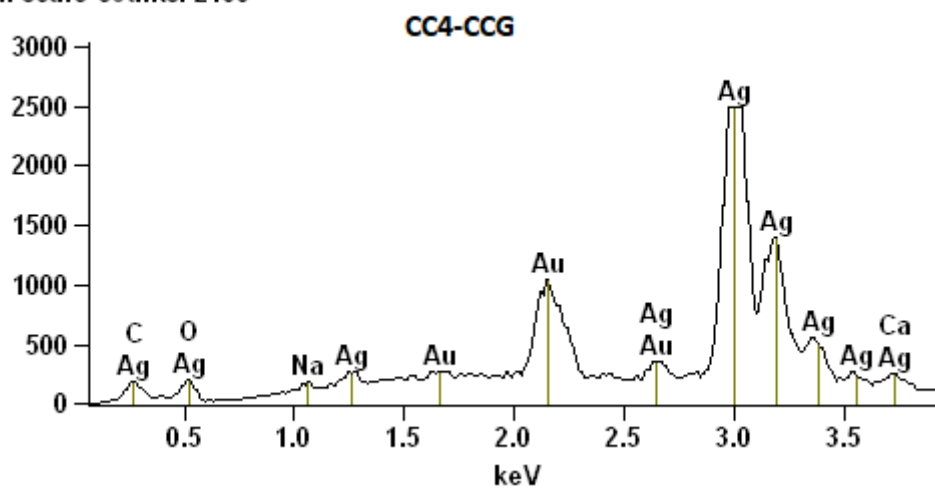
EDS assay details

Elements	C-K	O-K	Na-K	Mg-K	Cl-K	Ca-K	Ag-L	Au-M
Weight %	1.08	4.33	0.76	1.06	1.26	4.91	67.75	18.85
Atom %	6.84	20.50	2.51	3.31	2.68	9.29	47.61	7.25
Net Counts	513	736	554	977	919	2034	24093	8841

Figure 42 - SEM-EDS micrograph of AgNPs related to CC4-CCG extract from *M. citrifolia* leaves.



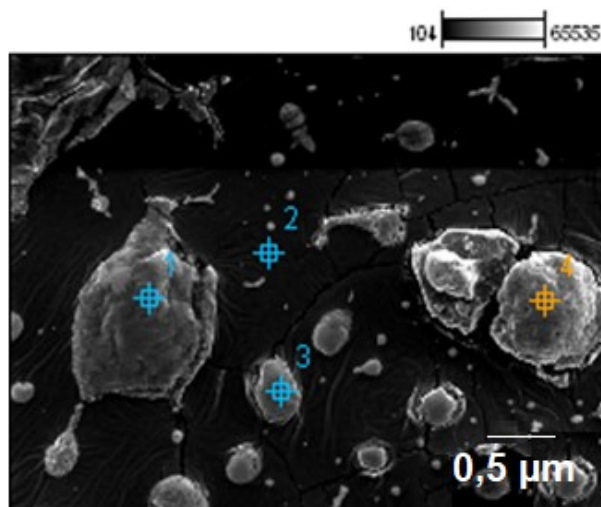
Full scale counts: 2488



EDS assay details

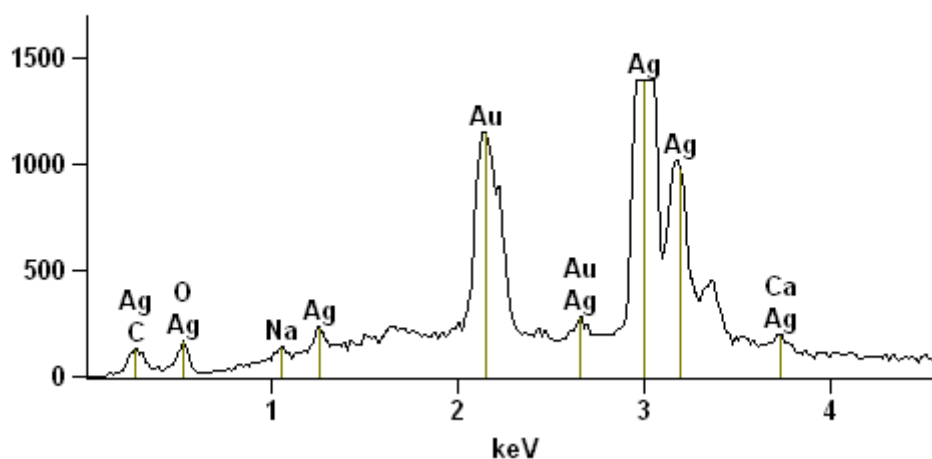
Elements	C-K	O-K	Na-K	Al-K	Ca-K	Rb-L	Ag-L	Au-M
Weight %	0.94	3.04	0.31	--	1.75	---	79.59	14.37
Atom %	6.88	16.72	1.20	--	3.84	--	64.94	6.42
Net Counts	1007	982	433	--	1400	--	55932	13107

Figure 43 - SEM-EDS micrograph of AgNPs related to CC4-CCM extract from *M. citrifolia* leaves.



Full scale counts: 1394

CC4-CCM



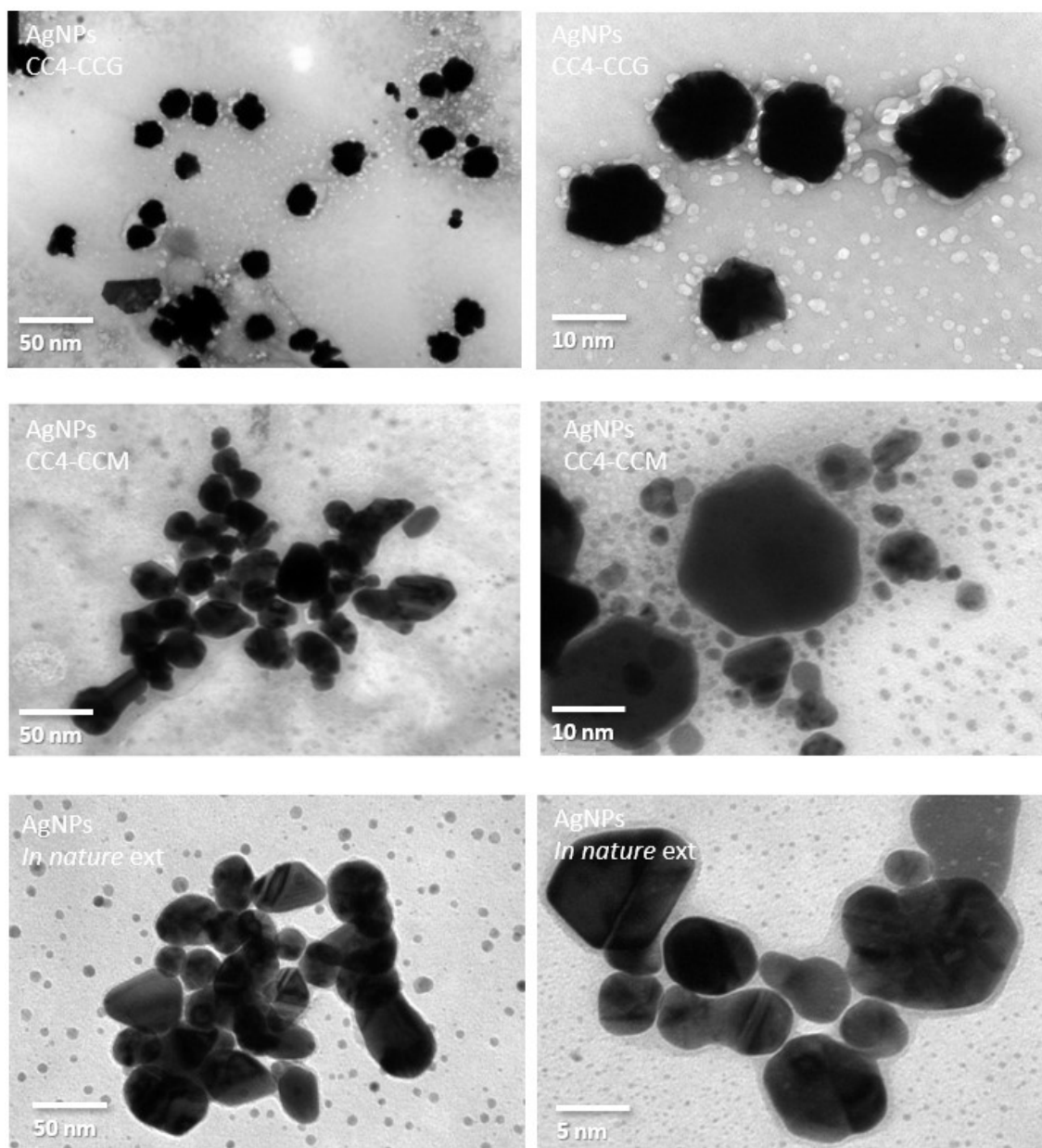
EDS assay details

Element	C-K	O-K	Na-K	Ca-K	Nb-L	Tc-L	Ag-L	Au-M
Weight %	0.96	3.25	0.26	2.08	--	--	71.36	22.10
Atom %	7.13	18.12	1.01	4.63	--	--	59.09	10.02
Net Counts	757	867	292	1330	--	--	39333	16117

Finally, the results of the TEM analysis are shown in Figure 44, which illustrates the AgNPs biosynthesized using *M. citrifolia* extracts concentrated by CCG and CCM, as well as by the extract *in natura* (Figure 44, from top to bottom). The TEM images confirm the presence of high-quality AgNPs, in terms of narrow size and polydispersity, also presenting a spheroidal, hexagonal, and uniformly distributed (monodisperse) shape without the detection of agglomerations. The average size of the AgNPs produced

using the extract *in natura*, CC4-CCG and CC4-CCM were 40 nm, 17 nm, and 29 nm respectively, a result that is similar and approximate to that presented by the DLS analysis of the Assays Protocol samples 1, as set out in Table 16 and Figure 31.

Figure 44 - TEM micrographs of AgNPs biosynthesized using the *in natura* extract and the extracts concentrated by CCG and CCM from the leaves of *M. citrifolia*.



6. CONCLUSIONS OF PART II

Given the general objective of this part of the study, we can conclude that biosynthesis of silver nanoparticles (AgNPs) through the use of cryoconcentrated extracts of *Morinda citrifolia* leaves was highly effective. The general results suggest that the biosynthesized AgNPs were characterized by high-performance techniques. yield, which are a set of essential tools in the verification of the presence of the obtained product.

The biosynthesis included an easy and scalable methodology, which allowed a quick, economic, simple and successful preparation of nanoparticles using extracts from *M. citrifolia* cryoconcentrated leaves by two different methods, gravitational and microwave-assisted.

It was studied how the concentrated substrate of *M. citrifolia* would provide the bioproduction of nanoparticles with improved properties. The AgNPs obtained from the cryoconcentrated extracts showed smaller particle size, better stability in colloidal medium, greater polydispersity, and color tone of the solution characteristic for AgNPs when compared with the AgNPs obtained from the *in natura* extract of *M. citrifolia* leaves. In addition, the biosynthesis of AgNPs using the concentrated extracts provided a higher concentration of NPs when again compared to the AgNPs from the extract *in natura*.

The FTIR spectroscopy assays revealed that the reductions in transmittance bands for AgNPs in relation to the same band referring to cryoconcentrated extracts are clearly due to the direct action of phenolic compounds such as flavonoids, triterphenoids present in the leaf extract that possibly influenced the reduction and stabilization of nanoscale silver particles. Furthermore, the differences between the FTIR spectra of the cryoconcentrated extracts and their respective AgNPs suggested the formation of chelates of Ag ions and –OH groups released by the bioactive agents present in greater amounts in the concentrated extracts.

The electron microscopy analyses allowed the visual verification of the AgNPs, of which the EDS tool allowed the elemental identification of Ag in the colloidal solutions of which they were uniformly distributed in a spherical shape.

The interference of the variation of several biosynthesis parameters on the size and stability of AgNPs was also studied. It was notable that both the increase of the metallic

precursor and the volume of the cryoconcentrate caused better stability results in ZP as a function of pH. It was notable that the best conditions for lower ZP values, consequently better stability, occurred in pH in the neutral range. and alkaline. However, higher volumes of concentrated extract did not cause a reduction in the size of AgNPs, suggesting a high amount of plant substrate with little available metallic reducing salt. It was also noticed that the most suitable temperature for AgNPs biosynthesis remained below 30 °C, since the increase in temperature caused an abrupt increase in particle size as well as greater instability reflected in ZP values close to 0 mV. It was also possible to verify the behavior of NPs against the storage time of AgNPs, from which it was possible to obtain stable nanosilver particles, with an average size below 100 nm in up to 30 days.

Overall, both cryoconcentration methods offered a valuable substrate in promoting AgNP biosynthesis. Both concentrated extracts were highly effective in terms of smaller size and stability of AgNPs when compared to biosynthesis involving the extract *in natura*. The fact that the biosynthesis involving the use of the extract from the CCG had better performance than the extract from the CCG, is due to the deposition of bioactive compounds present in the extract after the CCG.

FINAL CONCLUSION

The option to use block cryoconcentration techniques by the gravitational and microwave-assisted method was satisfactory and efficient in the retention process of bioactive compounds present in *M. citrifolia* leaf extracts. Given these methods, it is not necessary to use robust and expensive equipment, with easy process execution and high performance in the recovery of the final product.

Both cryoconcentration methods allowed the retention of large amounts of solids and phenolic compounds in the concentrated fractions, with high concentration factors in solute retention and high efficiency in the concentration of phenolic compounds. Although the use of the gravitational cryoconcentration technique resulted in a greater accumulation of retained solids and phenolic compounds; both methods are considered efficient for this purpose.

Both cryoconcentration methods also allowed obtaining a concentrated extract with proven potential for the synthesis of silver nanoparticles with improved properties. When compared with the *in natura* extract, the use of extracts more concentrated in phenolic compounds enabled the biosynthesis of nanoparticles of smaller size and greater stability.

Finally, taking into account that noni leaves are proven to contain a high amount of bioactive compounds with phytotherapeutic properties, the present study proved that the application of a non-thermal technology, known as cryoconcentration, for the separation and concentration of bioactive compounds from *Morinda citrifolia* was not only highly beneficial, but it also opened precedents for the exploitation of the product obtained in the broad field of nanobiotechnology, making the use of the technique in that plant raw material unprecedented. The results presented also suggest that the present study can contribute as a reference to the use of a cheap and sustainable technology in the reuse and treatment of residues from the food industry, in the generation of a promising product of high biological value, aiming to enhance the acquisition of bioactive, such as phenolic compounds; with broad functionality as well as enhanced nutritional and phytotherapy properties.

SUGGESTIONS FOR FUTURE WORK

The use of simpler technologies, with high yield and productivity in the acquisition of bioactive compounds from *M. citrifolia* proved to be effective in the biosynthesis of nanometals. The exploration of other methods of better yield in the concentration, as well as the expansion of scale is valid not only in the acquisition of a product of self-nutritional content but also in obtaining an even more valuable substrate for the biosynthesis of nanometals.

The tests of variation in the biosynthesis conditions of AgNPs had as main objective to verify their behavior in relation to the particle size and stability in a colloidal medium. However, the large number of results obtained allows, in further study, the development of a method for optimizing the biosynthesis of AgNPs to reach an optimal condition in the acquisition of these nanometals.

Finally, since the use of cryoconcentrated substrate, either by gravitational or microwave-assisted methods, has proven to result in nanosilver with even more improved properties than those obtained using the extract *in natura*. Such nanometals may allow for an even further application as an effective therapeutic agent against human pathogens.

REFERENCES

- Association of Official Agricultural Chemists (AOAC). **Official Methods of Analysis of AOAC International**. 18, Revisi. ed. [s.l: s.n.]
- AALBERSBERG, W. G. L.; HUSSEIN, S.; SOTHEESWARAN, S.; PARKINSON, S. Carotenoids in the Leaves of *Morinda citrifolia*. **Journal of Herbs, Spices & Medicinal Plants**, v. 2, n. 1, p. 51–54, 1993.
- ADNAN, A.; MUSHTAQ, M.; ISLAM, T. ul. Fruit Juice Concentrates. In: **Fruit Juices: Extraction, Composition, Quality and Analysis**. [s.l.] Elsevier Inc., 2018. p. 217–240.
- ADORNO, W. T.; REZZADORI, K.; AREND, G. D.; CHAVES, V. C.; REGINATTO, F. H.; DI LUCCIO, M.; PETRUS, J. C. C. Enhancement of phenolic compounds content and antioxidant activity of strawberry (*Fragaria × ananassa*) juice by block freeze concentration technology. **International Journal of Food Science and Technology**, v. 52, n. 3, p. 781–787, 2017.
- AIDER, M.; DE HALLEUX, D. Passive and microwave-assisted thawing in maple sap cryoconcentration technology. **Journal of Food Engineering**, v. 85, n. 1, p. 65–72, 2008.
- AIDER, M.; DE HALLEUX, D. Cryoconcentration technology in the bio-food industry: Principles and applications. **LWT - Food Science and Technology**, v. 42, n. 3, p. 679–685, 2009. Disponível em: <<http://dx.doi.org/10.1016/j.lwt.2008.08.013>>.
- AIDER, M.; DE HALLEUX, D.; AKBACHE, A. Whey cryoconcentration and impact on its composition. **Journal of Food Engineering**, v. 82, n. 1, p. 92–102, 2007.
- AIDER, M.; DE HALLEUX, D.; MELNIKOVA, I. Gravitational and microwave-assisted thawing during milk whey cryoconcentration. **Journal of Food Engineering**, v. 88, n. 3, p. 373–380, 2008.
- AIDER, M.; DE HALLEUX, D.; MELNIKOVA, I. Skim milk whey cryoconcentration and impact on the composition of the concentrated and ice fractions. **Food and Bioprocess Technology**, v. 2, n. 1, p. 80–88, 2009.
- AIDER, M.; HALLEUX, D. de. Production of concentrated cherry and apricot juices by cryoconcentration technology. **LWT - Food Science and Technology**, v. 41, n. 10, p. 1768–1775, 2008.
- AIDER, M.; OUNIS, W. Ben. Skim milk cryoconcentration as affected by the thawing mode: Gravitational vs. microwave-assisted. **International Journal of Food Science and Technology**, v. 47, n. 1, p. 195–202, 2012.
- AKINTELU, S. A.; FOLORUNSO, A. S.; OYEBAMIJI, A. K.; OLUGBEKO, S. C. Mosquito Repellent and Antibacterial Efficiency of Facile and Low-Cost Silver Nanoparticles Synthesized Using the Leaf Extract of *Morinda citrifolia*. **Plasmonics**, v. 16, p. 1645–1656, 2021.
- AL-WHAIBI, M. H.; FIROZ, M.; AL-KHAISHANY, M. Y. Role of Nanoparticles in Plants. In: **Nanotechnology and Plant Sciences**. 1. ed. [s.l.] Springer, Cham, 2015. p. 19–35.
- ALI, M.; KENGANORA, M.; MANJULA, S. N. Health Benefits of *Morinda citrifolia* (Noni): A

Review. **Pharmacognosy Journal**, v. 8, n. 4, p. 321–334, 2016.

ALMEIDA, É. S.; DE OLIVEIRA, D.; HOTZA, D. Characterization of silver nanoparticles produced by biosynthesis mediated by *Fusarium oxysporum* under different processing conditions. **Bioprocess and Biosystems Engineering**, v. 40, n. 9, 2017.

ALMEIDA, É. S.; DE OLIVEIRA, D.; HOTZA, D. Properties and Applications of *Morinda citrifolia* (Noni): A Review. **Comprehensive Reviews in Food Science and Food Safety**, 2019.

AREND, G. D.; ADORNO, W. T.; REZZADORI, K.; LUCCIO, M. Di; CHAVES, V. C.; REGINATTO, F. H.; PETRUS, J. C. C. Concentration of phenolic compounds from strawberry (*Fragaria X ananassa* Duch) juice by nano filtration membrane. **Journal of Food Engineering**, v. 201, p. 36–41, 2017.

ASHOK KUMAR, D.; PALANICHAMY, V.; ROOPAN, S. M. Photocatalytic action of AgCl nanoparticles and its antibacterial activity. **Journal of Photochemistry and Photobiology B: Biology**, v. 138, p. 302–306, 2014. Disponível em: <<http://dx.doi.org/10.1016/j.jphotobiol.2014.06.011>>.

ASSANGA, I.; L.M, L. L.; E.G., R.-C.; SALIDO, G.-; ACOSTA-SILVA, A. A.; MEZA-CUETO, C. Y.; L., R.-P. J. Effect of maturity and harvest season on antioxidant activity, phenolic compounds and ascorbic acid of *Morinda citrifolia* L. (noni) grown in Mexico (with track change). **African Journal of Biotechnology**, v. 12, n. 29, p. 4630–4639, 2013.

BENEDETTI, S.; PRUDÊNCIO, E. S.; NUNES, G. L.; GUIZONI, K.; FOGAÇA, L. A.; PETRUS, J. C. C. Antioxidant properties of tofu whey concentrate by freeze concentration and nanofiltration processes. **Journal of Food Engineering**, v. 160, p. 49–55, 2015.

BIRLA, S. S.; GAIKWAD, S. C.; GADE, A. K.; RAI, M. K. Rapid Synthesis of Silver Nanoparticles from *Fusarium oxysporum* by Optimizing Physicocultural Conditions. **The Scientific World Journal**, v. 2013, 2013.

BONILLA-ZAVALETA, E.; VERNON-CARTER, E. J.; BERISTAIN, C. I. Thermophysical properties of freeze-concentrated pineapple juice. **Italian Journal of Food Science**, v. 18, n. 4, p. 367–376, 2006.

BOURNE, M. C. **Food Texture and Viscosity: Concept and Measurement**. 2nd Editio ed. New York, USA: Academic Press, Elsevier Inc., 2002.

BRAND-WILLIAMS, W.; CUVELIER, M. E.; BERSET, C. Use of a free radical method to evaluate antioxidant activity. **Food Science and Technology**, v. 28, n. 1, p. 25–30, 1995.

CANO-SARMIENTO, C.; TÉLLEZ-MEDINA, D. I.; VIVEROS-CONTRERAS, R.; CORNEJO-MAZÓN, M.; FIGUEROA-HERNÁNDEZ, C. Y.; GARCÍA-ARMENTA, E.; ALAMILLA-BELTRÁN, L.; GARCÍA, H. S.; GUTIÉRREZ-LÓPEZ, G. F. Zeta Potential of Food Matrices. **Food Engineering Reviews**, v. 10, p. 113–138, 2018.

CAO, G. Physical Chemistry of Solid Surfaces. In: **Nanostructures and Nanomaterials - Synthesis, Properties, and Applications**. 2. ed. [s.l.] World Scientific Series in Nanoscience and Nanotechnology,

2011. 2p. 19–60.

CAMEL, S.; STAGNARO, S.; MARCHIONNI, M. Morinda citrifolia Plays a Central Role in the Primary Prevention of Mitochondrial-dependent Degenerative Disorders. **Asian Pacific Journal of Cancer Prevention**, v. 16, n. 4, p. 1675, 2015.

CARRILLO-LÓPEZ, A.; YAHIA, E. M. Noni (Morinda citrifolia L.). In: **Postharvest Biology and Technology of Tropical and Subtropical Fruits**. Elhadi M. ed. [s.l.] Woodhead Publishing Limited, 2011. 4p. 51–64.

CHAN-BLANCO, Y.; VAILLANT, F.; MERCEDES PEREZ, A.; REYNES, M.; BRILLOUET, J. M.; BRAT, P. The noni fruit (Morinda citrifolia L.): A review of agricultural research, nutritional and therapeutic properties. **Journal of Food Composition and Analysis**, v. 19, n. 6–7, p. 645–654, 2006.

CLARK, D. P.; PAZDERNIK, N. J. Nanobiotechnology. **Biotechnology**, p. 219–248, 2016. Disponível em: <<http://linkinghub.elsevier.com/retrieve/pii/B9780123850157000077>>.

CONIDI, C.; DRIOLI, E.; CASSANO, A. Membrane-based agro-food production processes for polyphenol separation, purification and concentration. **Current Opinion in Food Science**, v. 23, p. 149–164, 2018.

CORREA, L. J.; RUIZ, R. Y.; MORENO, F. L. Effect of falling-film freeze concentration on bioactive compounds in aqueous coffee extract. **Journal of Food Process Engineering**, v. 41, n. 1, p. 1–8, 2018.

CVETKOVIKJ, I.; STEFKOV, G.; ACEVSKA, J.; STANOEVA, J. P.; KARAPANDZOVA, M.; STEFOVA, M.; DIMITROVSKA, A.; KULEVANOVA, S. Polyphenolic characterization and chromatographic methods for fast assessment of culinary Salvia species from South East Europe. **Journal of Chromatography A**, v. 1282, n. 22, p. 38–45, 2013.

DAWSON, N. G. Sweating the Small Stuff: Environmental Risk and Nanotechnology. **Bioscience**, v. 58, n. 8, p. 690, 2008.

DE MORAIS, M. G.; MARTINS, V. G.; STEFFENS, D.; PRANKE, P.; DA COSTA, J. A. V. Biological applications of nanobiotechnology. **Journal of nanoscience and nanotechnology**, v. 14, n. 1, p. 1007–17, 2014. Disponível em: <<http://www.ncbi.nlm.nih.gov/pubmed/24730317>>.

DE SOUZA, M. V. N.; FERREIRA, S. B.; MENDONÇA, J. S.; COSTA, M.; REBELLO, F. R. Methodologies for the preparation and synthetic application of thiazoles, an important class of heterocyclic compounds. **Química Nova**, v. 28, n. 1, p. 77–84, 2005.

DEMIRBAS, A.; GROSZMAN, K.; PAZMIÑO-HERNANDEZ, M.; VANEGAS, D. C.; WELT, B.; HONDRED, J. A.; GARLAND, N. T.; CLAUSSEN, J. C.; MCLAMORE, E. S. Cryoconcentration of flavonoid extract for enhanced biophotovoltaics and pH sensitive thin films. **Biotechnology Progress**, v. 34, n. 1, p. 206–217, 2018.

DENG, S.; WEST, B. J.; JENSEN, C. J. Simultaneous characterisation and quantitation of flavonoid glycosides and aglycones in noni leaves using a validated HPLC-UV/MS method. **Food Chemistry**, v.

111, n. 2, p. 526–529, 2008.

DENG, S.; WEST, B. J.; JENSEN, C. J. A quantitative comparison of phytochemical components in global noni fruits and their commercial products. **Food Chemistry**, v. 122, n. 1, p. 267–270, 2010. Disponível em: <<http://dx.doi.org/10.1016/j.foodchem.2010.01.031>>.

DITTMAR, A. *Morinda citrifolia* L. - Use in Indigenous Samoan Medicine. **Journal of Herbs, Spices & Medicinal Plants**, v. 1, n. 3, p. 77–92, 1993.

DIXON, A. R.; MCMILLEN, H.; ETKIN, N. L. Ferment this: The transformation of noni, a traditional Polynesian medicine (*Morinda citrifolia*, Rubiaceae). **Economic Botany**, v. 53, n. 1, p. 51–68, 1999.

DOVA, M. I.; PETROTOS, K. B.; LAZARIDES, H. N. On the direct osmotic concentration of liquid foods. Part I: Impact of process parameters on process performance. **Journal of Food Engineering**, v. 78, p. 422–430, 2007.

DUSSOSSOY, E.; BONY, E.; MICHEL, A.; BOUDARD, F.; GIAIMIS, J.; BRAT, P.; VAILLANT, F. Anti-oxidative and anti-inflammatory effects of the *Morinda citrifolia* fruit (Noni). **Acta Horticulturae**, v. 1040, p. 69–74, 2014.

EL-RAFIE, H. M.; EL-RAFIE, M. H.; ZAHRAN, M. K. Green synthesis of silver nanoparticles using polysaccharides extracted from marine macro algae. **Carbohydrate Polymers**, v. 96, n. 2, p. 403–410, 2013. Disponível em: <<http://dx.doi.org/10.1016/j.carbpol.2013.03.071>>.

EL-SHERBINY, I. M.; SALIH, E. Green Synthesis of Metallic Nanoparticles Using Biopolymers and Plant Extracts. In: KANCHI, S.; AHMED, S. (Ed.). **Green Metal Nanoparticles: Synthesis, Characterization and Their Applications**. 1. ed. [s.l.] Scrivener Publishing LLC, 2018. p. 89–115.

ELKINS, R. M. H. **Hawaiian Noni: Prize Herb of Hawaii and the South Pacific**. [s.l.] Woodland Publishing. Pleasant Grove, UT, 1998.

ESCALANTE-MINAKATA, P.; IBARRA-JUNQUERA, V.; CHÁVEZ-RODRÍGUEZ, A. M.; DE JESÚS ORNELAS-PAZ, J.; EMPARAN-LEGASPI, M. J.; PÉREZ-MARTÍNEZ, J. D.; VILLAVELÁZQUEZ-MENDOZA, C. I. Evaluation of the freezing and thawing cryoconcentration process on bioactive compounds present in banana juice from three different cultivars. **International Journal of Food Engineering**, v. 9, n. 4, p. 445–455, 2013.

Food and Agriculture Organization of the United Nations (FAO). **Global food losses and food waste – Extent, causes and prevention**. [s.l.: s.n.]

H.Y., E.-K.; M.M., E.-S. Cytotoxic activity of biosynthesized gold nanoparticles with an extract of the red seaweed *Corallina officinalis* on the MCF-7 human breast cancer cell line. **Asian Pacific Journal of Cancer Prevention**, v. 15, n. 10, p. 4311–4317, 2014.

HAAS, I. C. da S.; ESPINDOLA, J. S. de; DE LIZ, G. R.; LUNA, A. S.; BORDIGNON-LUIZ, M. T.; PRUDÊNCIO, E. S.; DE GOIS, J. S.; FEDRIGO, I. M. T. Gravitational assisted three-stage block freeze concentration process for producing enriched concentrated orange juice (*Citrus sinensis* L.): Multi-

elemental profiling and polyphenolic bioactives. **Journal of Food Engineering**, v. 315, n. August 2021, 2022.

HENAO-ARDILA, A.; QUINTANILLA-CARVAJAL, M. X.; MORENO, F. L. Combination of freeze concentration and spray drying for the production of feijoa (*Acca sellowiana* b.) pulp powder. **Powder Technology**, v. 344, p. 190–198, 2019. Disponível em: <<https://doi.org/10.1016/j.powtec.2018.12.015>>.

HENGLEIN, A. Physicochemical properties of small metal particles in solution: “microelectrode” reactions, chemisorption, composite metal particles, and the atom-to-metal transition. **J. Phys. Chem.**, v. 93, n. 21, p. 5457–5471, 1993.

HUSEN, A.; SIDDIQI, K. S. Phytosynthesis of nanoparticles: Concept, controversy and application. **Nanoscale Research Letters**, v. 9, n. 1, p. 1–24, 2014.

INADA, A. C.; FIGUEIREDO, P. S.; DOS SANTOS-EICHLER, R. A.; FREITAS, K. de C.; HIANE, P. A.; DE CASTRO, A. P.; GUIMARÃES, R. de C. A. Morinda citrifolia Linn. (noni) and its potential in obesity-related metabolic dysfunction. **Nutrients**, v. 9, n. 6, p. 1–29, 2017.

JADOUN, S.; ARIF, R.; JANGID, N. K.; MEENA, R. K. Green synthesis of nanoparticles using plant extracts: a review. **Environmental Chemistry Letters**, v. 19, n. 1, p. 355–374, 2021. Disponível em: <<https://doi.org/10.1007/s10311-020-01074-x>>.

JAIN, K. K. Nanobiotechnology. **Comprehensive Biotechnology**, p. 599–614, 2011. Disponível em: <<http://linkinghub.elsevier.com/retrieve/pii/B9780080885049000684>>.

KANG, S.; VOGT, B. D.; WU, W.; PRABHU, V. M.; VANDERHART, D. L.; RAO, A.; LIN, E. K.; TURNQUEST, K. FTIR measurements of compositional heterogeneities. **Advances in Resist Materials and Processing Technology XXIV**, v. 6519, n. 301, p. 651916, 2007.

KISHEN, S.; MEHTA, A.; GUPTA, R. Biosynthesis and Applications of Metal Nanomaterials. In: **Green Nanomaterials. Advanced Structured Materials**. [s.l: s.n.]p. 139–157.

KUMAR, A.; CHISTI, Y.; CHAND, U. Synthesis of metallic nanoparticles using plant extracts. **Biotechnology Advances**, v. 31, n. 2, p. 346–356, 2013. Disponível em: <<http://dx.doi.org/10.1016/j.biotechadv.2013.01.003>>.

LACHENMEIER, K.; MUSSHOFF, F.; MADEA, B.; REUSCH, H.; LANCHENMEIER, D. Authentication of Noni (*Morinda citrifolia*) Juice. **Deutsche Lebensmittel-Rundschau**, v. 2, p. 58–61, 2006.

LAURENT, C.; BESANÇON, P.; CAPORICCIO, B. Flavonoids from a grape seed extract interact with digestive secretions and intestinal cells as assessed in an in vitro digestion/Caco-2 cell culture model. **Food Chemistry**, v. 100, n. 4, p. 1704–1712, 2007.

LEDWITH, D. M.; WHELAN, A. M.; KELLY, J. M. A rapid, straight-forward method for controlling the morphology of stable silver nanoparticles. **Journal of Materials Chemistry**, v. 17, n. 23, p. 2459, 2007.

LEE, A. L.; YU, Y. P.; HSIEH, J. F.; KUO, M. I.; MA, Y. S.; LU, C. P. Effect of germination on composition profiling and antioxidant activity of the polysaccharide-protein conjugate in black soybean [*Glycine max* (L.) Merr.]. **International Journal of Biological Macromolecules**, v. 113, p. 601–606, 2018. Disponível em: <<https://doi.org/10.1016/j.ijbiomac.2018.02.145>>.

LEWICKI, P. P. Design of hot air drying for better foods. **Trends in Food Science & Technology**, v. 17, p. 153–163, 2006.

LI, S.; SHEN, Y.; XIE, A.; YU, X.; QIU, L.; ZHANG, L.; ZHANG, Q. Green synthesis of silver nanoparticles using *Capsicum annuum* L. extract. **Green Chem**, v. 9, p. 852–858, 2007.

LI, X.; XU, H.; CHEN, Z.-S.; CHEN, G. Biosynthesis of Nanoparticles by Microorganisms and Their Applications. **Nanostructures for Medicine and Pharmaceuticals**, p. 1–16, 2011.

LIN, S.-Y.; LIAO, Y.-Y.; ROAN, S.-F.; CHEN, I.-Z.; CHEN, P.-A. Growth of noni fruits (*Morinda citrifolia* L.) and accumulation of phenolic compounds during fruit development. **Scientia Horticulturae**, v. 178, p. 168–174, 2014. Disponível em: <<http://dx.doi.org/10.1016/j.scienta.2014.08.013>>.

LIN, Y. L.; CHANG, Y. Y.; YANG, D. J.; TZANG, B. S.; CHEN, Y. C. Beneficial effects of noni (*Morinda citrifolia* L.) juice on livers of high-fat dietary hamsters. **Food Chemistry**, v. 140, n. 1–2, p. 31–38, 2013. Disponível em: <<http://dx.doi.org/10.1016/j.foodchem.2013.02.035>>.

LOGESWARI, P.; SILAMBARASAN, S.; ABRAHAM, J. Synthesis of silver nanoparticles using plants extract and analysis of their antimicrobial property. **Journal of Saudi Chemical Society**, v. 19, n. 3, p. 311–317, 2015.

LOWE, C. R.; LOWE, C. R. Nanobiotechnology: the fabrication and applications of chemical and biological Nanobiotechnology: the fabrication and applications of chemical and biological nanostructures. p. 428–434, 2015.

LUO, C.; CHEN, W.; HAN, W. Experimental study on factors affecting the quality of ice crystal during the freezing concentration for the brackish water. **Desalination**, v. 260, p. 231–238, 2010.

MANDUKHAIL, S. U. R.; AZIZ, N.; GILANI, A. H. Studies on antidyslipidemic effects of *Morinda citrifolia* (Noni) fruit, leaves and root extracts. **Lipids in Health and Disease**, v. 9, n. 1, p. 1–6, 2010.

MARTIN-DIANA, A. B.; IZQUIERDO, N.; ALBERTOS, I.; SANCHEZ, M. S.; HERRERO, A.; SANZ, M. A.; RICO, D. Valorization of Carob's Germ and Seed Peel as Natural Antioxidant Ingredients in Gluten-Free Crackers. **Journal of Food Processing and Preservation**, v. 41, n. 2, p. 1–13, 2017.

MAZZUCOTELLI, C. A.; GONZÁLEZ-AGUILAR, G. A.; VILLEGAS-OCHOA, M. A.; DOMÍNGUEZ-AVILA, A. J.; ANSORENA, M. R.; DI SCALA, K. C. Chemical characterization and functional properties of selected leafy vegetables for innovative mixed salads. **Journal of Food Biochemistry**, v. 42, n. 1, p. 1–12, 2018.

MITTAL, A. K.; BHAUMIK, J.; KUMAR, S.; BANERJEE, U. C. Biosynthesis of silver nanoparticles: Elucidation of prospective mechanism and therapeutic potential. **Journal of Colloid and Interface Science**, v. 415, p. 39–47, 2014. Disponível em:

<<http://dx.doi.org/10.1016/j.jcis.2013.10.018>>.

MITTAL, A. K.; CHISTI, Y.; BANERJEE, U. C. Synthesis of metallic nanoparticles using plant extracts. **Biotechnology Advances**, v. 31, n. 2, p. 346–356, 2013. Disponível em: <<http://dx.doi.org/10.1016/j.biotechadv.2013.01.003>>.

MORALES-LOZOYA, V.; ESPINOZA-GÓMEZ, H.; Z. FLORES-LÓPEZ, L.; SOTELO-BARRERA, E. L.; NÚÑEZ-RIVERA, A.; CADENA-NAVA, R. D.; ALONSO-NUÑEZ, G.; RIVERO, I. A. Study of the effect of the different parts of *Morinda citrifolia* L. (noni) on the green synthesis of silver nanoparticles and their antibacterial activity. **Applied Surface Science**, v. 537, n. September 2020, p. 147855, 2021. Disponível em: <<https://doi.org/10.1016/j.apsusc.2020.147855>>.

MORENO, F. L.; ROBLES, C. M.; SARMIENTO, Z.; RUIZ, Y.; PARDO, J. M. Effect of separation and thawing mode on block freeze-concentration of coffee brews. **Food and Bioproducts Processing**, v. 91, n. 4, p. 396–402, 2013. Disponível em: <<http://dx.doi.org/10.1016/j.fbp.2013.02.007>>.

MOTSHAKERI, M.; GHAZALI, H. M. Nutritional, phytochemical and commercial quality of Noni fruit: A multi-beneficial gift from nature. **Trends in Food Science & Technology**, v. 45, n. 1, p. 118–129, 2015. Disponível em: <<http://dx.doi.org/10.1016/j.tifs.2015.06.004>>.

MOURA, S. C. S. R. de; VISSOTTO, F. Z.; RUFFI, C. R. G.; ALVES JÚNIOR, P. Physical and rheological properties of fruit products. **Brazilian Journal of Food Technology**, v. 19, n. 0, p. 1–8, 2016.

MUÑOZ, I. de B.; RUBIO, A.; BLANCO, M.; RAVENTÓS, M.; HERNÁNDEZ, E.; PRUDÊNCIO, E. S. Progressive freeze concentration of skimmed milk in an agitated vessel: Effect of the coolant temperature and stirring rate on process performance. **Food Science and Technology International**, v. 25, n. 2, p. 150–159, 2019.

NAGRA, U.; SHABBIR, M.; ZAMAN, M.; MAHMOOD, A.; BARKAT, K. Review on Methodologies Used in the Synthesis of Metal Nanoparticles: Significance of Phytosynthesis Using Plant Extract as an Emerging Tool. **Current Pharmaceutical Design**, v. 26, p. 5188–5204, 2020.

NAIKOO, G. A.; MUSTAQEEM, M.; HASSAN, I. U.; AWAN, T.; ARSHAD, F.; SALIM, H.; QURASHI, A. Bioinspired and green synthesis of nanoparticles from plant extracts with antiviral and antimicrobial properties: A critical review. **Journal of Saudi Chemical Society**, v. 25, n. 9, p. 101304, 2021. Disponível em: <<https://doi.org/10.1016/j.jscs.2021.101304>>.

NASH, M. A.; SHOSEYOV, O. Editorial overview: Nanobiotechnology at a crossroads: moving beyond proof of concept. **Current Opinion in Biotechnology**, v. 39, p. vii–ix, 2016. Disponível em: <<http://dx.doi.org/10.1016/j.copbio.2016.04.024>>.

NATH, D.; BANERJEE, P. Green nanotechnology - a new hope for medical biology. **Environ. Toxicoll. Pharmacol.**, v. 36, n. 3, p. 997–1014, 2013.

NEIL SOLOMON. **Noni juice (*Morinda citrifolia*): the tropical fruit with 101 medicinal uses**. 2nd editio ed. [s.l.] Pleasant Grove, Utah: Woodland Publishing, 1999.

NELSON, S. Noni Seed Handling and Seedling Production. **Fruits and Nuts**, p. 8–11, 2005.

NELSON, S. C. Noni cultivation in Hawaii. **Fruits and Nuts**, n. 4, p. 2–5, 2001.

NELSON, S. C.; ELEVITCH, C. R. Making noni products. In: **Noni: the complete guide for consumers and growers**. Holualoa, Hawaii.: Permanent Agriculture Resources, 2006. p. 67–80.

ORELLANA-PALMA, P.; GONZÁLEZ, Y.; PETZOLD, G. Improvement of Centrifugal Cryoconcentration by Ice Recovery Applied to Orange Juice. **Chemical Engineering and Technology**, n. 4, p. 925–931, 2019.

ORELLANA-PALMA, P.; PETZOLD, G.; GUERRA-VALLE, M.; ASTUDILLO-LAGOS, M. Impact of block cryoconcentration on polyphenol retention in blueberry juice. **Food Bioscience**, v. 20, n. August, p. 149–158, 2017a. Disponível em: <<http://dx.doi.org/10.1016/j.fbio.2017.10.006>>.

ORELLANA-PALMA, P.; PETZOLD, G.; PIERRE, L.; PENSABEN, J. M. Protection of polyphenols in blueberry juice by vacuum-assisted block freeze concentration. **Food and Chemical Toxicology**, v. 109, p. 1093–1102, 2017b.

ORELLANA-PALMA, P.; PETZOLD, G.; TORRES, N.; AGUILERA, M. Elaboration of orange juice concentrate by vacuum-assisted block freeze concentration. **Journal of Food Processing and Preservation**, v. 42, n. 2, p. 1–6, 2018.

OU, B.; HUANG, D.; HAMPSCH-WOODILL, M.; FLANAGAN, J. A.; DEEMER, E. K. Analysis of antioxidant activities of common vegetables employing oxygen radical absorbance capacity (ORAC) and ferric reducing antioxidant power (FRAP) assays: A comparative study. **Journal of Agricultural and Food Chemistry**, v. 50, n. 11, p. 3122–3128, 2002.

PAI, A. R.; KAVITHA, S.; S, S. R. A. J.; PRIYANKA, P.; VRINDA, A.; VIVIN, T. S.; SASIDHARAN, S. Green synthesis and characterizations of silver nanoparticles using fresh leaf extract of *Morinda citrifolia* and its anti-microbial activity studies. **International Journal of Pharmacy and Pharmaceutical Sciences**, v. 7, n. 3, p. 459–461, 2015.

PERALTA-VIDEA, J. R.; HUANG, Y.; PARSONS, J. G.; ZHAO, L.; LOPEZ-MORENO, L.; HERNANDEZ-VIEZCAS, J. A.; GARDEA-TORRESDEY, J. L. Plant-based green synthesis of metallic nanoparticles: scientific curiosity or a realistic alternative to chemical synthesis? **Nanotechnology for Environmental Engineering**, v. 1, n. 1, p. 1–29, 2016.

PETER, P. I.; PETER, K. V. Noni (*Morinda citrifolia* L.): Research and Development. **New Age Herbals**, p. 55–69, 2018.

PETZOLD, G.; AGUILERA, J. M. Centrifugal freeze concentration. **Innovative Food Science and Emerging Technologies**, v. 20, p. 253–258, 2013. Disponível em: <<http://dx.doi.org/10.1016/j.ifset.2013.05.010>>.

PETZOLD, G.; MORENO, J.; LASTRA, P.; ROJAS, K.; ORELLANA, P. Block freeze concentration assisted by centrifugation applied to blueberry and pineapple juices. **Innovative Food Science and Emerging Technologies**, v. 30, p. 192–197, 2015. Disponível em: <<http://dx.doi.org/10.1016/j.ifset.2015.03.007>>.

PETZOLD, G.; NIRANJAN, K.; AGUILERA, J. M. Vacuum-assisted freeze concentration of sucrose solutions. **Journal of Food Engineering**, v. 115, n. 3, p. 357–361, 2013. Disponível em: <<http://dx.doi.org/10.1016/j.jfoodeng.2012.10.048>>.

PETZOLD, G.; ORELLANA, P.; MORENO, J.; CERDA, E.; PARRA, P. Vacuum-assisted block freeze concentration applied to wine. **Innovative Food Science and Emerging Technologies**, v. 36, p. 330–335, 2016.

PHILIP, D.; UNNI, C.; AROMAL, S. A.; VIDHUA, V. K. *Murraya Koenigii* leaf-assisted rapid green synthesis of silver and gold nanoparticles. **Spectrochimica Acta Part A: Molecular and Biomolecular Spectroscopy**, v. 78, n. 2, p. 899–904, 2011.

PILATTI-RICCIO, D.; DOS SANTOS, D. F.; MEINHART, A. D.; KNAPP, M. A.; HACKBART, H. C. dos S.; PINTO, V. Z. Impact of the use of saccharides in the encapsulation of *Ilex paraguariensis* extract. **Food Research International**, v. 125, n. June, p. 108600, 2019. Disponível em: <<https://doi.org/10.1016/j.foodres.2019.108600>>.

PRASAD, R. Synthesis of Silver Nanoparticles in Photosynthetic Plants. **Journal of Nanoparticles**, v. 2014, p. 1–8, 2014.

PRAWITWONG, P.; TAKIGAMI, S.; PHILLIPS, G. O. Phase transition behaviour of sorbed water in Konjac mannan. **Food Hydrocolloids**, v. 21, n. 8, p. 1368–1373, 2007.

PRUDÊNCIO, A. P. A.; PRUDÊNCIO, E. S.; AMBONI, R. D. M. C.; MURAKAMI, A. N. N.; MARASCHIN, M.; PETRUS, J. C. C.; OGLIARI, P. J.; LEITE, R. S. Phenolic composition and antioxidant activity of the aqueous extract of bark from residues from mate tree (*Ilex paraguariensis* St. Hil.) bark harvesting concentrated by nanofiltration. **Food and Bioprocess Processing**, v. 90, n. 3, p. 399–405, 2012. Disponível em: <<http://dx.doi.org/10.1016/j.fbp.2011.12.003>>.

RAI, M.; YADAV, A.; GADE, A. Silver nanoparticles as a new generation of antimicrobials. **Biotechnology Advances**, v. 27, n. 1, p. 76–83, 2009. Disponível em: <<http://dx.doi.org/10.1016/j.biotechadv.2008.09.002>>.

RAJAN, R.; CHANDRAN, K.; HARPER, S. L.; YUN, S. II; KALAICHELVAN, P. T. Plant extract synthesized silver nanoparticles: An ongoing source of novel biocompatible materials. **Industrial Crops and Products**, v. 70, p. 356–373, 2015. Disponível em: <<http://dx.doi.org/10.1016/j.indcrop.2015.03.015>>.

RICO, C. M.; PERALTA-VIDEA, J. R.; GARDEA-TORRESDEY, J. L. Chemistry, Biochemistry of Nanoparticles, and Their Role in Antioxidant Defense System in Plants. In: **Nanotechnology and Plant Sciences**. [s.l.] Springer, Cham, 2015. p. 1–17.

ROSS, I. A. **Medicinal Plants of the World: Chemical Constituents, Traditional and Modern Medicinal Uses, Volume 2**. 1. ed. [s.l.] Humana Press, 2001.

RYU, D.; KOH, E. Stability of anthocyanins in bokbunja (*Rubus occidentalis* L.) under in vitro gastrointestinal digestion. **Food Chemistry**, v. 267, n. February, p. 157–162, 2018. Disponível em: <<https://doi.org/10.1016/j.foodchem.2018.02.109>>.

SAFIEI, N. Z.; NGADI, N.; JOHARI, A.; ZAKARIA, Z. Y.; JUSOH, M. Grape Juice Concentration by Progressive Freeze Concentrator Sequence System. **Journal of Food Processing and Preservation**, v. 41, n. 1, p. 1–11, 2017.

SAMATEH, M.; POTTACKAL, N.; MANAFIRASI, S.; VIDYASAGAR, A.; MALDARELLI, C.; JOHN, G. Unravelling the secret of seed-based gels in water: the nanoscale 3D network formation. **Scientific Reports**, v. 8, p. 1–8, 2018.

SÁNCHEZ, J.; RUIZ, Y.; AULEDA, J. M.; HERNÁNDEZ, E.; RAVENTÓS, M. Review. Freeze Concentration in the Fruit Juices Industry. **Food Science and Technology International**, v. 15, n. 4, p. 303–315, 2009.

SANG, S.; CHENG, X.; ZHU, N.; STARK, R. E.; BADMAEV, V.; GHAI, G.; ROSEN, R. T.; HO, C. Flavonol Glycosides and Novel Iridoid Glycoside from the Leaves of *Morinda citrifolia*. **Journal of Agricultural and Food Chemistry**, v. 49, p. 4478–4481, 2001a.

SANG, S.; CHENG, X.; ZHU, N.; WANG, M.; JHOO, J. W.; STARK, R. E.; BADMAEV, V.; GHAI, G.; ROSEN, R. T.; HO, C. T. Iridoid glycosides from the leaves of *Morinda citrifolia*. **Journal of Natural Products**, v. 64, n. 6, p. 799–800, 2001b.

SANG, S.; WANG, M.; KAN, H.; LIU, G.; DONG, Z.; BADMAEV, V.; ZHENG, Q. Y.; GHAI, G.; ROSEN, R. T.; HO, C.-T. Chemical Components in Noni Fruits and Leaves (*Morinda citrifolia* L). In: HO, C.-T.; ZHENG, Q. Y. (Ed.). **Quality Management of Nutraceuticals**. Washington, DC: American Chemical Society, 2002. p. 134–150.

SARATALE, R. G.; SARATALE, G. D.; SHIN, H. S.; JACOB, J. M.; PUGAZHENDHI, A.; BHAIASARE, M.; KUMAR, G. New insights on the green synthesis of metallic nanoparticles using plant and waste biomaterials: current knowledge, their agricultural and environmental applications. **Environmental Science and Pollution Research**, v. 25, n. 11, p. 10164–10183, 2018.

SATHISHKUMAR, G.; GOBINATH, C.; KARPAGAM, K.; HEMAMALINI, V.; PREMKUMAR, K.; SIVARAMAKRISHNAN, S. Phyto-synthesis of silver nanoscale particles using *Morinda citrifolia* L. and its inhibitory activity against human pathogens. **Colloids and Surfaces B: Biointerfaces**, v. 95, p. 235–240, 2012. Disponível em: <<http://dx.doi.org/10.1016/j.colsurfb.2012.03.001>>.

SCHRAMM, G. **Reologia e Reometria: Fundamentos Teóricos e Práticos**. 1ª ed. ed. [s.l.] Artliber LTDA, 2006.

SHALAN, N. A. A. M.; MUSTAPHA, N. M.; MOHAMED, S. Noni leaf and black tea enhance bone regeneration in estrogen-deficient rats. **Nutrition**, v. 33, p. 42–51, 2017a. Disponível em: <<http://dx.doi.org/10.1016/j.nut.2016.08.006>>.

SHALAN, N. A. A. M.; MUSTAPHA, N. M.; MOHAMED, S. Chronic toxicity evaluation of *Morinda citrifolia* fruit and leaf in mice. **Regulatory Toxicology and Pharmacology**, v. 83, p. 46–53, 2017b. Disponível em: <<http://dx.doi.org/10.1016/j.yrtph.2016.11.022>>.

SHIMANOUCI, T. **Tables of Molecular Vibrational Frequencies: Consolidated Volume I**. Washington, D.C.: National Standard Reference Data System, 1973. v. 1

SIDDIQUI, M. H.; AL-WHAIBI, M. H.; MOHAMMAD, F. **Synthesis of metallic nanoparticles using plant extracts.** [s.l: s.n.]

SILVERSTEIN, R. M.; WEBSTER, F. X.; KIEMLE, D. J. **Spectrometric Identification of Organic Compounds.** [s.l: s.n.]

SINGH, D. R.; SINGH, S. Phytochemicals in plant parts of noni (*Morinda citrifolia* L.) with special reference to fatty acid profiles of seeds. **Proceedings of the National Academy of Sciences India Section B - Biological Sciences**, v. 83, n. 3, p. 471–478, 2013.

SINGH, J.; DUTTA, T.; KIM, K.-H.; RAWAT, M.; SAMDDAR, P.; KUMAR, P. 'Green' synthesis of metals and their oxide nanoparticles: applications for environmental remediation. **Journal of nanobiotechnology**, v. 16, n. 84, p. 1–24, 2018.

SINGH, P.; KIM, Y. J.; ZHANG, D.; YANG, D. C. Biological Synthesis of Nanoparticles from Plants and Microorganisms. **Trends in Biotechnology**, v. 34, n. 7, p. 588–599, 2016. Disponível em: <<http://dx.doi.org/10.1016/j.tibtech.2016.02.006>>.

SINGLETON, V. L.; ROSSI, J. A. Colorimetry of total phenolics with phosphomolybdic-phosphotungstic acid reagents. **American Journal of Enology and Viticulture**, v. 16, n. 3, p. 144–158, 1965.

SMITHA, S. L.; PHILIP, D.; GOPCHANDRAN, K. G. Green synthesis of gold nanoparticles using *Cinnamomum zeylanicum* leaf broth. **Spectrochimica Acta Part A: Molecular and Biomolecular Spectroscopy**, v. 74, n. 335–739, 2009.

SOCRATES, G. **Infrared and Raman characteristic group frequencies. Tables and charts.** Third Edit ed. West Sussex, England: John Wiley & Sons, LTD, 2001.

SRIVATSAN, T. S. *Nanomaterials: Synthesis, Properties, and Applications*, A. S. Edelstein and R. C. Cammarata, Editors. **Materials and Manufacturing Processes**, v. 27, n. 10, p. 1145–1145, 2012. Disponível em: <<http://www.tandfonline.com/doi/abs/10.1080/10426914.2012.689458>>.

SU, B. N.; PAWLUS, A. D.; JUNG, H. A.; KELLER, W. J.; MCLAUGHLIN, J. L.; KINGHORN, A. D. Chemical constituents of the fruits of *Morinda citrifolia* (Noni) and their antioxidant activity. **Journal of Natural Products**, v. 68, n. 4, p. 592–595, 2005.

SUÁREZ-CERDA, J.; ALONSO-NUÑEZ, G.; ESPINOZA-GÓMEZ, H.; FLORES-LÓPEZ, L. Z. Synthesis, kinetics and photocatalytic study of “ultra-small” Ag-NPs obtained by a green chemistry method using an extract of Rosa ‘Andeli’ double delight petals. **J Colloid Interface Sci**, v. 15, n. 458, p. 169–77, 2015.

SUMAN, T. Y.; RADHIKA RAJASREE, S. R.; KANCHANA, A.; ELIZABETH, S. B. Biosynthesis, characterization and cytotoxic effect of plant mediated silver nanoparticles using *Morinda citrifolia* root extract. **Colloids and Surfaces B: Biointerfaces**, v. 106, p. 74–78, 2013. Disponível em: <<http://dx.doi.org/10.1016/j.colsurfb.2013.01.037>>.

SUMAN, T. Y.; RADHIKA RAJASREE, S. R.; RAMKUMAR, R.; RAJTHILAK, C.; PERUMAL, P.

The Green synthesis of gold nanoparticles using an aqueous root extract of *Morinda citrifolia* L. **Spectrochimica Acta - Part A: Molecular and Biomolecular Spectroscopy**, v. 118, p. 11–16, 2014. Disponível em: <<http://dx.doi.org/10.1016/j.saa.2013.08.066>>.

SUMAN, T. Y.; RAVINDRANATH, R. R. S.; ELUMALAI, D.; KALEENA, P. K.; RAMKUMAR, R.; PERUMAL, P.; ARANGANATHAN, L.; CHITRARASU, P. S. Larvicidal activity of titanium dioxide nanoparticles synthesized using *Morinda citrifolia* root extract against *Anopheles stephensi*, *Aedes aegypti* and *Culex quinquefasciatus* and its other effect on non-target fish. **Asian Pacific Journal of Tropical Disease**, v. 5, n. 3, p. 224–230, 2015.

SUNDRARAJAN, M.; BAMA, K.; BHAVANI, M.; JEGATHEESWARAN, S.; AMBIKA, S.; SANGILI, A.; NITHYA, P.; SUMATHI, R. Obtaining titanium dioxide nanoparticles with spherical shape and antimicrobial properties using *M. citrifolia* leaves extract by hydrothermal method. **Journal of Photochemistry and Photobiology B: Biology**, v. 171, n. February, p. 117–124, 2017. Disponível em: <<http://dx.doi.org/10.1016/j.jphotobiol.2017.05.003>>.

SYAFIUDIN, A.; SALMIATI; HADIBARATA, T.; SALIM, M. R.; KUEH, A. B. H.; SARI, A. A. A purely green synthesis of silver nanoparticles using *Carica papaya*, *Manihot esculenta*, and *Morinda citrifolia*: synthesis and antibacterial evaluations. **Bioprocess and Biosystems Engineering**, v. 40, n. 9, p. 1349–1361, 2017.

TANAKA, K.; CHUJO, Y. Design of functionalized nanoparticles for the applications in nanobiotechnology. **Advanced Powder Technology**, v. 25, n. 1, p. 101–113, 2014. Disponível em: <<http://dx.doi.org/10.1016/j.appt.2013.07.002>>.

TANAKA, M.; SATO, M. Microwave heating of water, ice, and saline solution: Molecular dynamics study. **Journal of Chemical Physics**, v. 126, n. 3, p. 1–10, 2007.

THANI, W.; VALLISUTA, O.; SIRIPONG, P.; RUANGWISES, N. Anti-proliferative and antioxidative activities of Thai noni/Yor (*Morinda citrifolia* Linn.) leaf extract. **The Southeast Asian Journal of Tropical Medicine and Public Health**, v. 41, n. 2, p. 482–489, 2010.

THOO, Y. Y.; HO, S. K.; ABAS, F.; LAI, O. M.; HO, C. W.; TAN, C. P. Optimal binary solvent extraction system for phenolic antioxidants from mengkudu (*morinda citrifolia*) fruit. **Molecules**, v. 18, n. 6, p. 7004–7022, 2013.

TONTRONG, S.; KHONYOUNG, S.; JAKMUNEE, J. Flow injection spectrophotometry using natural reagent from *Morinda citrifolia* root for determination of aluminium in tea. **Food Chemistry**, v. 132, n. 1, p. 624–629, 2012. Disponível em: <<http://dx.doi.org/10.1016/j.foodchem.2011.10.100>>.

TRIPATHY, A.; RAICHUR, A. M.; CHANDRASEKARAN, N.; PRATHNA, T. C.; MUKHERJEE, A. Process variables in biomimetic synthesis of silver nanoparticles by aqueous extract of *Azadirachta indica* (Neem) leaves. **Journal of Nanoparticle Research**, v. 12, n. 1, p. 237–246, 2010.

VAHUR, S.; TEEARU, A.; PEETS, P.; JOOSU, L.; LEITO, I. ATR-FT-IR spectral collection of conservation materials in the extended region of 4000–80 cm⁻¹. **Analytical and Bioanalytical Chemistry**, v. 408, n. 13, p. 3373–3379, 2016. Disponível em: <<http://dx.doi.org/10.1007/s00216-016->

9411-5>.

VAN BEEK, T.; BUDDE, M.; VAN ESCH, J. Membrane-Freeze Concentration Hybrid for Temperature-Sensitive Biomolecules. Investigation, Application, and Techno-Economic Benefits. **Chemical Engineering and Technology**, v. 41, n. 12, p. 2385–2392, 2018.

WANG, M.-Y.; WEST, B. J.; JENSEN, C. J.; NOWICKI, D.; SU, C.; PALU, A. K.; ANDERSON, G. *Morinda citrifolia* (Noni): a literature review and recent advances in Noni research. **Acta pharmacologica Sinica**, v. 23, n. 12, p. 1127–1141, 2002.

WU, Y. Y.; XING, K.; ZHANG, X. X.; WANG, H.; WANG, Y.; WANG, F.; LI, J. M. Influence of freeze concentration technique on aromatic and phenolic compounds, color attributes, and sensory properties of cabernet sauvignon wine. **Molecules**, v. 22, n. 6, p. 1–18, 2017.

XAVIER, M. M. M.; MACHADO, A. V.; COSTA, R. de O. Bleaching of fruit and vegetables: A literature review. **Brazilian Journal of Agrotechnology**, v. 4, n. 1, p. 6–9, 2014.

YUAN, Y.; LI, C.; ZHENG, Q.; WU, J.; ZHU, K.; SHEN, X.; CAO, J. Effect of simulated gastrointestinal digestion in vitro on the antioxidant activity, molecular weight and microstructure of polysaccharides from a tropical sea cucumber (*Holothuria leucospilota*). **Food Hydrocolloids**, v. 89, n. November 2018, p. 735–741, 2019. Disponível em: <<https://doi.org/10.1016/j.foodhyd.2018.11.040>>.

ZHANG, C.; HU, Z.; DENG, B. Silver nanoparticles in aquatic environments: Physiochemical behavior and antimicrobial mechanisms. **Water Research**, v. 88, p. 403–427, 2016. Disponível em: <<http://dx.doi.org/10.1016/j.watres.2015.10.025>>.

ZHANG, X.; YAN, S.; TYAGI, R. D.; SURAMPALLI, R. Y. Synthesis of nanoparticles by microorganisms and their application in enhancing microbiological reaction rates. **Chemosphere**, v. 82, n. 4, p. 489–494, 2011. Disponível em: <<http://dx.doi.org/10.1016/j.chemosphere.2010.10.023>>.

ZIELINSKI, A. A. F.; ZARDO, D. M.; ALBERTI, A.; BORTOLINI, D. G.; BENVENUTTI, L.; DEMIATE, I. M.; NOGUEIRA, A. Effect of cryoconcentration process on phenolic compounds and antioxidant activity in apple juice. **Journal of the Science of Food and Agriculture**, v. 99, n. 6, p. 2786–2792, 2019.